Estimation of carrying capacity of offshore milkfish farm environments through mathematical modeling

(数理モデルによるサバヒー養殖場の環境容量に関する研究)

A dissertation for the degree of

Doctor of Philosophy in Engineering

in

Graduate School of Urban Innovation
Institute of Urban Innovation

Yokohama National University

by

SUMBING, JOEMEL GENTELIZO

YOSHIYUKI NAKAMURA

Academic Adviser

ABSTRACT

The model set-up for milkfish marine cage culture with environmental and harvest weight criteria is presented. The motivation of the model is the growing concern of aquaculture fish kills in active production areas in the Philippines and the deficient environmental quality standards on sediment conditions in tropical regions. The model was divided into four sub-models, (1) growth sub-model, (2) carbon box sub-model, (3) particle dispersion model, and (4) sediment degradation model.

Four growth trials were used for the proposed logistic growth model. Fish density, temperature and feed rates were the factors identified to estimate the maximum attainable (*K*) (R^2=0.68) and intrinsic growth rate (*r*) (R^2 = 0.66). The proposed growth curve model was used as the principal sub-model for the model-setup. The particulate carbon flux was calculated using carbon balances equations with routine metabolism rate at 1.55 gC/kg day. Proximate analysis data on feed and fish body were also used to the estimation. Carbon and nitrogen content in the feed was found at 45% and 12%, respectively and in the fish body, it was at 36% and 11% respectively.

Probability density function was used to elucidate the distribution of the particulate carbon flux in the sediment area. Experimental data on AVS spatial concentrations and milkfish feed and faeces sinking rates (7.1 cm/s and 0.9 cm/s) were used to estimate the current standard deviation and was found at 0.0104m/s. This value was used for the model set-up simulations for milkfish cage. Sediment AVS generation was calculated from the particulate carbon flux distribution using the assumptions from theory. The calculated and actual AVS data were compared and exhibits moderate correlation.

Simulations on single net cage culture and multiple cages were done using different environmental criteria, depth and current standard deviation. The results of the simulations were used to establish a relationship of the index of suitable location and the harvest biomass. The stocking density of the milkfish was then calculated to ensure economic and environmental sustainability.

TABLE OF CONTENTS

Chapter 1 - INTRODUCTION

1.1 Background of the study

Aquaculture has rapidly developed over the past decades and considered as the fastest growing food industry in the world. This rapid growth was caused mainly by the declining trend in global capture fisheries (Chopin et al. 2008; Troell et al. 2009). From 2009 to 2014, global aquaculture production had increased from 55.7 to 73.8 million tonnes while wild capture had increase only from 90.2 to 93.4 million tonnes (FAO 2016). This shows that nearly a second fish consumed is coming from aquaculture operations. The constant increasing demand for fish food supply has resulted to conversion of coastal resources to fish production and has caused the deterioration of many coastal ecosystems which resulted to coastal eutrophication and marine habitat destruction. The introduction of inorganic and organic wastes into the coastal environment has led to internal, local and regional impacts which increases the risk of disease outbreaks and introduction of non-native species affecting the local biodiversity (Silvert 1992). While aquaculture provides food security, diversification of income and food sources, improved marginal economies and reduced food prices, it can also modify ecosystem resilience through water and sediment nutrient enrichment which in regional scale can result to irreversible environmental deterioration (Frankic and Hershner 2003).

In the Philippines, milkfish *(Chanos chanos*) is the most predominant species produced from aquaculture and shares 64% of produced fish species in 2016 (FAO 2016). As it is considered as the country's national fish, it is best suited for aquaculture because of its fast growth, adaptability to variety of feed sources, resistance to disease and handling, and tolerance to wide range of environmental conditions (Crear 1980). With the increasing fish demand, milkfish cage aquaculture has expanded to marine coastal waters due to the eutrophication of freshwater resources.

Although cage aquaculture has been practiced for centuries (such as transporting wild caught fish to shore), it has rapidly grown for this past 30 years. In the Philippines, marine milkfish cage aquaculture production has increased rapidly from 1998 at 7.5×10^3 metric tonnes to 2016 at 117.15

× 10^3 metric tonnes. This growth can be accounted for the limited brackish and freshwater sites that can be converted to aquaculture. The sites suitable for cage aquaculture may often be found in coves and estuaries where waves and water current are minimal. Since these sites have insufficient water exchange, carrying capacity is limited and the environment suffers adverse impacts. These impacts may not only affect the immediate coastal environment but also directly affect the fish stocks. When the conditions are right, intensive cage farming may result to mass fish kill. One recorded economic loss of fish stocks in the Philippines was in year 2015, with a total loss of PhP 220 million (500 million yen) in Bolinao, Pangasinan, where intensive milkfish pens and cages aquaculture were carried out. At the same site in 2011, PhP 44.17 worth of fish perished and in 2002, PhP 400 million worth of fish perished.

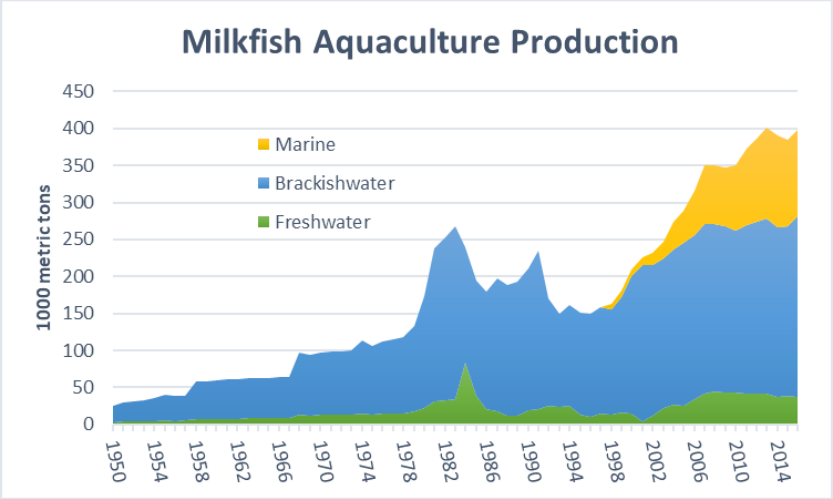

Figure 1.1. Philippine milkfish aquaculture production in different water classification.

These incidents of mass fish kills have prompted researchers to study the impacts of cage aquaculture (San Diego-McGlone et al. 2008). Most of the studies in milkfish aquaculture were based on increasing the production efficiency through the manipulation of feed nutrition (Wu et al. 1994). Through adjusting the feed nutrition, the time it takes for the fish to reach marketable size can be minimized. Although these factors are important to lessen the environment burden, environment factors such as inorganic and organic loading should also be considered (Troell et al. 2003).

Inorganic and organic wastes derived from aquaculture are diverse and can be in the form of particulate and dissolved. While most dissolved waste cause internal impacts, such as low dissolved oxygen concentration in the water column, particulate waste can cause locals impacts such as sediment degradation, that may lead to regional impacts (Silvert 1992). To prevent these impacts, environmental criteria need to be established before or during the start of aquaculture activities. Since the amount of feed input is directly proportional to the amount of organic waste loads, it is necessary to identify the number of fish that a certain cage dimension can sustain without surpassing the set environmental criteria.

In this study, the amount of the organic matter waste was estimated through material box model. Through sediment degradation reactions, the evolved AVS concentration derived from the accumulation of organic matter was also computed. Lastly, the carrying capacity of the marine milkfish cage were estimated based on the sediment acid volatile sulfide (AVS) criteria based on the "Law to Ensure Sustainable Aquaculture Production (1999)" in Japan (Yokoyama 2003).

1.2 Objectives of the study

There are two management feeding protocols being practice in milkfish cage aquaculture are: (1) satiation feeding scheme, and (2) ration feeding scheme. In satiation feeding scheme, the milkfish exhibits fast growth and less stress due to handling, however, in this scheme, high amount of feeds is required causing high sediment deposition. On the other hand, in ration feeding scheme, fish growth parameters measurements were done, and calibrated amount of feed was given. This causes stress to fish during sampling and often optimum growth is not reached. However, since the feed amounts were calibrated, sediment deposition is low. It is apparent that there is a need to combine the positive aspects of both schemes to prevent sediment pollution at the same time ensuring optimum growth. To ensure sustainable milkfish aquaculture production, carrying capacity should be estimated using

appropriate models. These models can serve as a management tool where fish farmers can utilize before or during production runs.

Taking these factors in consideration, the main objective of this study is to recommend a management scheme that would serve as basis for milkfish cage aquaculture production to maintain sustainable operations based on AVS concentration as an environmental criterion. The sub-objectives of the study are as follows:

- Propose a generalized milkfish growth curve based on the fish physical parameters.
- Estimate the amount of organic particulate waste derived from milkfish cage operation using material box model.
- Estimate the diffusion of organic particulate waste through probability density function.
- Calculate the evolution of hydrogen sulfides using the estimated organic particulate waste through aerobic and anaerobic degradation reactions.

These sub-objectives will serve as the basis for generating a mathematical model for milkfish farming. The goal of this study is to create a model that would serve as a management tool to ensure optimum fish growth in a given number of fish at a given duration and to ensure that the production does not exceed the set environmental criteria, in this case, the sediment acid volatile sulfides (AVS) concentration.

1.3 Significance of the study

In milkfish cage aquaculture, feed must be supplied, and waste product must be regulated, since the accumulation of these waste products have directly or indirectly adverse effects to the fish stocks. However, the amount of feed is identified by the number of cultured stocks. The interaction between the number of cultured stocks and the surrounding environment must be quantified and understood. The models for interpreting this interaction has been commonly used in temperature

regions, where most aquaculture techniques were standardized (Wu et al. 1994). However, in tropical regions there are limited studies made on elucidating this mechanism, thus, it is necessary to postulate a model that can establish these relationships.

Box models are one of the effective tools in estimating the amount of feacal material derived from aquaculture (Satoshi Watanabe et al. 2014). In marine species, these models were widely used in forecasting the amount of excess carbon, nitrogen, and phosphate in the feacal material of fish after feed ingestion. With the aid of tracer compounds, the apparent digestibility of feeds in milkfish can also be calculated. However, this procedure was used in feed nutrition studies and recommendations were made only on the amount of feed input and not on the number of cultured species. Previously, these models would focus on the feed characteristics, however as the feed wastage was reduced, the component of modeling shifted to the faecal material of the target fish species (Chamberlain and Stucchi 2007).

Particle dispersion model is a useful tool in explaining the distribution of particulate wastes from marine fish cages. This model can help in deciding the suitable site for culture and the orientation of the cages. Furthermore, it can also aid the farmers in deciding when and where to take samples for analyzing environmental parameters. Finally, the model can be used to identify the specific impacts and its extent associated with marine fish cages (Stucchi et al. 2005)

Sediment degradation model, on the other hand, was constructed to predict the formation of pollutant such as ammonia, carbon dioxide and hydrogen sulfides. In some models, environmental changes were also accounted for instance changes in dissolved oxygen concentration and changes in the amount of organic material. However, the main purpose of this sediment degradation model is to predict the nutrient released or buried from and into the sediment and served as the basis for setting an environmental criterion.

In this study, four different models were used to estimate the carrying capacity of the milkfish cage culture. Moreover, this model can also be used to explain the extent and expanse of the

particulate waste accumulation and the resulting AVS concentrations derived from the culture cage. This model can also be used as a guide in determining the if the identified site is suitable for milkfish cage culture operations.

1.4 Scope and limitations

This study includes a proposal of a growth curve derived from four experiment trials using the fish average body weight and the duration of culture as the main parameters for the derivation. The growth constants were also estimated using the fish density, average site temperature and the given feed amount. Environmental factors which cause stress to the fish stocks such as salinity, turbidity, dissolved oxygen, ammonia, and phosphate were not included in the growth curve derivation. Furthermore, the age of the milkfish stocks was not considered in the modeling.

This study also includes carbon and nitrogen material balance models. These models were dependent on the stable isotope ratio of both feed and milkfish body composition thus the type of feed for all trials were assumed to be the same. In this study, it was also assumed that the amount of uneaten or waste feeds was at 5% which was also based in theory. The respiration and excretion rate needed for the material balance were also taken from available principles based on the metabolism of fish. Though most nutrition studies based the growth of fish through using tracer compounds, the apparent digestibility of feed was not taken into consideration. The results of the nitrogen balance were not used for modeling however it can be used for future considerations.

As for the particle dispersion model, it was assumed that the north-south and east-west direction has equal diffusion characteristics. This means that turbulent diffusion was not considered. In addition, the cultured site was assumed to have no unidirectional current, thus the maximum particulate carbon wastes can be found at the center of the cage. It was also assumed that the only source of particulate carbon settling onto the seabed is only coming from the cage and no intervention from external sources.

For the sediment degradation model, dissolved oxygen was assumed at 6mg/L to signify that the site is not polluted before the start of any trials. This assumption is important since organic matter undergoes aerobic degradation before and when it reaches the seabed. The higher the dissolved oxygen the lower the organic matter that undergoes anaerobic degradation. Assumptions on the diffusivity of solutes were also made for the conversion of material fluxes to concentrations and vice versa. The diffusive boundary layer and the hydrogen sulfide diffusive layer were also assumed to aid with the conversion. However, unlike other models, only one layer per reaction was taken into consideration. Nitrate, manganese, and iron degradation were not calculated but instead a ratio was used to estimate the carbon flux which can undergo either of the three degradation reactions. Furthermore, the sediment degradation model did not include the hydrogen sulfide release to the water column but instead it was assumed to be buried within 1cm of the sediment depth parallel to the sampling protocol for measure sediment AVS.

All assumptions on each of the sub-models were considered to produce the model-setup for milkfish farming as an aid in estimating the carrying capacity of the milkfish cage.

1.5 Definition of the keywords

Average body weight (ABW)

The mean milkfish wet body weight with sampling size of 10% of the total number of fish in each the cage. Measured every 28 or 30 days from the start of the experiment. This parameter is reported in grams.

Days/Duration of culture

Number of days where the milkfish was cultured until harvest in marine cage. In standard cages operations it was estimated to be from 120 to 180 days (4-6 months), but in this study it ranges from 83 to 189 days.

Fish Count / Fish Density

The total number of milkfish in a marine cage. The initial number at the start of culture is called stocking density and the final number is harvest density. In marine cages, the standard stocking density was suggested at 30 individuals/m3.

Biomass

The product of ABW and Density. The total fish wet mass in a marine cage. This parameter is used for the calculation of daily feed ration and represents carrying capacity in the model-setup.

Feed rate

The feed amount in percentage, based on the ABW of milkfish as suggested by theory or commercial feed producers. As ABW increases the feed rate decreases. For commercial feeds it was suggested that for ABW of 5-25g, feed rate is 10-8%; for 25-150g, 8-6%; 150-280g, 6-4% and 250-500g, 4-2%.

Feed ration

The calculated amount of daily feed be given in per cage. This is the product of ABW, Feed rate and Density and usually rounded off to the nearest kilogram for ease of weighing and preparations.

Uneaten feeds

The estimated amount of leftover (not consumed) feed of milkfish. This parameter depends highly on the quality of feed and the amount unformed feeds (ground feeds resulted from milling). In theory it was suggested that 1-5% of feeds are wasted due to milling, handling, and feeding issues. In this study, this parameter was assumed at 5%.

Routine Metabolism Rate (RMR)

The rate of oxygen used by milkfish through respiration and metabolism. At this rate, it was assumed that the milkfish is not under stress. The rate of metabolism was converted into the amount of glucose needed for the fish energy demand.

Particulate carbon flux/ carbon flux/ organic matter flux (OM_P)

The resulting product of carbon balance which includes feacal carbon and uneaten carbon divided by the duration and the area of the cage.

Acid volatile sulfides (AVS)

Defined operationally as the sulfide fraction that is evolved from sediment when treated with acid. It is a complex and variable fraction of sediment represented by a variety of reduced sulfur components. Greater AVS concentrations are associated typically with organic-rich, anoxic deposits and lower levels are found usually in anoxic sediments having low organic content (Hammerschmidt and Burton 2010).

Chapter 2 - REVIEW OF LITERATURE

2.1 Fish growth curves

Numerous models have been introduced to model the growth of biological systems. These models address population dynamics, either modelled discretely or for large populations. Some models include the actual physical growth for some properties that may hinder or accelerate growth rate for an organism or as a part of a whole. The simple exponential growth model can provide an adequate approximation to such growth for the initial period. However, for populations, no predation or intraspecific competition is included. The population would therefore continue to increase unhindered (or inevitably reduce to zero if an initial growth reduction were present). Even in the case where predation was at most negligible, the model does not accommodate reductions due to intraspecific competition for environmental resources such as food and habitat. For the case of growth per se, unrestricted growth is also unrealistic (Tsoularis and Wallace 2002; Vogels et al. 1975).

Verhulst considered that, for the population model, a stable population would consequently have a saturation level characteristic: this is typically called the carrying capacity, *K*, and forms a numerical upper bound on the growth size. To incorporate this limiting form, he introduced the logistic growth equation which is shown later to provide an extension to the exponential model. This logistic equation can also be seen to model physical growth provided *K* is interpreted, rather naturally, as the limiting physical dimension. It is parameterized by the initial population size (or physical dimension), the initial growth rate, and *K*. For typical values of these, particularly, where the initial population size (or dimension) is smaller than *K*, the resulting logistic growth rate curve is sigmoidal (Mawhin 2004; Mujib et al. 2019).

The simplest realistic model of population dynamics is the one with exponential growth

$$\frac{dN}{dt} = rN\left(1-\frac{N}{K}\right) \qquad \textbf{(1)}$$

with the solution:

$$N(t) = \frac{KN_0}{(K - N_0)e^{-rt} + N_0} \quad \textbf{(2)}$$

where:
N_0 is the population size at time t=0,
r is the intrinsic growth rate that represents growth per capita.

The three key features of the logistic growth curve are:

(1) $\lim_{t\to\infty} N(t) = K$, the population will ultimately reach its carrying capacity.
(2) The relative growth rate , $\frac{1}{N}\frac{dN}{dt}$, declines linearly with increasing population size.
(3) The population at the inflection point (where growth rate is maximum), N_{inf}, is the exactly half the carrying capacity, $N_{inf} = \frac{K}{2}$.

In all kinds of food production, especially in aquaculture, the growth performance of organisms is the most important influencing factor regarding economic benefit (Lugert et al. 2016). As the rate of growth in weight approaches an asymptotic value, the economic value of the yield harvest is at its peak and afterwards, if the duration of culture was prolonged, the economic value of the harvest decreases. This shows that the optimum growth rate was already reached, and the continuation of the culture after the highest growth rate was attained, would result to a higher feed conversion ratio which in turn would increase the cost of production thus, it is not economically viable (Martinez, Tseng, and Yeh 2006).

Growth curves for fish in the wild are usually fitted to data on size at yearly intervals. Either length or weight can be fitted, but length is usually easier because the inflection point for length has usually been passed by age 1, so it is only the part of the curve having decreasing curvature that needs to be described by a formula. By contrast, the absolute rate of increase in weight often continues to increase for several years before decreasing; hence in order to fit the whole of a weight curve it is necessary to find an S - shaped curve having the correct curvature on both sides of the inflection point. (Ricker 1979).

There are three existing measures when reporting fish growth: absolute growth rate, relative growth rate and specific growth rate. Less frequently, Von Bertalanffy growth functions are used. Each of these measures is a numerical representation of growth which can be used for various purposes, including statistical evaluation of the effects of various treatments of growth presentation of growth data in a standard format which allows experimenter's to compare growth in different experiments and providing the basis for management decisions (Hopkins 1992). In most cases, stocking and harvest data are used to compute growth rates and do not consider growth during the whole duration period. When doing so only the simplest form of the absolute growth rate is appropriate. Also, this leads to the absence of the intermediate data during the duration of the experiment and it can often be neglected. The commonly used curves to study growth when measured by weight are the Logistics (Figure 2.1), Gompertz (Figure 2.2), Von Bertalanffy (Figure 2.3) and Richards (Figure 2.4). Little emphasis has been placed on the statistical properties of these conventional nonlinear models (Hernandez-Llamas and Ratkowsky 2004).

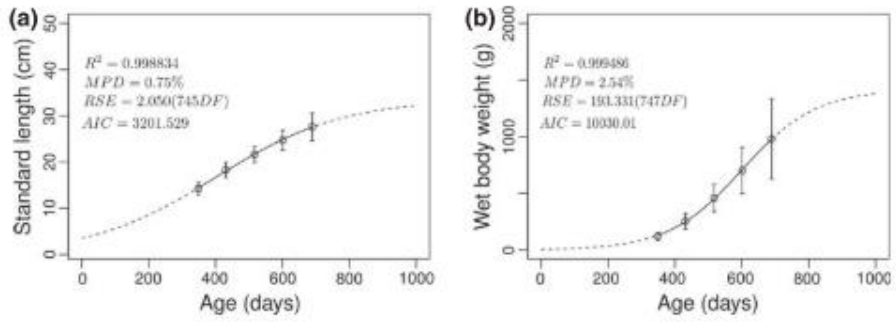

Figure 2.1. Logistics growth curve in average wet body weight and standard length.

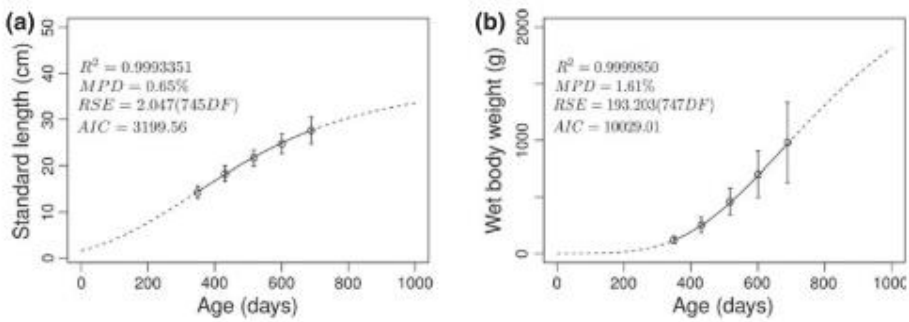

Figure 2.2. Gompertz growth curve in average wet body weight and standard length.

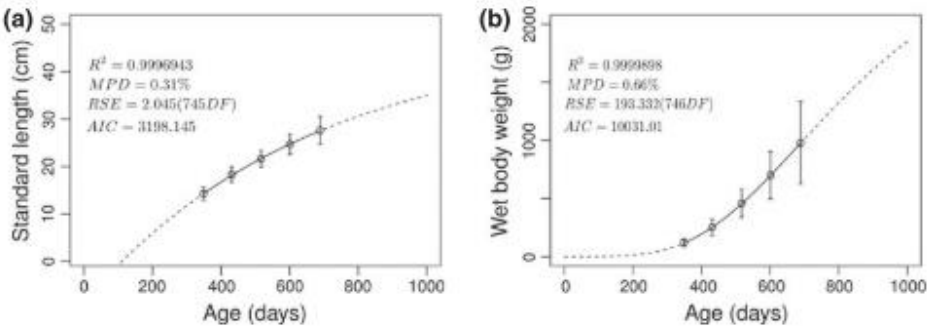

Figure 2.3. Von Bertalanfy growth curve in average wet body weight and standard length.

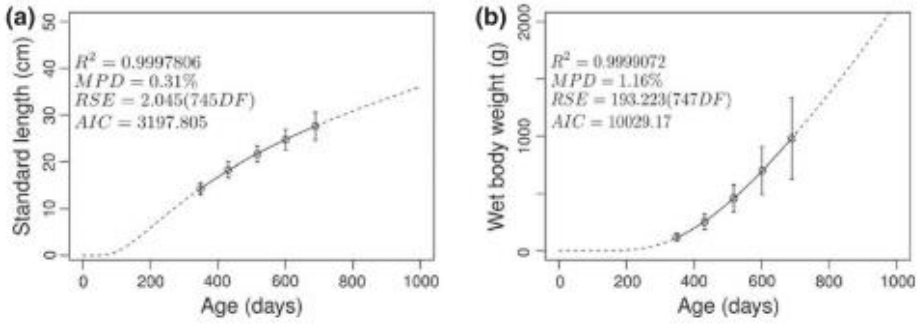

Figure 2.4. Richards growth curve in average wet body weight and standard length.

The growth of fish underlies a wide range of positive or negative impacting factors. In fish, growth mainly depends on feed consumption and quality, stocking density, biotic factors such as sex and age; genetics variance; and abiotic factors such as water chemistry, temperature, photo period, and oxygen level (Bagarinao 1991; Kumagai, Bagarinao, and Unggui 1985; Lugert et al. 2016). In other cases, estimates of growth parameters may be functionally dependent on specific environmental or management variables, such as temperature or stocking density. In every circumstance, as statistically well behaved, close to linear growth model is highly desirable (Grover and Juliano 1976; Hernandez-Llamas and Ratkowsky 2004).

Originating from population studies, the logistic function describes the curve with the perfect S-shape character. It is one of several bipartite expressions as possible descriptions of the succession of age frequencies in human populations. In ichthyology, it has been used mainly to describe the

increase in weight of populations, rather than individuals (Ricker 1979). It can be a prototype of S-curves, being perfectly symmetric (Figure 2-5). As the ideal curve of fish growth in length describes a bounded curve, it is unfavorable to use a function that mathematically provides POI or point of inflection and has an S-shape. In contrast, it is obvious that the perfect S curve could adequately describe fish growth in weight because growth in weight shows a strong S-shape character. You do it symmetric form, it gains strong limitations from the time scale of the data set, because growth curves are often skewed to the right. In order to improve the estimation of the logistic growth curves, several factors need to be included in the estimation of fish growth. Examples of these factors may include fish density, temperature, salinity, and feed consumption.

$$w = \frac{W_\infty}{1 + ce^{-gt}} \qquad \textbf{(3)}$$

Logistics Growth Curve:

where:

w = weight at any time
t = time
W_∞ = asymptotic weight
g = instantaneous rate of growth
c = inflection point of the curve

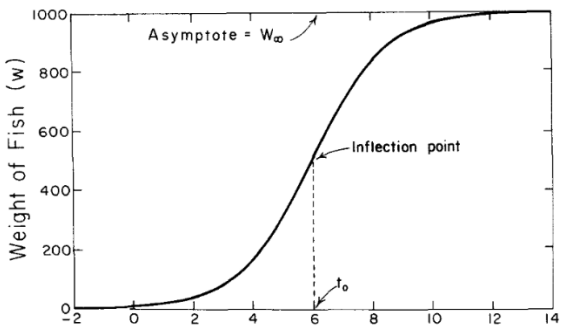

Figure 2.5. An example of logistics growth curve with point of inflection and asymtotic weight.

In many growth studies, the estimation of fish growth only includes the average body weight, average body length and the duration of culture. As for the logistics growth curve, the asymptotic weight and instantaneous growth rate can mathematically represent certain environmental factors,

which can directly affect the growth of the fish more specifically on the marine cage culture. In milkfish marine cage experiment for the development of integrated multi-trophic aquaculture, a logistic curve was fitted from culture day 1 to 200 days (i.e. 61-260 days of age) with the equation of BW(g) = 400.5 / (1 + $e^{-0.0202x\ (t-192.0)}$); (r2= 0.996) where t is age in days (Satoshi Watanabe et al. 2014). Through accurate forecast of fish growth, farmers and regulators could use the approach for sitting decisions and to determine optimal stocking density to avoid the adverse effect of marine cage farming to the marine ecosystem (Price et al. 2015).

2.2 Material balance

Coastal farming of fish through the use of floating net cage is a rapid expanding method in aquaculture (FAO 2016). It provides a significant portion of the world's fish production. For the milkfish industry, the typical method of cultivation is using pens in brackish water environment, however, the availability of the ponds for milkfish cultivation are declining (Holmer et al. 2002). In order to maintain the supply of milkfish, sheltered coastal areas were developed as aquaculture sites. This impacts the marine environment primarily through the release and accumulation of waste products (Noroi et al. 2011). Since these areas often have a little water exchange, the environment may be heavily affected. Likewise, particulate organic carbon and ammonia from the farmed fish can cause eutrophication which can lead to mass fish kills. Particulate waste products in the form of fish food and faeces quickly sink to the sea floor. The higher deposition of waste particles in the sediment near aquaculture operations stimulates metabolic activity in the settlement and hence the consumption of electron acceptors resulting in changed pathways for carbon and nitrogen mineralization and nutrient regeneration (Corner et al. 2006; Halwart, Soto, and Arthur 2007; Soto et al. 2008).

For sustainable management of the impacted ecosystems, it is imperative to understand how they function and how they respond to increased loading of nutrients and organic matter. The ability to forecast the loading of nutrients and organic matter can be solved using detailed information of

husbandry data which depends on the length and complexity of the study. Feed input data in terms of kilograms per cage per day are most used, but information on fish species, numbers, average weight, total biomass, and feed diameter should be obtained where available. However, knowing the real amount of feed ingested by fish in cage farming is practically impossible hence, as a more accurate approximation, the amount of uneaten feed can be assumed (Ballester-Moltó et al. 2017). With this mentioned factors, daily data can be obtained for the estimation of the organic and nutrient loading.

2.2.1 Organic matter waste

Intensive fish farming in coastal waters generates large amounts of particulate organic waste in the form of waste feed and fecal matter. The particulate organic wastes settle onto the seabed and produced enriched sediments, which can result in deoxygenation of the bottom water, the production of reduced compounds such as ammonium and sulfides, and changes in the structure of benthic communities (Pearson and Black 2001; Yokoyama, Abo, and Ishihi 2006). Ensuring sustainable aquaculture production in coastal areas requires careful attention to environmental interactions with the benthos and water column. The eutrophication of sediments underlying fish farm cages due to deposition of organic- rich solid waste represent a major factor influencing productive capacity. The generation and release of organic waste to the environment mostly depend on the fish farm size and husbandry practices. Once at the bed, waste can accumulate or be degraded, buried, or resuspended in the water column. Degradation of organic waste (by aerobic and anaerobic respiration) is a function of the supply of oxidants to surface sediments and the composition and successional stage of benthic communities carrying out degradation. These factors also define the recovery rate of fallowed sites and the return of your chemical and biological indicators to the bounds of natural variation (Bravo and Grant 2018).

In this regard, it is necessary to determine the ration level, which may be variable depending on the culture species, it's body size and the environmental temperature (Yokoyama, Inoue, and Abo

2004). Similarly, obtaining detailed husbandry data should be the topmost priority. The number of daily feeding events as well as the feeding method should also be known. However, few studies exist in the scientific literature on feed wastage as generalizations are difficult given the variation in husbandry feeding practices. Current modeling studies use uneaten feed as 1 to 5% of feed input, with 5% representing a worst-case scenario (Cromey and Black 2005).

In simple terms, of all of the organic matter that is provided to the fish in the feed, most is ingested by the fish and a small portion is uneaten or wasted.

$$\mathrm{OM}_{\mathrm{feed}} = \mathrm{OM}_{\mathrm{ingested}} + \mathrm{OM}_{\mathrm{waste\ feed}} \quad \textit{(4)}$$

The fate of the organic matter that is ingested may be further partitioned into three components: fish growth, respiratory/soluble wastes and faecal waste- the first three terms on the right-hand side of the following equation:

$$\mathrm{OM}_{\mathrm{feed}} = \mathrm{OM}_{\mathrm{growth}} + \mathrm{OM}_{\mathrm{resp.\ \&\ sol.\ waste}} + \mathrm{OM}_{\mathrm{feces}} + \mathrm{OM}_{\mathrm{waste\ feed}} \quad \textit{(5)}$$

The amount of organic matter in the respiration and soluble waste can be calculated using the complete aerobic respiration of glucose with standard vertebrate stoichiometry:

$$\mathrm{C_6H_{12}O_6} + 36\mathrm{ADP} + 36\mathrm{P_i} + 36\mathrm{H^+} + 6\mathrm{O_2} \Rightarrow 6\mathrm{CO_2} + 36\mathrm{ATP} + 42\mathrm{H_2O} + \mathrm{Heat} \quad \textit{(6)}$$

Both oxygen and carbon dioxide are gases at the range of temperatures and pressures encountered by fishes on earth, and their stoichiometric consumption or release can be monitored to gauge the rate of this reaction. By quantitatively transforming the emanated carbon dioxide into a solid, we could estimate the oxygen consumed by air- breathing organisms through measuring the loss of respirometer volume. Because each major food stuff (protein, fat, or carbohydrate) produces different amounts of energy per amount of oxygen consumed or carbon dioxide emanated, accurate use of indirect calorimetry for bioenergetics requires a strict accounting of the substrate being oxidized and the energy lost through excretion of waste nitrogen. The relationship between the enthalpy change and the amount of oxygen consumed is less dependent upon the foodstuff being

oxidized than is the caloric coefficient of carbon dioxide release which, makes oxygen a much better gas to use if the investigator is only going to use one gas (Nelson 2016). In the estimation of the respired and soluble carbon, routine metabolism rate in terms of oxygen consumption is necessary (Table 2-1).

Table 2-1. Experiment results on routine metabolism rate of euryhaline milkfish.

	Overall[a]		Daily[b]		Fish[c]	
Salinity (‰)	RMR ($mg\,O_2\,kg^{-1}\,h^{-1}$)	$U_{routine}$ ($L\,s^{-1}$)	RMR ($mg\,O_2\,kg^{-1}\,h^{-1}$)	$U_{routine}$ ($L\,s^{-1}$)	RMR ($mg\,O_2\,kg^{-1}\,h^{-1}$)	$U_{routine}$ ($L\,s^{-1}$)
15	132.3±3.2 (93)	0.79±0.01 (93)	132.7±5.6 (16)	0.77±0.03 (16)	136.0±6.8 (7)	0.77±0.04 (7)
35	170.4±4.1 (93)	0.97±0.02 (93)	167.2±7.8 (15)	0.96±0.04 (15)	171.7±10.3 (9)	1.02±0.05 (9)
55	126.0±2.4 (119)	0.67±0.02 (119)	126.5±3.4 (21)	0.67±0.03 (21)	127.7±4.2 (9)	0.70±0.05 (9)

The routine metabolism rate describes the oxygen required to cover basic cost in a resting animal, such as osmotic and ionic regulation, the constitutive turnover of proteins and basic cardiorespiratory functions. For the euryhaline species like the milkfish, the routine metabolism rate would be reduced in low salinity environment like brackish water compared the fresh or full seawater (Ern et al. 2014). In the study to check the interactive effects of salinity on metabolic rate of milkfish, it was found out that, at the salinity of 35, the routine metabolism rate of milkfish was at 171.7 ± 10.3 mgO_2/kg-hr (Swanson 1998).

Using the stoichiometry of fish respiration, the total amount of particulate organic matter can be calculated using the following equation:

$$\mathrm{OM}_{\mathrm{feces}} = \mathrm{OM}_{\mathrm{feed}} - \mathrm{OM}_{\mathrm{growth}} - \mathrm{OM}_{\mathrm{respired}} - \mathrm{OM}_{\mathrm{soluble\ waste(excreted)}} - \mathrm{OM}_{\mathrm{waste\ feed}} \quad \textit{(7)}$$

Similarly, if the apparent that just stability coefficient for organic matter is available, the carbon balance will greatly be dependent on the amount of carbon found on the feces. However, in this study, the apparent digestibility coefficient of the commercial feed with milkfish is not available.

2.2.2 Nitrogen waste

One of the major water quality problems in intensive aquaculture systems is the accumulation of toxic inorganic nitrogenous species like ammonia and nitrite in the water (Colt and Armstrong 1981). Aquatic animals, such as fish and shrimp, typically needs protein-rich feed for cell development, because their energy production pathways depend on the oxidation and catabolism of proteins (Czamanski et al. 2011). In marine environment, degradation of ammonia is solely dependent on the bacterial activity that is present in the surface water and underlying seabed, and the nitrates available in the sediment. Since nitrogen is the limiting nutrient in many marine environments, the input of ammonium might lead to increased primary production and changes in the plankton community. Such effects are usually not observed at the fish farm itself but increase nutrient loading from fish farming may cause such effects on a regional scale (Avnimelech 1999; Islam 2005). Pelagic effects are highly dependent on hydrographic and nutrient status in the farming area (Huiwen and Yinglan 2007).

To estimate the quantity of nitrogen waste loading of the culture system, fish nitrogen digestibility and excretion needs to be established. The resulting estimation can then be used to predict waste assimilation and eutrophication of the culture system. Nitrogen loss can be decreased through optimization of the protein: energy ratio and balancing of amino acid content in fish diets (Wu 1995). At present, many commercial feeds are available for intensive culture which are based on nutritional requirements of milkfish (Bergheim and Asgard 1996; Lim, Borlongan, and Pascual 2002). The effects of these feeds on water quality in brackish water ponds were initially investigated, however its effects on marine cage culture were not. In addition, there is limited information of specific sources and the amount of waste generated from milkfish digestion and excretion.

The utilization of nitrogen is dependent on diet quality and size of fish. In one study, the total nutrient wastage from faeces and excretion ranged from 55.1% to 71.5% of the total nitrogen consumed. The biological value of nitrogen may vary depending on the source of dietary protein or ingredients. Most commercial feeds for milkfish aquaculture have fish meal as the main ingredient

and it is moderately digestible in milkfish with digestibility values ranging from 50% to 90%. Compared to the growth of milkfish in wild, cultured milk fish had a faster growth rate since animal sources are known to be more digestible than plant sources. Considering that in the wild milkfish has only plant diet.

According to one study (Sumagaysay-Chavoso 2003), small milkfish was observed to excrete more nitrogen relative to their body size then larger fish. The is because small fish have higher weight - specific metabolic rates than adults Moreover, an inverse relationship between food consumption and fish weight may also affect excretion rate. The study also established the relationship of the milkfish body weight in relation to the dissolve inorganic nitrogen excreted by the milkfish (Figure 2.6).

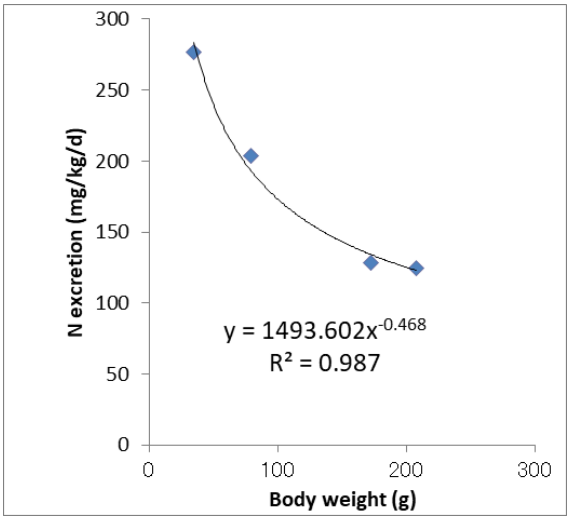

Figure 2.6. Nitrogen excretion rate of milkfish based on average wet body weight.

The derived relationships show that the fish total body weight can be used to estimate the amount of nitrogen excreted by the milkfish with the assumption that the fish was fed in satiation (Sumagaysay-Chavoso 2003). Commercial feed nitrogen was calculated to be 7% ± 0.23 (n=3) of the feed. In addition, the total fish body nitrogen equation was derived with the use of an EA-1108 element analyzer at National Research Institute of Fisheries Science, Japan (Satoshi Watanabe et al. 2014)

$$\text{Total Body N} = \text{ABW x } 0.05824 \text{ x Biomass} \quad \textit{(8)}$$

In this study the relationships derived from theory based on total excreted nitrogen and total body nitrogen of the milkfish is going to be used for the calculations of the particulate nitrogen with the aid of nitrogen box models.

2.3 Waste dispersion model

Almost studies on the environmental impact of marine fish farming were carried out in temperate regions. While there has been a rapid growth in marine fish farming activities in the tropical and sub-tropical countries, virtually nothing is known of the impacts of fish farming activities in those waters. It is important to note that the environmental impact of mariculture in the tropics and sub-tropics may be very different from their temperate counterparts. First, unlike the temperate countries (e.g., Scotland, Norway, and Canada) where pelleted feed is used, trash fish is used in the tropical/sub-tropical fish farms (e.g., Hong Kong, Indonesia, Philippines, Thailand, Japan, and Singapore). The use of trash fish also generates food wastes of much smaller particle size and hence may facilitate a wider dispersion and greater impact upon a much larger area. Second, the higher water temperature regime in the tropics and sub-tropics also allows a higher rate of biological processes in the water, and the plankton dynamics are very different. Furthermore, despite the fact that the environmental impact of marine fish farming would, theoretically, depend upon both the density of fish stock and hydrographic conditions of culture sites, no studies have ever attempted to compare the impact of marine fish farming under different culture and hydrographic conditions (Wu et al. 1994).

With the constant expansion of fish farming, environmental concerns have been raised regarding the fate of aquaculture waste materials such as feed pellets and fecal material. To date, research has focused primarily on the deposition of organic waste immediately under or adjacent to

fish cages and pens, termed the 'near-field'. Increasingly accurate models use the settling characteristics of feed pellets and feces to map the areal extent of the near-field depositional footprint (Chamberlain and Stucchi 2007; Cromey, Nickell, and Black 2002; Pearson and Black 2001)

The effect on model predictions of two important data types (drifter and hydrographic data) and two less important processes (cage movement and waste release time) are explored. Drifter and hydrographic data are a fundamental component of a detailed site study and can be analyzed and implemented into the model in many ways. Timing of feeding and defecation events appear to be an unnecessary detail in most studies, apart from short-term sediment trap validation studies. The main objective of a fish farm drifter study is to provide information on dispersion and circulation patterns so that this can be incorporated into modelling studies of the discharge. Typically, in aquaculture modelling studies, dispersion coefficients are resolved for east-west and north-south axes. Meanwhile, the main objective of using hydrographic data is to provide the least and most dispersive day period to set the mean surface and near-bed speed for the prediction the deposition footprint (Cromey and Black 2005). In the case of hydrographic data, it has small area of deposition compared to using drifter analysis. This difference was caused by the near-seabed speed which falls between the highest and lowest current. In this study, an assumption of the standard deviation of currents will be used to explain the fate of the particulate waste.

2.3.1 Sinking rates of feed and faecal material

Lagrangian (particle tracking) models used in the assessment of aquaculture impact are commonly made up of some or all the following components: grid generation, fish bioenergetics, particle tracking, resuspension, biochemical and benthic faunal response. Given wastage rates of fish food and faeces from a bioenergetics model, hydrodynamic data and settling velocity of wastes, initial deposition of particles on the sea bed can be predicted with a particle tracking component (Cromey and Black 2005; Panchang, Cheng, and Newell 2006). Aquaculture wastes comprise both particulate

material (mainly uneaten food and fish faeces) and soluble material consisting principally of carbon, nitrogen, and phosphorus compounds. Fish faeces, along with uneaten food, is an important component of solid wastes that can cause increased sediment deposition and nutrient enrichment of the receiving waters (Chen, Beveridge, and Telfer 1999).

All particle dispersion models require that the solid wastes (waste feed and faeces) be characterized by their settling rates and mass fraction to calculate their horizontal displacement and sedimentation rates. In salmon aquaculture modelling studies, the mass fraction was determined through experiment and estimation and was estimated in Table 2-2. Several investigators have undertaken laboratory experiments to determine the sinking rates of feed pellets (Stucchi et al. 2005). The sinking rate will depend on the size and composition of the feed pellet as well as the pelleting conditions used in its production. In this study, the feed sinking rate was assumed at 10 cm/s.

Table 2-2. Salmon feacal material mass fraction at different settling rates.

Fraction	Sinking rate ($cm\ s^{-1}$)	Mass fraction (%)
1	4	15
2	3	70
3	2	15

The determination of the sinking rate for faecal material is not as straight-forward as for feed pellets. Faecal material is often not in the form of a well- defined pellet or solid mass but rather exists as a gelatinous mass that may disintegrate. Thus, careful methodology of collecting and handling faecal material are important factors to consider, specially that the faecal material from fish can disperse easily. In one laboratory study for determination of sinking rates of fecal material, it was found out that it is normally distributed (Cromey et al. 2002). In addition it was also determined that the mean sinking rate of 5.3 cm/s was observed with range from 4-6 cm/s in salmon (Chen et al. 1999). Further, another study observed a similar sinking rate and found that 70% of the observations fell within 2-4 cm/s range. These setting rates were all found in salmonid species which can be similarly

used for milkfish. Given the range of settling rates, to have a good estimate, a partition of the amounts that undergo a certain settling rate is necessary.

2.3.2 Diffusion and particle dispersion

The dispersion of the solid waste from the fish farm is approach from statistical perspective. Simply stated, the statistics of the circulation are assumed to determine the distribution of the solid waste on the bottom. The important hydrodynamic variable is the depth average horizontal current. Flat bottom or constant depth is assumed throughout the model domain. In one dimensional problem of calculating the distribution of particles on the bottom from a point source of identical particles, the particles were assumed to fall at constant vertical distance to the bottom. It was also assumed that the depth average velocity had a normal or gaussian distribution. The probability density function $f(x)$ that describes the distribution of the particles on the bottom is then completely determined by the statistics (the mean v_u and standard deviation σ_u) of the depth-averaged velocity field.

$$f(x) = \frac{1}{\sigma_x\sqrt{2\pi}}\, e^{-1/2\left(\frac{x-v_x}{\sigma_x}\right)^2} \qquad (9)$$

$$v_x = \left(\frac{h}{u}\right) v_u \qquad \sigma_x = \left(\frac{h}{u}\right) \sigma_u \qquad (10)$$

where:

v_u = average velocity
σ_u = standard deviation velocity
v_x = depth average velocity
σ_x = depth average standard deviation
h = distance from cage bottom to sea bottom
u = sinking rate

For the two-dimensional problem, we assumed that the velocity field was rep- resented by a bivariate normal distribution and that the velocity components u and w could be rotated so that they were uncorrelated. The probability density function for the distribution of the particles on the bottom is accordingly given by the equation:

$$f(x,y) = \frac{1}{\sigma_x\sqrt{2\pi}}\, e^{-1/2\left(\frac{x-v_x}{\sigma_x}\right)^2} \cdot \frac{1}{\sigma_y\sqrt{2\pi}}\, e^{-1/2\left(\frac{y-v_y}{\sigma_y}\right)^2} \qquad \textit{(11)}$$

$$v_x = \left(\frac{h}{u}\right) v_u \quad \sigma_x = \left(\frac{h}{u}\right)\sigma_u$$
$$v_y = \left(\frac{h}{u}\right) v_w \quad \sigma_y = \left(\frac{h}{u}\right)\sigma_w \qquad \textit{(12)}$$

A fish cage is not a point source but rather an area source (Cromey et al. 2002; Panchang et al. 2006; Stucchi et al. 2005). Integration of the two-dimensional equation over the area of the bottom of the net pen transforms the point source into an area source. These equations are applied to each size fraction of the solid waste characterized by its own sinking rate. Each waste fraction falling through the bottom of the net pens is then distributed on the ocean bottom using statistics.

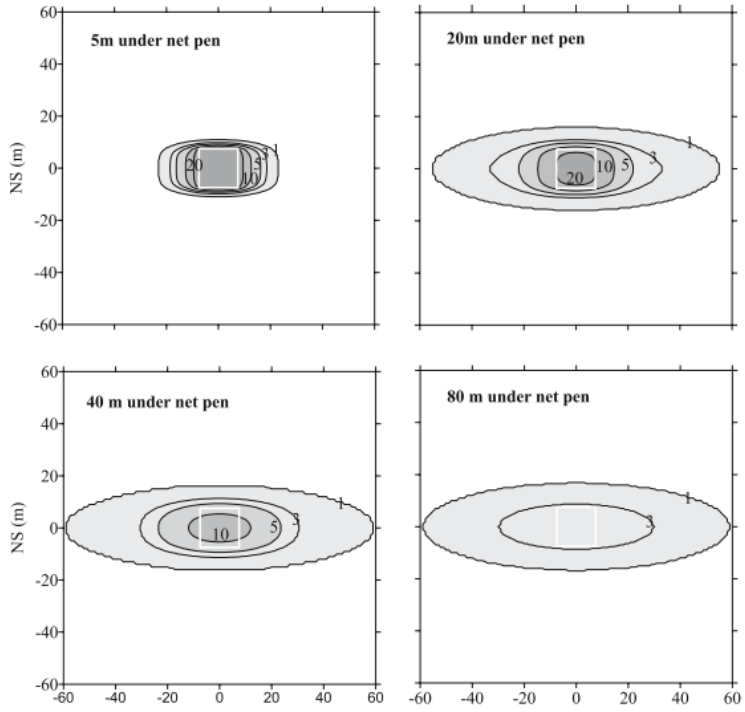

Figure 2.7. Organic matter dispersion in salmon cages at variable depths.

The simulations for the single net pen were run at four different depths (5 m, 20 m, 40 m, and 80 m) from the bottom of the net pens to the ocean bottom with a calculated carbon flux of 72 g/m^2-

day. There were several features of the computed footprints that were noted to be common to all the simulations. First, the shape of the footprint was determined by the relative sizes of the standard deviations of the two velocity components. For these simulations, the standard deviation in the EW direction was four times larger than in the north/south (NS) direction. Consequently, the footprint was observed to be elongated in the EW direction relative to the NS direction (Fig. 2-7). Second, in all the simulations, the maximum depositional flux was found to be directly under the net pen. Although not shown because the current means in the EW and NS direction were set to zero, the effect of a mean flow would have shifted the footprints in the direction of the mean flow. Third, most of the wastes fell within a short distance (< 60 m) from the net pen (Stucchi et al. 2005).

Changing the depth under the net pens while maintaining the same current characteristics and feed inputs was found to alter the footprint in two different ways. First, the maximum depositional flux, which was directly under the center of the net pen, decreased as the depth under the net increased (Fig. 2). For depths of 20 mand 80 m under the net pens, the maximum depositional fluxes of organic matter were calculated to be 27 and 5 g/ m^2-day, respectively. Second, the area of the depositional field increased as the depth under the net pen increased and this is evident from the area of the 1 g/m^2-day contour given in Fig. 2. However, the area within a given contour of organic matter flux did not increase for all depths under the net pen. For example, the area bounded by the 10 g/m^2-day contour was larger for 20m under the net pen than for 5 m and 40 m under the net pen and was zero (not present) for the simulation with 80m under the net pens.

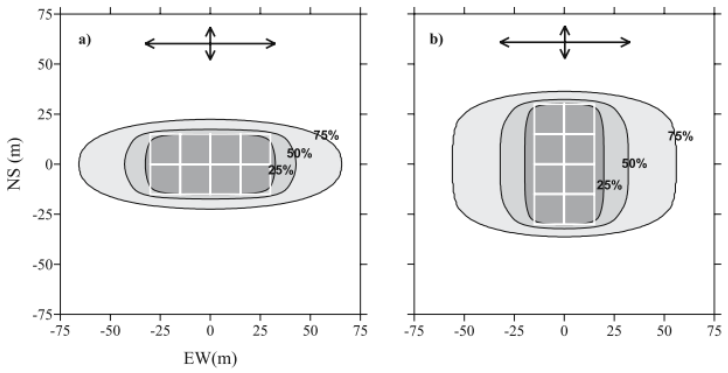

Figure 2.8. Organic matter dispersion of multiple cages at east-west and north-south orientation.

With the same current statistics, instead of a single 15 m × 15 m by 20 m deep net pen, eight pens of a similar size configured in a two by four linear grouping (Figure 2-8). The first one was with the net pen group aligned in the EW direction or parallel to the main direction of the flow. The second was with the group aligned in a NS direction or perpendicular to the main direction of flow (Fig. 2.8). The differences in the depositional field were found to be significant. First, the peak fluxes of organic matter were larger for the farm configuration having net pen groups aligned with, as opposed to perpendicular to, the dominant EW current axis (57 vs. 45 g/m^2-day, respectively). Second, the wastes were dispersed over a larger area when the net pen grouping was oriented perpendicular to the main direction of the flow. For example, the area of the depositional field containing 50% of the wastes was approximately 40% larger for the orientation perpendicular to the flow than for the parallel orientation (Stucchi et al. 2005).

Another method of determining the dispersion coefficient, is through the use of drifter technology. Most of its application has been in the global ocean and shelf seas. In early studies, the methods employed are as easy as studying the release of objects, and later compared to aerial photography and GPS. The spatial and temporal information provided by these studies varies considerably, and the most appropriate method will depend on the environment and the scale of the process being studied. For oceanic applications where the study area is potentially massive, the frequency and accuracy of the positional information can be reduced so that a long survey period is achieved. While the use of drifter technology in the coastal environment has been mainly used for assessment of domestic sewage or industrial discharges with studies around aquaculture operations not so common in the literature. The use of the drifter method typically involves GPS (Cromey and Black 2005).

The main objective of a fish farm drifter study is to provide information on dispersion and circulation patterns so that this can be incorporated into modelling studies of the discharge. The

variance of positional data (x, y) at time t for N drifters is (Okubo, Ebbesmeyer, and Sanderson 1983; Yanagi, Murashita, and Higuchi 1982):

$$\sigma_x^2 \equiv \frac{1}{N-1}\sum_{i=1}^{N}[x_i(t)-\overline{x}(t)]^2 \quad \sigma_y^2 \equiv \frac{1}{N-1}\sum_{i=1}^{N}[y_i(t)-\overline{y}(t)]^2 \tag{13}$$

$$\sigma_{xy}^2 \equiv \frac{1}{N-1}\sum_{i=1}^{N}[x_i(t)-\overline{x}(t)][y_i(t)-\overline{y}(t)] \tag{14}$$

Dispersion coefficients (k_x and k_y) are then calculated as:

$$k_x(t) = \frac{1}{2}\frac{\partial\sigma_x^2}{\partial t}, \quad k_y(t) = \frac{1}{2}\frac{\partial\sigma_y^2}{\partial t} \tag{15}$$

In aquaculture modelling studies, dispersion coefficients are resolved for east-west and north-south axes. As a result, k_x is representative of dispersion along the east-west axis and k_y representative of the north- south axis. Although convenient to resolve in this manner, more accurate representation of the data may be obtained if the dispersion coefficients are resolved according to major and minor axes of flow.

Table 2-3. Results of the diffusivity coefficient (k) and the calculated fluxes from Scotland and Eastern Mediterranean salmon cages.

Environment	Scotland			Eastern Mediterranean	
Species	Salmon	Salmon	Salmon	Sea bream	Sea bream
Source of k data	Measured	Measured	Theoretical	Measured	Measured
Major – k_ζ (m^2s^{-1})	0.108	0.386	0.1	0.108	0.446
Minor – k_η (m^2s^{-1})	0.278	0.001	0.1	0.353	0.015
Major axis (°)	0	58	0	0	118
	Predicted vertical flux at sea bed[a] ($g\,m^{-2}\,yr^{-1}$)				
0 m	9381	10 855	10 396	8048	9806
5 m	–	–	–	5591	7412
10 m	–	–	–	4168	5539
25 m	6572	8126	6848	1305	1829
50 m	2240	3009	2294	326	469
100 m	733	934	655	–	–

[a] An increase in flux at stations between scenarios is associated with a reduction in the mean flux directly underneath the cages so that mass balance is preserved.

In Table 2-3, dispersion coefficients were resolved for east-west (x) and north-south (y) axes respectively using site-specific data for a North Atlantic salmon site (k_x = 0.278 m^2/s, k_y = 0.108 m^2/s). Table 1 also shows the difference between data resolved for North Atlantic and Mediterranean sites and the effect on predicted flux at varying distances from the cages.

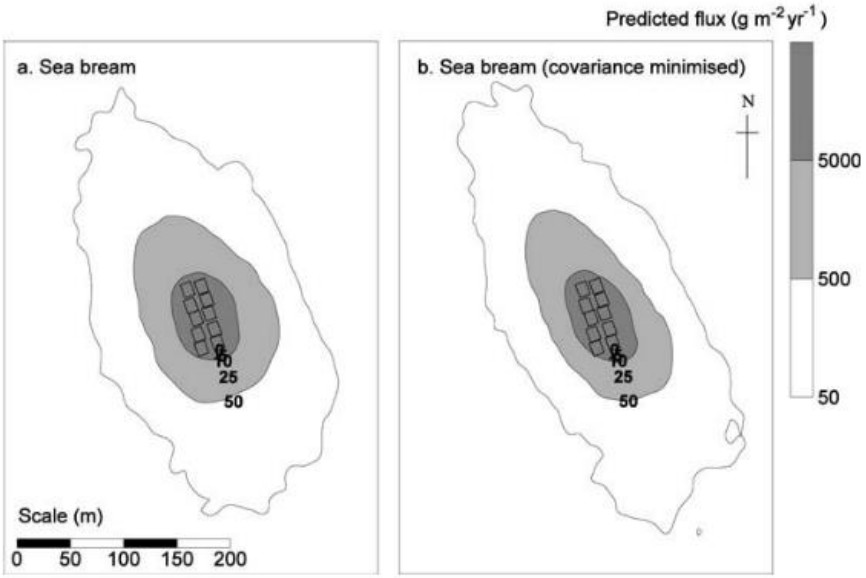

Figure 2.9. Predicted flux from sea bream aquaculture site with minimization of covariance through depth average current velocities and direction.

Figure 2.9 is showing the Mediterranean example that demonstrates the difference in deposition footprint shape. Model predictions of discharges containing fine, slow settling sea bream faecal material will be influenced the most by this effect due to the long period in which particles are being subject to random walk processes. Correlations between the current velocity component and *k* resolved for the major axis may well exist, as well as correlations between the major axis and the residual current direction.

Moreover, in one the study (Okubo 1971), using dye diffusion methods, the author defined the criteria for diffusion experiments suitability which are: (1) The release of dye should be as close to a type of instantaneous point source as possible. The duration of release and the initial size of dye patch must be reported. At least the initial size must be estimated somehow to an order of magnitude.

For a known initial size or more precisely a known initial variance, a critical time after which the diffusion is regarded practically as from a point source can be estimated from a theoretical relationship for the rate of change of variance.

$$\sigma_0^2 = 6\,P^2 t_0^2 \qquad \textit{(16)}$$

where σ^2_0 is the variance associated with the initial distribution of patch; P is a diffusion velocity being taken 1 cm/sec as a representative value, and t_0 is a characteristic time of diffusion during which a patch from a point source grows into the size. (2) The dye patch should maintain a sufficient distance from vertical boundaries so that the field of diffusion is regarded as extending to infinity in the horizontal direction. (3) The horizontal distribution of dye concentration should be observed in such a manner that the variance can be computed directly from the distribution. Figure 2.10 shows the estimated diffusion in different study location.

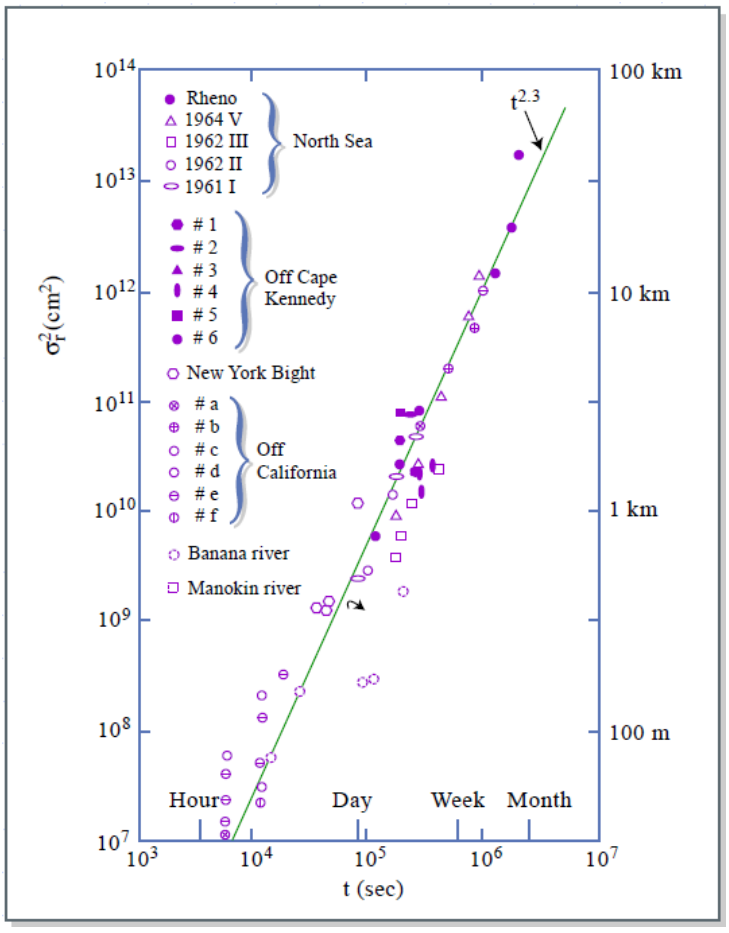

Figure 2.10. Estimated values of diffusion in different study areas and the variances versus diffusion time

However, the study of (Okubo 1971), was meant to analyze the solvent diffusivity coefficient which is not parallel to the particle diffusion wherein depth can influence the behavior of diffusion. However, for future considerations of dissolved wastes diffusion, this concept can be relevant to particle dispersion.

In order to quantify the growth of a cloud in a turbulent flow (Richardson 1926), introduced the distance–neighbour function $q(r,t)$, which is defined as the probability density function at time t for the separation r between two fluid particles chosen randomly from a puff released (or marked) at time $t = 0$. The puff can be described by continuous concentration field $c(x,t)$, which we may normalize so that $\int c(x,t)d^3x = 1$, and we derive the following equation:

$$q(\boldsymbol{r}) = \int \langle c(\boldsymbol{x})c(\boldsymbol{x}+\boldsymbol{r})\rangle \, \mathrm{d}^3\boldsymbol{x}, \tag{17}$$

Assuming homogeneity, isotropy and stationarity, Richardson proposed a simple first-order closure for q:

$$\frac{\partial q(r,t)}{\partial t} = \frac{1}{r^2}\frac{\partial}{\partial r} r^2 K \frac{\partial}{\partial r} q(r,t), \tag{18}$$

where $K = K(r, t)$ is a diffusivity, and $r = |\mathrm{r}|$ is the absolute value of the separation vector r. Richardson used a one-dimensional equation, but that does not change results qualitatively. Richardson argued further that K is proportional to $r^{4/3}$ (Ott and Mann 2000). This model was found to be similar with probability function mentioned earlier in this chapter. Diffusion modelling through the use of Richardson's proposed equations were widely used in many studies, and the 4/3 dispersion rule was further developed. Under the 4/3 Richardson's Law, $\mathrm{E}(\sigma)$ is a scale dependent diffusion, which means that the larger the area being considered, the higher is the diffusivity coefficient, and it is given by the equation:

$$E_r = \frac{d\sigma_r^2}{4dt} \tag{19}$$

through Richardson's 4/3 Law interpreted as shear dispersion:

$$E \sim \sigma^{4/3} \quad \textit{(20)}$$

In summary, the comparison of the solution for diffusivity coefficient is given by Table 2-4.

Table 2-4. Summary of relationships for the estimation of diffusion from diffrerent theories.

	Fickian	*Okubo*	*Richardson*
σ(t)	$\sigma^2 \sim t$	$\sigma^2 \sim t^{2.34}$	$\sigma^2 \sim t^3$
E(t)	$E \sim$ const	$E \sim t^{2.34}$	$E \sim t^2$
E(σ)	$E \sim$ const	$E \sim \sigma^{1.15}$	$E \sim \sigma^{4/3}$

In this study, the estimation of the diffusivity coefficient of the experiment site was employed using the particle dispersion model through probability density function. The cage in study was set to be an area source and the prevailing water current is a factor to superposition the highest concentration of the particulate waste flux. The main factor to be considered for the dispersion is the standard deviation of the current and was used to estimate the diffusivity coefficient of the site. The distribution of the particulate waste was based only on the spatial concentration of acid volatile sulfides that was taken from the experiment site.

2.4 Organic matter degradation

The degradation of organic material takes place through the primary reactions such as respiration with oxygen, denitrification, respiration with manganese and iron, respiration with sulfate and methanogenesis. Several studies have shown that this organic material deposited on marine sediments can be divided into several pools: (1) rapidly degraded pools (within few weeks or months),

(2) a pool that is degraded significantly more slowly (typically over several years, and (3) a pool that is non-degradable (Fossing et al. 2004).

Most aquaculture system uses of the coastal zone result in increasing release of nutrients. In a culture site where water exchange is often restricted, this leads to nutrient and organic matter enrichment or eutrophication. Progressive stages of enrichment include increased inorganic and organic nutrients, microbial biomass and enzymatic decomposition of substrates, nitrification, denitrification and benthic oxygen and nutrient fluxes. Evidence is also accumulating to show that with increasing eutrophication the ratio of autotrophic to heterotrophic microbial processes is reduced as increasing amounts of organic matter are respired in sediments than in the water column. As organic enrichment of aquatic ecosystems increases, the balance between pelagic and benthic metabolism appears to shift to become dominated by benthic processes (Holmer, Wildish, and Hargrave 2005). In eutrophic temperate regions, nutrient-rich areas however, heterotrophy predominates based largely on stored organic matter in sediments, which may be reflected seasonally, unlike in tropical regions. When finfish and shellfish aquaculture facilities are located in coastal areas that receive other sources of organic waste, soluble and particle matter products released because of aquaculture operations are added to what may be an already high supply of organic matter.

Although no single method exists for differentiating sources of organic matter, stable isotope analysis appears to offer a general methodology that might be useful. Stable carbon isotopes were used to determine sediment organic carbon from salmon farm sites was derived from fish pen wastes (Gondwe, Guildford, and Hecky 2012). In an aquaculture system, the differentiation of organic matter input is mainly based on the feed composition, and the particulate waste generated from the culture can be best estimated by carbon and or nitrogen balance. This is largely because substantial amounts of refractory material in sediment add to the organic content but do not affect the composition rates. It is also well known that input of labile organic waste products to sediments increases microbial activity and sulfate reduction rates are particularly sensitive to stimulation through enrichment. As a result, the determination of sulfide levels in the sediments using electrochemical methods is a widely

used monitoring tool for assessing benthic environmental effects (Chang et al. 2014; Holmer et al. 2005; Yokoyama et al. 2006).

The ratio of the flux of undegraded organic matter to total organic matter flux is calculated from the concentration of organic matter at the bottom (20 cm) of the model and the sedimentation rate. Therefore, it is a prerequisite to the calculation that all degradable organic material has been degraded when this depth is reached. The ratio of the flux of readily degradable organic matter to the total organic matter flux was determined from literature values and is presented by the relationship (Fossing et al. 2004):

$$\frac{OM_D}{OM_P} = 0.42 \qquad \textbf{(21)}$$

where:

OM_P = total particulate carbon (gC/m^2-day)
OM_D = degradable particulate carbon (gC/m^2-day)

Aquaculture organic waste are mostly considered as labile wherein the degradation takes place within weeks to months. For this study, this relationship plays an important role in estimating the evolution of organic matter.

2.4.1 Aerobic degradation

Seabed sediment is an important habitat for organisms living in marine environment. Characteristics of the sediment play an important role in determining the population structure, abundance, and distribution of marine organisms. Environmental factors that influenced sediment and water qualities are mainly coming from the activities in the sea and runoff from the coastal areas which gathered the organic matter and eventually washed down to be accumulated on to the sea bottom. On the basis of actual rate measurements of organic matter decomposition, it was proposed that the organic matter itself could be divided into various groups of compounds with different reactivity (Middelburg 1989). Organic matter is decomposed by microbes that require oxygen for

degradation. In certain locations, benthic deposits maybe responsible for around 50% of the total oxygen depletion, apart from the depletion caused by sulfides. This depletion is referred to as sediment oxygen demand (SOD) although many researchers coined it as benthic oxygen demand (BOD); and is given by the stoichiometry:

$$CH_2O + O_2 \rightarrow CO_2 + H_2O \quad \textit{(22)}$$

Sediment oxygen demand is a term that includes oxygen demand from two separate processes: (1) biological respiration of all living organisms in the sediment and (2) the chemical oxidation of reduced substances in the sediment such as divalent iron and manganese and sulfide (Bowman and Delfino 1980).

It is well documented that the dissolved oxygen in the water column is one of the most important factor for maintaining life of cultured organisms (Demirak, Balci, and Tüfekçi 2006; Yokoyama 2003). In organic matter degradation reaction, dissolved oxygen plays an important role into the first step of degradation. The organic matter cycle can be divided into a series of sub cycles that dominate organic matter degradation to varying degrees at different depths within the sediment. For instance, the nitrogen cycle is specially dominating in the upper few millimeters of the sediment below the oxidized zone.

Bottom-water oxygen and nutrient concentrations are of great importance to the chemical processes in the sediment and to nutrient exchange between seabed and bottom water (Sorensen et al. 2001). To mathematically describe the transport and nutrient cycling taking place in the sediment, we perceive the seabed to be composed of different layers. The first layer where organic matter degradation happens is called the diffusive boundedly layer. This layer differs from the rest of the water column in that transport of solutes takes place mainly by molecular diffusion. In many sediment modeling studies this layer can range from 0.1 - 0.5 mm (Fossing et al. 2004). The substance transfer between the water column and the sediment is assumed controlled by three mechanisms: (1) Diffusion of dissolved substance through the hydraulic laminar film at the sediment surface. (2) Net

deposition of solids from the water column to the sediment surface constant in time. (3) Diffusion of dissolved substance within the sediment pores. In a natural system continuous deposition of solids will take place on the sediment surface. These solids will adsorb substance in the water and thus participate in the transfer of substance from the water column into the sediment (Sorensen et al. 2001). The diffusion transport flux of dissolved substance through the laminar layer to the sediment surface is given by the equation:

$$Flux_{diff} = -D \frac{\partial C_{diss}}{\partial x} \quad \textbf{(23)}$$

where $Flux_{diff}$ is the substance flux (Mass/m2-s), C_{diss} is the dissolved substance concentration, D is the diffusion coefficient (m^2/s), and x is the distance. This equation is used in the following analysis in order to investigate the influence on the substance transfer due to both diffusion and the deposition of solids on the sediment surface. Similarly, the oxygen flux can be calculated through with the assumption that oxygen concentration is very small or almost negligible at the lower boundary of the diffusive layer:

$$Flux_{O_2} = D_{O_2} \frac{C_{O_2}}{\delta} \quad \textbf{(24)}$$

where:

$Flux_{O2}$ = sediment oxygen demand (g O_2/ m^2-day)
D_{O2} = oxygen diffusion coefficient (m^2-day)
C_{O2} = dissolved oxygen concentration (g/m^3)
δ = thickness of diffusive boundary layer (m)

Values of D, or rather, temperature-dependent values of D, can be found in the literature for all solutes, and apparently vary considerably within each separate material. Thus, temperature significantly influences the amount of oxygen that is transported into the sediment and is presented through the empirical equation (Fossing et al. 2004):

$$D_{O_2} = (11.7 + 0.344T + 0.00505T^2) \times 10^{-6}\ cm^2 s^{-1\ *\ 2} \quad \textit{(25)}$$

Where T is the temperature in degrees centigrade. In addition, based on the model developed for Aarhus Bay sediment and nutrient flux, to estimate the amount of oxygen flux on the sediment surface, the diffusive boundary layer was assumed at 0.3 mm where the width of the part of the oxygen profile exhibiting a linear decline in oxygen concentration. This was a result of the study made for measuring dissolved oxygen concentration using microelectrodes with a depth resolution of 100 µm. As mentioned in the earlier part of this chapter, this value of the DBL thickness agrees with the estimated values for most studies.

2.4.2 Sulfate degradation

Fish farming serves as a source of sediment organic enrichment and if oxygen is deficient, the decomposition proceeds without oxygen, and with the presence of sulfates hydrogen sulfide (H_2S) is produced. (Wongsin et al. 2015). A major portion of organic matter in oxygen deprived aquatic sediments undergoes oxidation processes where microbes utilize sulphate as the electron receptor (Allen, Fu, and Deng 1993; Chaikaew and Sompongchaiyakul 2018; Pawar, Matsuda, and Fujisaki 2002). Hydrogen sulphide is an evil-smelling and highly poisonous waste product and at high concentrations the redox potential of the sediment can reach as low as -200mV (Eh). Through secondary reactions H_2S is removed from the seabed, either by reaction with the oxidized compounds O_2, MnO_2 and FeOOH, or as an iron-sulphide precipitate formed by reaction with Fe^{2+} (Fossing et al. 2004).

In a previous study conducted in Seto Inland Sea, on Yokota and Tashima fish farming sites, a relationship of organic carbon and acid volatile sulfide contents was established (Figure) (Pawar et al. 2002). The organic matter flux to the sediment, which is determined by the amount of farm waste and the hydrographic conditions of the area, is a major factor governing the sediment quality. If the aquaculture practices in an area are similar, variation in the sediment quality should be largely

explained by the variation in the feed input. The study was also carried out to understand the magnitude of the effect of organic carbon input to the fish farm on sediment. Data on feed input were collected and their relationship with the annual as well as seasonal sediment quality (ignition loss, redox potential, and acid volatile sulfide sulfur (AVS-S) content) of the fish farms was analyzed. The role of temperature in describing the seasonal variability of sediment quality was also examined.

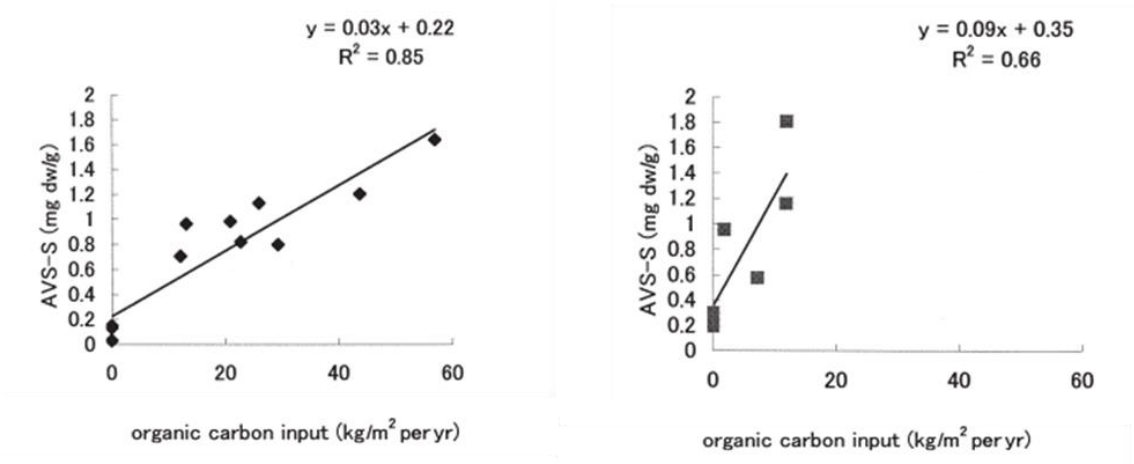

Figure 2.11. AVS concentration in Yokota (left) and Tashima area along Seto Inland Sea.

Figure 2.11 shows that the amount organic matter supplied to the sediment is directly proportional to the evolution of hydrogen sulfide. The degradation of sulfate is given by the following stoichiometry:

$$SO_4^{2-} + 2CHO_2O + 2H^+ \rightarrow H_2S + 2CO_2 + 2H_2O \quad \textbf{(26)}$$

Of all bacterial anaerobic degradation processes in marine sediment, sulfate reduction is the most important and approximately 60% of anaerobic degradation is sulfate reduction (Fossing et al. 2004) . Compared to nitrate, iron and manganese respiration, in most environmental standards, the production of hydrogen sulfide place an important role in determining environmental capacity (Yokoyama 2003; Yokoyama et al. 2010, 2006).

The increase of hydrogen sulfide content corresponded to the depth of the sediment. The higher accumulation was found in the deeper levels. It was also found that the total amount of sulfide accumulation in sediments is proportional to the type, organic composition, and total amount of

organic matter in the sediment, because the total amount of sulfide in sediment is caused by sulfate reduction process. The potential amount of hydrogen sulfide in the sediment can be best described by the distribution of dissolved substances found in the measurable parameter in terms of acid volatile sulfides (AVS). Understanding these substances in AVS is important for understanding the biogeochemistry of sulfidic natural systems (Rickard and Morse 2005). These dissolved substances can be divided into two groups: (1) dissolved iron and sulfur species and their complexes and (2) aqueous iron sulfide clusters, commonly referred to as FeS_{aq}. The clusters bridge the molecular gap between simple complexes, with a well-defined equilibrium stability constant and true condensed phases, which possess a surface. The metastable iron sulfides include the minerals mackinawite (FeS) and greigite (Fe_3S_4).

In one study based on sediment core sampling method, the distribution of AVS-S on cores in the figure generally exhibits the same pattern; activities were lowest in the topmost increment and increased with depth (Figure 2.12). Formation of other end products like CO_2 appeared to be proportional to the formation of AVS and also are expected to increase with depth (Urban et al. 1994). It is safe to say that the sulfate reduction rates may therefore be underestimated if the sulfate transformation are based only on the formation of AVS.

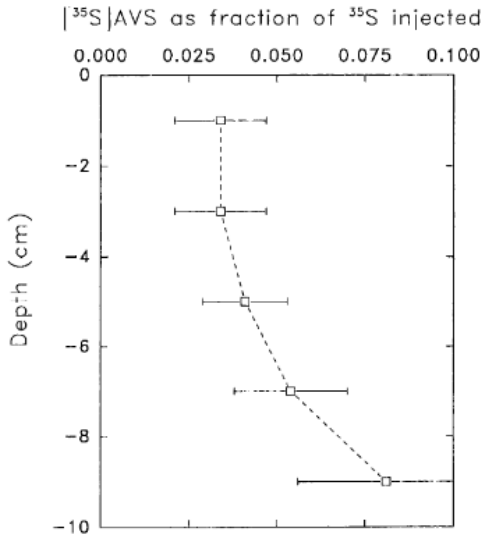

Figure 2.12. Depth profiles of AVS generally showed increasing activities with depth.

Acid-volatile sulfide is defined operationally as the sulfide fraction that is evolved from sediment when treated with concentrated hydrochloric acid or sulfuric acid . It is a complex and variable fraction of sediment represented by a variety of reduced sulfur components, although often dominated by relatively labile Fe and Mn monosulfides. Greater AVS concentrations are associated typically with organic-rich, anoxic deposits and lower levels are found usually in oxic sediments having low organic content (Hammerschmidt and Burton 2010). The most popular method of measuring AVS-S is using Hedorotec-S 330 (GASTEC CORPORATION, Kanagawa, Japan) following the standard method prescribed by the Japan Fisheries Resource Conservation Association (Pawar et al. 2002; Sumbing et al. 2019; S. Watanabe, Sumbing, and Lebata-Ramos 2014). In this method, sediment thickness for AVS-S analysis was determined at 1cm from the surface of the seabed. Though the sedimentation rate for organic matter in intensive fish farming can reach 1cm in a year, the resulting AVS-S concentration at the depth of 1cm can best represent the evolution of hydrogen sulfide as sorbed with Mn and Fe substrates (Holmer et al. 2002; Piedrahita 2000; Roden and Tuttle 1992). It was observed that within 1 cm sediment thickness, the H_2S concentration distribution follows a linear trend (Figure 2.13).

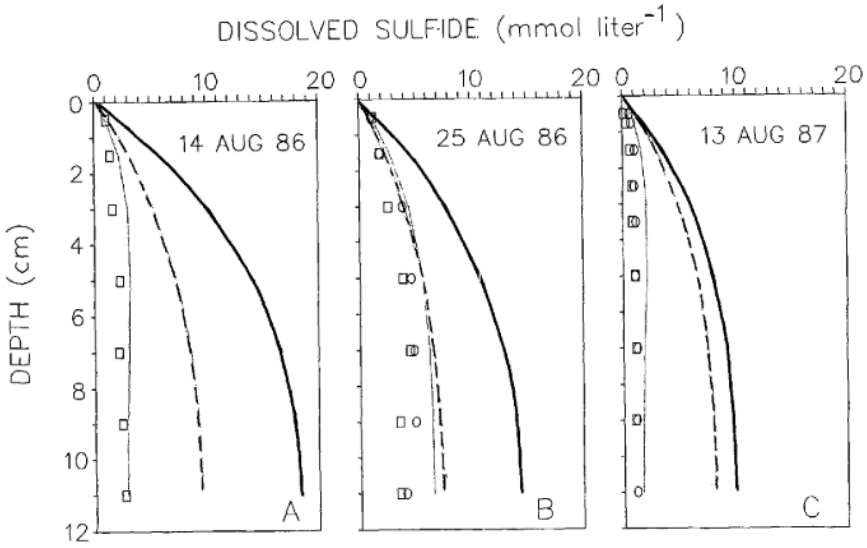

Figure 2.13. Measured (symbols) and modeled profiles of AVS (solid and dashed lines) in Chesapeake Bay.

Based on the diffusion transport flux of substance through the 1 cm layer of the sediment, the relationship of hydrogen sulfide flux and concentration is given by:

$$Flux_{H_2S} = D_{H_2S} \frac{C_{iH_2S} - C_{\delta H_2S}}{\delta} \quad \textit{(27)}$$

where:

$Flux_{H2S}$ = hydrogen sulfide production (g H_2S/ m^2-day)
D_{O2} = hydrogen sulfide diffusion coefficient (m^2-day)
$C_{\delta H2S}$ = hydrogen sulfide concentration at the given thickness (g/m^3)
C_{iH2S} = hydrogen sulfide concentration at the surface (g/m^3)
δ = thickness sediment layer (0.01m)

However, sulfate concentration is negligible on the sediment surface, thus it is assumed that there is no production of hydrogen sulfides, yielding C_{iH2S} = 0. In addition, the diffusion coefficient, like the oxygen, is temperature dependent. Marine sediments may experience temperature changes on both temporal and spatial scales. Seasonal changes in ambient temperature affect processes in the upper sediment layers, while the temperature increase with burial may influence biogeochemical rates in the deep biosphere (Arndt et al. 2013) .The effect of temperature to H_2S diffusivity coefficient was illustrated in Aarhus Bay sediment flux model (Fossing et al. 2004):

$$D_{H_2S} = (8.74 + 0.264T + 0.004T^2) \times 10^{-6}\ cm^2 s^{-1\ *\ 2} \quad \textit{(28)}$$

In this study, only the estimation of the evolved hydrogen sulfide with organic matter reaction will be estimated and not the different species that resulted into the secondary degradation reaction. Though the secondary degradation reaction plays an important role on the hydrogen sulfide production, it is assumed that high percentage of hydrogen sulfide production are the result of sulfate reduction.

2.5 Carrying capacity

Carrying capacity is defined as the maximum biomass of a farmed species that can be supported without violating the maximum acceptable impacts to the farmed stock and its environment (Stigebrandt 2011). The maximum acceptable impacts are expressed through water quality and/or sediment quality where adverse effects to both fish and environment were observed. Significant negative impact may cause low productivity and harvest of the farmed stock, or even worse, mass fish kills. However, these environmental criteria are mainly determined through political processes that may or may not be based on science. The scientific part of the problem to estimate the carrying capacity is to develop reliable, objective methods or models for estimating the response of both the environment and the farmed stock to farming. Using such models together with field observations from a specified locality and the quality standards in force, the carrying capacity for the locality can be estimated. The carrying capacity are site-specific, however the environmental criteria may be generalized in regional and national levels (Silvert 1992). Models must properly deal with hydrodynamic, biogeochemical, and ecological processes in the environment as well as with oxygen consumption and sources and sinks of organic matter and nutrients due to farm activity.

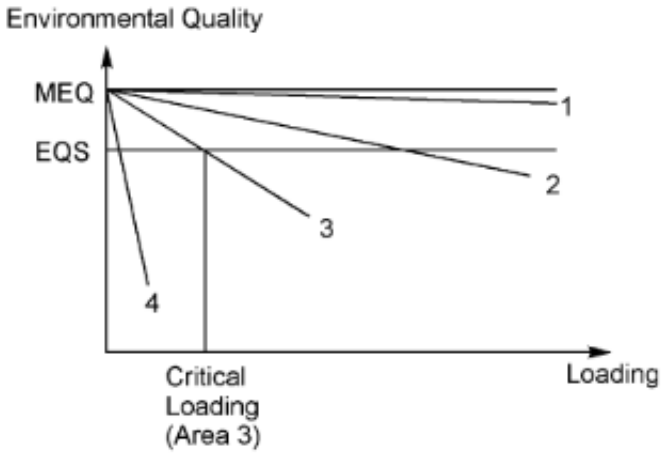

Figure 2.14. Environmenrtal quality as a function for four loading areas with different water exchange (1-4)

Idealized relationships between environmental impact, measured by an environmental quality para meter, and loading are sketched in Figure 2.14 for four areas with different water exchange. Area 1 has high and area 4 has low water exchange. Maximum environmental quality is associated here with the absence of anthropogenic loading. The lowest water quality that can be accepted is specified by one or several EQS. Figure 2.14 shows how the critical loading is defined as the loading that yields environmental quality equal to the EQS. To apply this to aquaculture, one must estimate the relationship between loading and biomass of the farmed species. In practice, there may be contributions to the loading other than those from aquaculture and these must be considered.

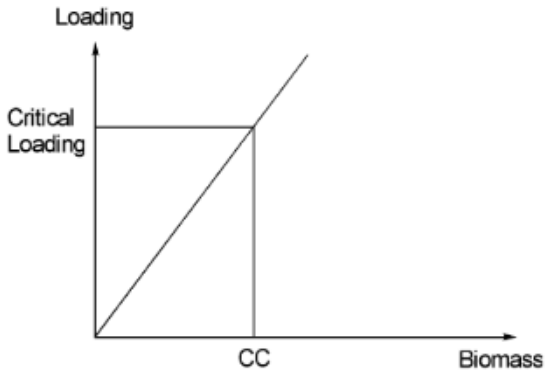

Figure 2.15. Idelaized relationship between critical loading and carrying capacity.

The carrying capacity CC is obtained for the biomass that yields critical loading, Figure 2.15. The loading caused by farming of a certain biomass of a species is in general dependent on the farm configuration, i.e., the cage size and cage separation, feed composition and feeding routines, current conditions in the water column and water depth. To estimate the carrying capacity at a site, we need to find the relationship between the biomass of a farm and environmental impact. We do this in two steps. The first step is to find how a specified loading influences environmental quality (i.e., using a dose-response relationship). The second step is to determine the relationship between loading (i.e., the dose) and biomass in a farm. The relationship between loading and environmental impact can be

estimated using a water quality model. Such a model may be general and need not be developed specifically for aquaculture purposes (Stigebrandt 2011).

The nature of the benthic community at a certain location is dependent on the supplies of feed loading and oxygen. If the feed supply is small and the oxygen concentration high, the benthic community can be expected to have a small biomass density and a high diversity. In areas with a high supply of organic matter, the biomass density may be higher. If the oxygen concentration is low permanently or episodically, the diversity may be low (Pearson and Black 2001). At some limit value of the loading, the benthic infauna disappears, and organic matter will accumulate on the bottom. The limit value will depend on the oxygen supply, which depends mainly on the bottom water current (oxygen exchange), oxygen concentration above the benthic boundary layer and the capacity of the upper sediment layer to absorb oxygen. In addition, the health of the fish farm is mainly dependent on the water quality. This means that the site capacity to supply oxygen and remove waste from the farm is the most important factor. However, sediment and water interaction specially with hydrogen sulfide production should also be considered. The requirement of good water quality should also include good sentiment quality and it should be beast both on the carrying capacity of the aquaculture site.

The common practice is that carrying capacity is determined only when aquaculture was already established in a certain area. This should not be the case, carrying capacity should be predetermined on aquaculture site. Next, when a representative aquaculture system has been established, constant monitoring should be employed to show whether the estimated carrying capacity is factual. Then, through this process the expansion of the aquaculture site can be planned.

Aquaculture impacts occur on several space and time scales, which are classified as internal, local, and regional. Internal impacts are those involving the effects of a particular farm on itself and its immediate environment, generally on a scale of at most a few 100 meters and fluctuations over times measured in minutes or even seconds. One example of an internal impact is the depletion of

oxygen by the fish within the boundaries of the fish farm. This can be caused by plankton bloom where the entire water body can be significantly depressed, but even in well oxygenated sites, it is still possible that the dissolved oxygen concentration can fall below safe levels especially those coastal sites near to river outlets and surface run-offs. The rate of oxygen consumption by the fish is directly proportional to the annual production of the farm. So careful estimation of the fish stocking density should be the primary consideration. Unusual conditions, such as abnormally low currents, especially in estuaries and cove, or pollution and abrupt temperature changes can cause the fish oxygen demand to increase. Deposition of faecal material and unconsumed feed pellets on the seabed are obvious forms of local impact in aquaculture. High depositional rates can cause an accumulation of organic detritus in the sediments which overwhelm the feeding capacity of the benthos and result in the formation of bacterial mats and anoxic conditions. This leads in turn to the anaerobic generation of hydrogen sulfide and methane. These effects are well recognized because they affect both the farms and the environment, with visible changes to the benthos and recognizable changes in wild benthic populations in the vicinity of fish farms. The question of regional impact is critical in areas where there is pressure to expand the number of aquaculture sites. Eutrophication is one example of the regional impact. Such impact leads to the increased frequency of toxic algal blooms. Eutrophication between marine and freshwater systems are most pronounced, and the most important nutrients in marine systems are ammonia and other nitrogenous compounds, although in some cases phosphate can be a factor in marine eutrophication (Silvert 1992). The calculation of eutrophication can be done using internal and local impacts, although it may involve large quantities it should include environmental criteria to prevent such impact.

2.6 Environmental marine criteria

Fish farming causes artificial loading of organic matter and due to its oxidation and degradation, results to the increase of nutrients such as nitrides and phosphates. These compounds

adversely affect the primary production in aquatic ecosystems. The temporary increase in primary production can lead to hypoxia, and with the addition of the particulate waste coming from the aquaculture site, the bottom sediment quality deteriorates. With the eutrophic effect of the artificial load, a criteria should be developed to make fish farming environmentally sustainable as excessive organic loading leads to over-exploitation of the coastal ecosystems (Omori, Hirano, and Takeoka 1994).

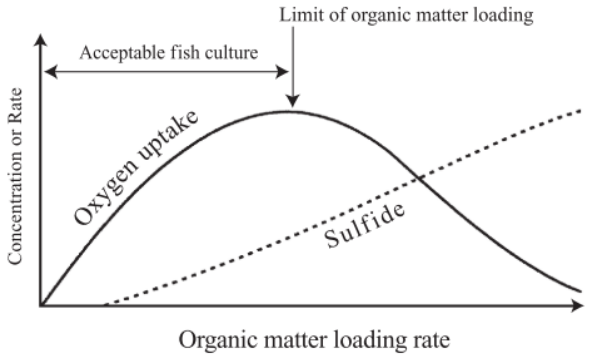

Figure 2.16. Schematic model for determining the limit of organic loading from fish farming. (Yokoyama 2000)

In a model presented by Omori et al. 1994, they determined the limit of organic loading to the bottom sediment using the rate of benthic oxygen uptake (BOU), which was defined as the in situ oxygen consumption by sediments, as an indicator of the activity of the benthic ecosystem. It was observed that a peak of BOU along a gradient of organic loading and took this peak as an indicator of the maximum phase in the process of remineralization (Figure 2.16). Based on this model, a method to determine the assimilative capacity of fish farms by using AVS-S was presented (Takeoka and Omori 1996). The concept was later named the “Omori-Takeoka theory” which was adopted as a criterion for drafting the “Law to Ensure Aquaculture Production”.

In 1999, the “Law to Ensure Aquaculture Production” was stipulated in under the Decree of the Ministry of Aquaculture, Forestry and Fisheries of Japan. As a fundamental guide for putting the Law into practice, the Minister of Agriculture, Forestry and Fisheries produced the ‘‘Basic Guidelines

to Ensure Sustainable Aquaculture Production'', which detailed the matters relevant to the goal of aquacultural improvement. The Law stipulates that fisheries cooperative associations should enact the ''Aquaculture Ground Improvement Program'' to ensure sustainable aquaculture and get approval from the prefectural governor. This system is legally based on voluntary activities of the licensed cooperative associations. The Law also stipulates the mechanism to make the system effective in practice,(i.e., a recommendation made by the prefectural governor). If a cooperative association does not utilize its aquaculture grounds in line with the Basic Guidelines, and the environmental conditions of its aquaculture grounds deteriorate, the prefectural governor may recommend that the cooperative association take measures necessary for improving aquaculture included in the development of the ''Aquaculture Ground Improvement Program''. If the cooperative association does not follow the recommendation, the prefectural governor may make the environmental status public (Yokoyama 2003). To indicate a practical goal for aquacultural improvement, environmental guidelines were established (Table 2-5) (Yokoyama 2000). Moreover, based on these findings, the Minister of Agriculture, Forestry and Fisheries established environmental criteria under the provision of the Basic Guidelines by using only three indicators: dissolved oxygen of the water within fish cages, sulfide content (AVS) of the sediment and macrofauna beneath the fish cages (Table 2-5).

The farm environments are considered in healthy condition when the values of these parameters are under the suggested threshold (Table 2-6). In cases where the limits of these thresholds were surpassed, the Japan Fisheries Agency can plan immediate countermeasures to keep these criteria under acceptable levels. One of the most significant parameters in water quality modelling is dissolved oxygen. Low DO concentrations (<2 mg/L) can cause suffocation of gill-breathing aquatic organisms which leads to massive fish kill. During the fish kill event in 2002, in Bolinao, Philippines, the dissolved oxygen in entire water column of the fish farming site was less than 4 mg/L (San Diego-McGlone et al. 2008). The mass fish kill event was greatly caused by wasted feeds and the decay of algae which consumed oxygen to a very fast rate. Based on the "Law" in Japan, the

critical farms should have a minimum limit of 2.5ml/L (3.6 mg/L) and the DO for the normal growth should be greater than 4.0ml/L (5.7 mg/L).

Table 2-5. Excerpt of environmental criteria from the Law to Ensure Sustainable Aquaculture Production in Japan

Item	Standard Value(content)	Description
Farm water standard		
(1) Dissolved O_2	>6 mg/L	Normal growth of marine species
(2) Dissolved O_2	>5.7 mg/L	Conditions necessary for the sound cultivation of aquaculture; goals for improving aquaculture grounds
(3) Dissolved O_2	<3.6 mg/L	Aquaculture grounds whose condition has deteriorated significantly
Criteria for Bottom layer/sediment environment (Environmental indicators that are easily changed by organic matter load)		
(4) Dissolved O_2 in bottom water	4.3 mg/L	Marks the beginning of pollution; must be maintained at a minimum in the inner bay fishing grounds
(5) Dissolved O_2 in bottom water	<2.9mg/L	Shows a polluted environment
(6) Sediment SOD_5	3.0 mg O_2/g dry	Indicates the beginning of pollution
(7) Sediment SOD_5	>7.0 mg O_2/g dry	Shows a polluted environment
(8) Sediment $SOD_{0\text{-}60\ mins}$	0.3 mg O_2/g dry	Indicates the beginning of pollution
(9) Sediment $SOD_{0\text{-}60\ mins}$	>0.5 mg O_2/g dry	Shows a polluted environment
(10) Sediment COD	20 mg O_2/g dry	Indicates the beginning of pollution
(11) Sediment COD	>30 mg O_2/g dry	Shows a polluted environment
(12) Sediment Sulfide	0.2 mg S/g dry	Marks the beginning of pollution
(13) Sediment Sulfide	>1.0 mg S/g dry	Shows a polluted environment
(14) Sediment Sulfide	>2.5 mg S/g dry	Aquaculture grounds whose condition has deteriorated significantly

Table 2-6. Adopted environmental criteria in the Law to Ensure Sustainable Aquaculture Production

Environmental criteria adopted in the Law to Ensure Sustainable Aquaculture Production

Item	Indicator	Criteria for identifying healthy farms	Criteria for identifying critical farms
Water in cages	Dissolved oxygen	>4.0 ml/l	<2.5 ml/l
Bottom environment	Sulfide (AVS-S)	Less than the value at the point where the benthic oxygen uptake rate is maximum	>2.5 mg/g dry sediment
	Benthos	Occurrence of macrobenthos throughout the year	Azoic conditions for >6 months

In the Philippines, in Table 2-7, the DO criteria for milkfish farms were established at 5.0 mg/L which is almost similar to the environment criteria established in Japan. However, in the Philippine setting, there is no mention on the critical DO level. This leads to some regulation issues that fish farms tend to exploit the coastal area for fish production and latter becomes an irreversible problem and worse the loss of the culture stocks.

As for the sediment quality criteria, in Japan, the "Law" states that the AVS-S concentration should be less than the value at the point where the benthic oxygen uptake rate is maximum. Based on Table 2-5, AVS-S at 0.20 mgS/g dry, marks the start of pollution and at 1.0 mgS/g dry, it signifies polluted sediment. According to a study done by Yokoyama 2003, < 0.20 mgS/g dry is considered as healthy sediments. However, those AVS-S concentrations that falls between 0.2 and 1.0 mgS/g dry are considered as the start of pollution. When AVS-S levels reached 1.0 mgS/g dry, the sediment is considered polluted or in a cautionary level. This means the macrobenthos activity on the sediment, including bacterial degradation rate is lessened due to the hypoxic nature of hydrogen sulfide. Countermeasures need be acted to allow the burial of hydrogen sulfide at the deeper part of the sediment. These countermeasures may include relocation of the fish farm or changes of production management and may greatly depend on the regulations placed by the ruling body, in Japan's case, The Ministry of Agriculture. The "Law" also suggested that farms with AVS-S bottom concentration of 2.5 mgS/g dry are considered critical. In this case the cooperative association should take all necessary measures on improving the aquaculture site. It is not clear with the "Law" of how penalties are sanctions are handed for failure to follow the guidelines, however, the prefectural governor can make this violation public.

For the case of the Philippines, no standard criteria for the bottom sediment were stated. This is alarming since the local impacts of aquaculture was not placed into consideration. Accumulation of organic waste in the bottom sediment causes increased rate of ammonia, carbon dioxide and hydrogen sulfide which increase sediment oxygen demand. In cases when a turbulent bottom current occurs, overturning and resuspension of the sediment would allow these unwanted compounds to

aggressively react with the dissolved oxygen in the water column which would result to a larger case of hypoxia leading to massive fish kills. It also follows that, from local impacts of cage operations, in a large-scale expansion, regional impacts such as eutrophication and habitat destruction are highly possible. This creates an imbalance in marine ecosystem where frequent algal blooms occur.

Table 2-7. Excerpt from the Code of Good Aquaculture Practices for Finfishes in the Philippines.

Parameters	Unit	Freshwater	Coastal and Marine Waters	
		Class C	Class SB	Class SC
Temperature	˚C rise	3	3	3
pH		6.5-8.5	6.0-8.5	6.0-8.5
DO	% sat'n; mg/L	60; 5.0	70; 5.0	70; 5.0
BOD (5-day, 20˚C)	mg/L	7	5	7
Color	pcu	Normal	Normal	Normal
Total Suspended Solids	mg/L (increase)	30 mg/L	30 mg/L	30 mg/L
Oil/Grease	mg/L	2	2	3
Phenols	mg/L	0.02	0.01	-
Total Coliforms	mpn/100 ml	5,000	1,000	5,000
Chloride	mg/L	350	-	-
Copper	mg/L	0.05	0.02	0.05

Legend: Class C – fishery waster for the propagation of growth of fish and other aquatic resources
Class SB – fishery water class I (spawning areas for milkfish and similar species)
Class SC – fishery water class II (commercial and sustenance fishing)

In many studies on macrofaunal population in aquaculture sites, it was found out that the diversity of these organism (presence of multiple species), best indicates how the sediment bottom is polluted. The presence of opportunistic species of polychaete, such as *Capitella capitata*, *Cirratulus cirratus* ,and *Prionospio sp*., that flourish in sediments with high levels of sulfide and low levels of oxygen indicates heavily polluted sediments (Huang et al. 2012). The criteria used in the "Law", however, only specifies that the benthos should be present. A healthy environment is identified in terms of the existence of live macrofauna throughout the year, while a critical environment is identified from the azoic conditions during half a year or more. This criterion has no biological basis

since there are polychaete species that can thrive on high sulfide and low oxygen concentrations and can coexist with sulfide fixing bivalves.

Based on the criteria in Philippine setting (Table 2-7), macrobenthos population in aquaculture areas was not considered and yet to be investigated. Since there are no conditions on the existing status of the bottom sediment, it is difficult to determine if the fish farms on active aquaculture sites in the country are in cautionary or critical levels. Without basis of sediment relationships and fish farming management, it is imperative that a model needs to be constructed.

Chapter 3 - METHODOLOGY

3.1 Brief overview

The methods used for the elucidation and simulation of the marine milkfish cage culture from generation to accumulation and degradation are divided in four parts: (1) analysis of milkfish physical parameters to derive a general growth model, (2) estimation of particulate waste with the aid of material balances equations, (3) approximation of the extent of dispersion of particulate waste through statistical analysis and (4) calculation of acid volatile sulfide concentration through aerobic and anaerobic sediment degradation reactions.

Several experiment growth trials were used to generate a general growth curve which is used for the simulation. The population density growth equation (logistics growth equation) was used and later generalized. The parameters used for fitting the growth curve are average wet body weight (ABW) and duration of culture (DC). Moreover, the temperature and fish cage density were then used as additional parameters to propose a growth curve. For waste estimation, the daily growth of milkfish was interpolated in between sampling schedules. Using the daily growth of milkfish and the daily feed ration, material balance (carbon and nitrogen) was employed to calculate the amount of particulate waste generated daily. The summation of the organic matter based on the carbon balance was then converted to carbon flux using the duration and cage dimensions. The calculation of the distribution of the carbon flux was carried out using the probability density function with depth average water current data. The evolution of carbon flux to acid volatile sulfide (AVS) concentration was calculated using the sediment reactions for oxygen and sulfate degradation. Majority of the constants and equations for the sediment degradations were based on the model set-up for an oxygen and nutrient flux model for Aarhus Bay (Denmark).

The simulation of the marine milkfish cage culture used the proposed generalized growth curve, the carbon balance mechanisms, the diffusivity coefficient based on probability density function, and the equations for sediment degradation taken from theory.

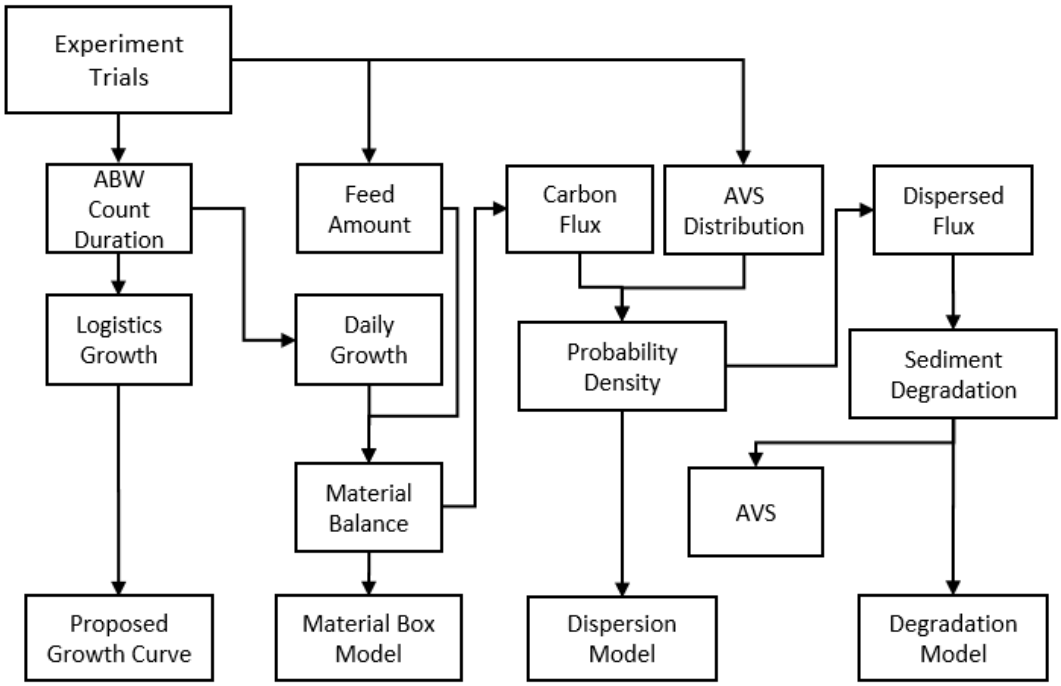

Figure 3.1. Schematic flowchat of the methods used for model-setup generation

3.2 Site and sampling methods

3.2.1 Experiment site

The cage culture experiment was performed in Southeast Asian Fisheries Development Center Aquaculture Department (SEAFDEC-AQD), Igang Marine Sub-Station, Nueva Valencia, Guimaras, Philippines. The site is located along the mouth of the Iloilo Straits which is known to have a strong current that behaves like a funnel for the incoming current from the south-west of Panay Island. The station is composed of four islets and clusters of fish cages for breeding and production experiments. The station also maintains hundreds of brood stocks of various commercially important species. Around the vicinity of the station, bamboo fish traps are commonly found, which are used by local fishermen to catch wild fish for their livelihood. The site is also protected by small islands at the mouth of the cove and surrounded by coral reefs and is suitable for marine pollution cage experiments since it is not greatly affected by river surges and surface run-offs.

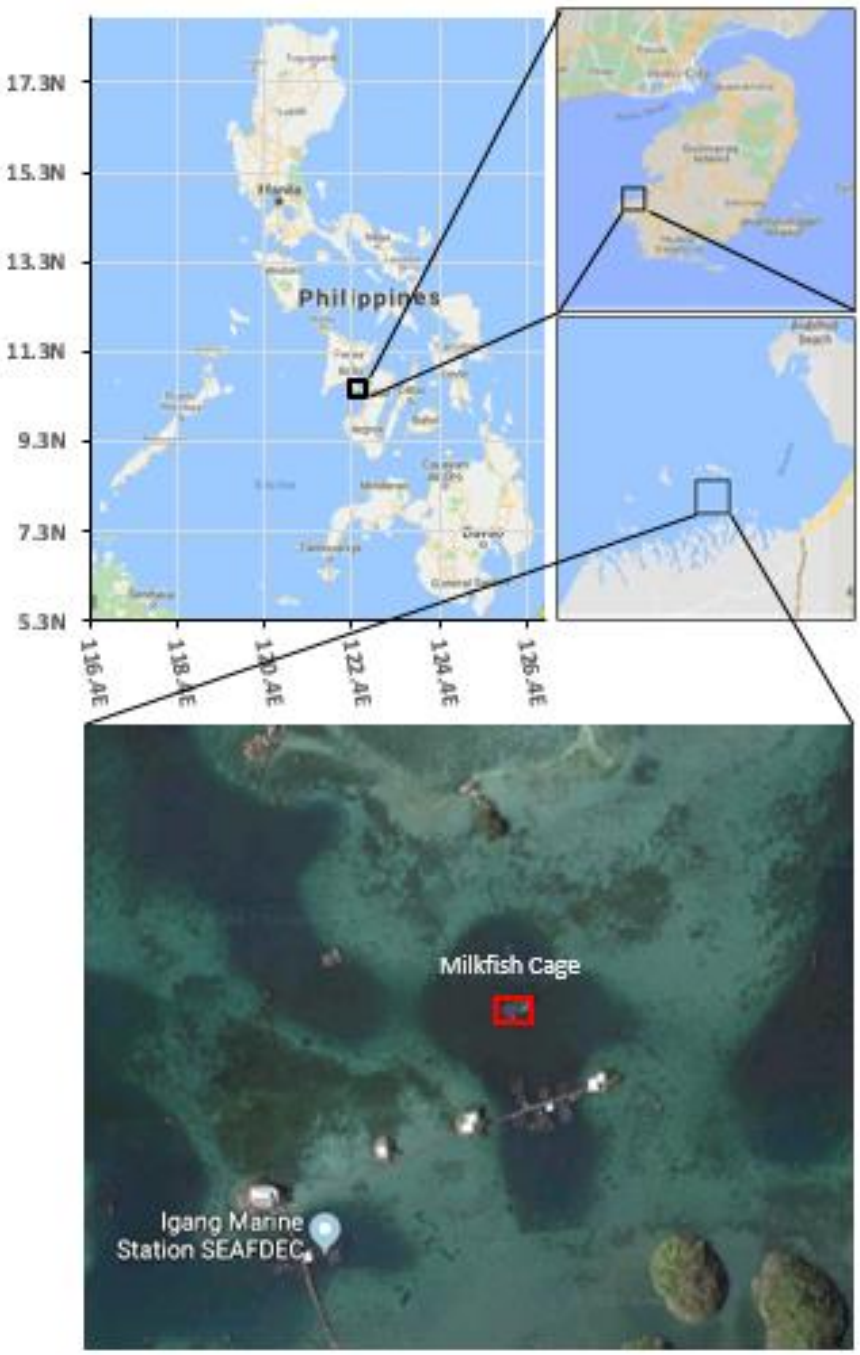

Figure 3.2. Location of the the experiment site in Igang, Nueva Valencia, Guimaras, Philippines.

The average depth of the cage experiment site is between 12-15m (Figure 3.3). The cage was detached from the clusters of cages to prevent contamination from other fish cages. The cage site was also selected because of good water exchange compared to the cages situated between the islets and, bamboo traps for local fisheries were not installed near the experiment area. The north side of cage

shows an island that served as a protection from big waves. It also served as an obstacle which routes the current on the east-west direction to the cage resulting to the prevailing current in east-west direction. Since the average depth around the experiment area is between 1-3m, it expected that most of the particulate waste coming from the milkfish cage, settles just below it.

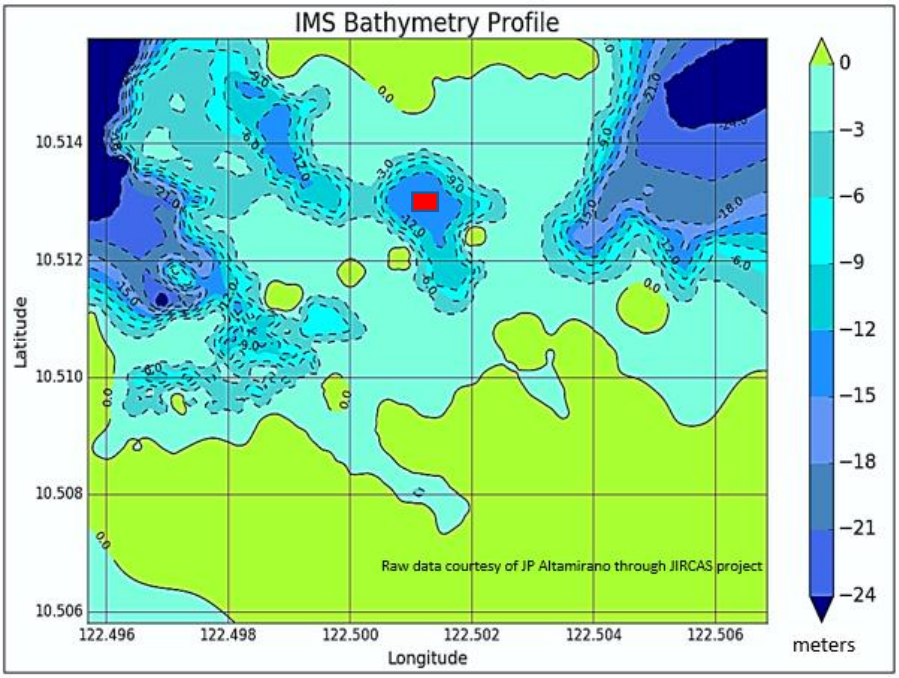

Figure 3.3. Bathymetry contour map of the experriment site (cage location red marked)

3.2.2 Trials and sampling methods

Four experiment trials were performed with fish density and cage dimension variations (Table 3-1). The number of fish stock and initial average body weight (ABW) was predetermined by the availability of juveniles' supply. Trials 1 and 2, were done during the coldest months of the year while Trials 3 and 4, were done during the hottest months. Moreover, the initial stocking weight of the milkfish from Trials 1-2 was lower compared to the Trials 3-4. While the temperature was taken from the average temperature for the whole experiment duration through the data from the chlorophyll logger that was installed midway from the water surface to the seabed. As for the Trials 3 and 4, the orientation of the 6 cages was set at 3 cages east-west direction and 2 cages north-south direction.

Table 3-1. Experiment trials with physical parameters and duration.

Trials	Start	End	No. of fish (pcs)	Cage Dimension	Initial ABW(g)	Final ABW (g)	Average Temperature ˚C	Duration (days)
T1	21-Nov-2011	28-May-2012	3,674	1 × (5 × 5 × 4m)	33.91	299.17	28.24	189
T2	20-Aug-2012	14-Feb-2013	3,780	1 × (5 × 5 × 4m)	19.45	342.28	28.70	178
T3	29-Apr-2015	21-Jul-2015	17,039	6 × (5 × 5 × 4m)	61.05	390.94	29.83	83
T4	24-Apr-2018	17-Jul-2018	7,038	6 × (5 × 5 × 4m)	50.82	413.97	29.61	84

Approximately, every 28 days, measurements of the 10% of the total number of fishes was done to the closest graduation of 1 gram and reported as average body weight (ABW). Table 3-2 to 3-5 shows the result of the ABW per trial. Based on the growth data of the experiments, Trial 1 has the longest culture duration while having the lowest ABW on the harvest date (terminal sampling). On the other hand, Trial 4 showed the highest growth with shorter duration of culture. These data were used for the derivation of the proposed generalized growth curve for milkfish culture.

Table 3-2. Experiment Trial 1 average wet body weight data.

Trial 1	21-Nov-11	12-Dec-11	10-Jan-12	6-Feb-12	5-Mar-12	2-Apr-12	30-Apr-12	28-May-12
Duration (days)	0	21	50	77	105	133	161	189
ABW (g)	33.91	41.71	65.04	101.60	136.00	203.72	266.54	299.17

Table 3-3. Experiment Trial 2 average wet body weight data.

Trial 2	20-Aug-12	20-Sep-12	22-Oct-12	20-Nov-12	15-Dec-12	15-Jan-13	14-Feb-13
Duration (days)	0	31	63	92	117	148	178
ABW (g)	19.45	50.76	97.01	159.47	222.06	291.64	342.28

Table 3-4. Experiment Trial 3 average wet body weight data.

Trial 3	29-Apr-15	27-May-15	23-Jun-15	21-Jul-15
Duration (days)	0	28	55	83
ABW (g)	61.05	138.72	273.98	390.94

Table 3-5. Experiment Trial 4 average wet body weight data.

Trial 4	24-Apr-18	22-May-18	19-Jun-18	17-Jul-18
Duration (days)	0	28	56	84
ABW (g)	50.82	135.48	275.94	413.97

Daily fish mortality was also recorded daily and reported as monthly mortality in every sampling schedule. The reported mortality was later interpolated between sampling schedules for the estimation of the biomass component as a prerequisite for material balance.

For Trial 1, sediment samples were collected approximately every 14 days from each sampling points at 0, 5, 10, 25 and 50m away from the cage starting at the northeast side (Figure 3-4). The sampling points were then converted to coordinates relative to the orientation and center of the cage single cage. Ekman grab was used to retrieve sediment samples from the sea bottom and 3 samples from the upper 1 centimeter of the sediment were pooled, mixed, and analyzed for AVS-S composition. The acid volatile sulfide content was measured following the standard method prescribed by the Japan Fisheries Resource Conservation Association. The instrument used to measure the sulfide content is the Hedorotec GASTEC 201L/H which was used by most marine sediments studies.

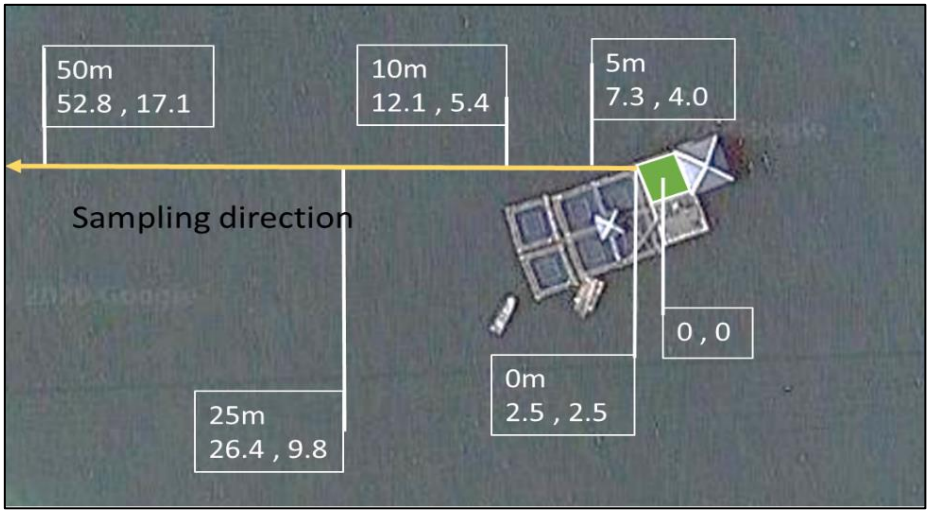

Figure 3.4. Trial 1 AVS sampling points relative to cage orientation. The cage used was marked in green.

Similar sampling methods were employed for Trial 3 with the number of cages were six 5 × 5 × 4m cages with 3 cages in horizontal orientation and 2 cages in vertical. This time, instead of 14-day sampling interval, monthly sediment sampling was done. The sampling points were determined at 0, 10, 25, 50m away from the northeast edge of the cage cluster (Figure 3-5). Sampling distance was also

converted to coordinates relative to the orientation and center of the 6 cages. The six cages for Trial 3 were treated as one single cage with 15 × 10 × 4m dimensions. Through the analysis of AVS-S, moisture content of the sample sediment was computed and later be used for the estimation of AVS-S from organic loading calculations. The AVS-S from Trials 1 and 3, were used for the estimation of the diffusivity coefficient of the experiment site and for the verification and comparison of the organic matter loading and formation of hydrogen sulfides.

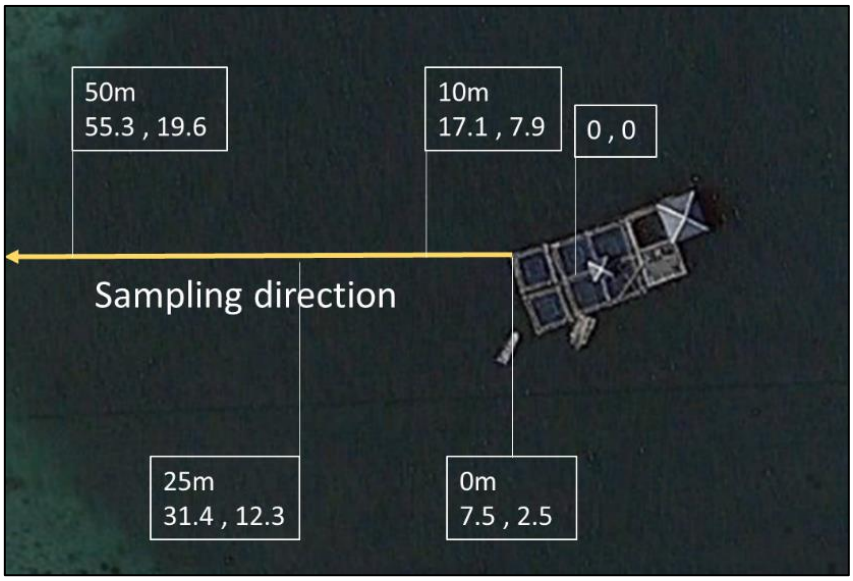

Figure 3.5. Trial 3 AVS sampling points. the 0m signifies the edge of the 6 cages used for the trial.

3.3 Methods of Analysis

3.3.1 Growth curve derivation

The Verhulst Logistic Growth equation was used to estimate the growth behavior of milkfish constrained in the cages. Redefining this equation allows the integration of properties that affects the carrying capacity of for this instance, the maximum weight of fish that the cage can handle in an infinity number of days. The logistics growth curve can be written as:

$$u(t) = \frac{Ku_{(0)}}{u_{(0)} + \left(K - u_{(0)}\right)\exp\left(-rt\right)} \quad \textit{(29)}$$

where:

$u(t)$ = body weight of fish in t days
K = maximum body weight coefficient (grams)
$u_{(0)}$ = initial weight at t= 0; stocking weight
r = intrinsic growth rate (%/day)
t = duration of culture (day)

Using the ABW and duration of culture data from Trials 1-4, regression analysis was used to estimate the values of K, r and $u_{(0)}$. The factors that affect the maximum body weight coefficient (K) and intrinsic growth rate (r), were then added to the equation using multiple linear regression analysis. The factors considered for the estimation K and r were fish density (ρ_c), temperature (T), and average feed rate (f_r). The fish density, was computed using the count of the milkfish at the end of the trial, ensuring the optimum biomass for the calculation, and the volume of the cage. The fate rate was calculated in a daily basis using the ratio of daily feed ration and the computed daily biomass (biomass = fish count × ABW) and was reported as percentage. The following equations for the estimation of K and r are as follows:

$$K = \mathrm{A}_K\rho_c + \mathrm{B}_K T + C_K fr \quad \textit{(30)}$$

$$r = \mathrm{A}_r\rho_c + \mathrm{B}_\mathrm{r} T + \mathrm{C}_r fr \quad \textit{(31)}$$

Where A, B, and C are the coefficient for each of the factors. Moreover, statistical tests such as R-squared and Chi-test were also employed to check the goodness of fit of the calculated values from the estimated values. The resulting growth curve from the analysis of the four Trials, were used for the model set-up for milkfish farming.

3.3.2 Estimation of particulate waste using material balance

As prerequisite for the material balance, the ABWs and fish counts were linearly interpolated between sampling schedules to get the daily biomass. Since the feed rations were recorded daily, the

amount of uneaten feed in terms of carbon and nitrogen were calculated using the stable isotope ratio of feed which was assumed to be constant on all trials. It was also assumed that the amount of the uneaten feed for all the trials were at 5%, also follows 95% daily feed ingestion. In addition, the carbon and nitrogen body composition were also taken from the stable isotope ratio of the milkfish body with the acquired data through communication. A box model for carbon and nitrogen balance was employed to estimate the amount of waste (particulate and dissolved) originated from each of the experiment trials.

3.3.2.a.Carbon balance

The amount of carbon waste derived from milkfish aquaculture was estimated using a box model. The carbon box balance model is illustrated by the Figure 3.6,

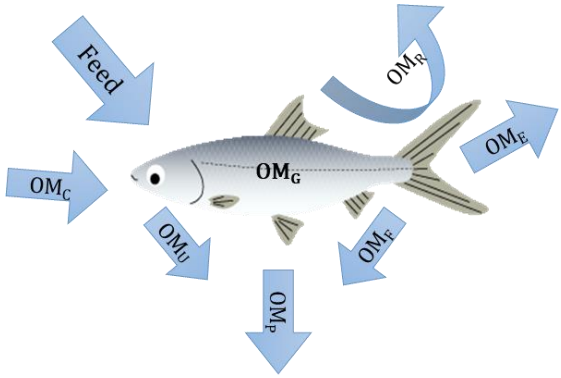

Figure 3.6. Schematic diagram of the carbon box model.

where:

OM_C = Consumed Carbon (g)
OM_U = Uneaten Carbon (g)
OM_G = Carbon used for Growth (g)
OM_E = Excreted Carbon = Dissolve Organic Carbon (DOC) (g)
OM_R = Respired Carbon (g)
OM_F = Carbon in Feacal Matter (g)
OM_P = Particulate Carbon = Particulate Organic Carbon (POC) (g)

Table 3-6.Feed and milkfish body carbon content (stable isotope data, Kodoma Masashi unpublished)

	Feed C	Body C
Average	0.450	0.360
STD	0.0771	0.0474
Count	7	3

The carbon content of the feed was calculated using the data of Feed C from Table 3-6 (*Kodama, Masashi unpublished data*). The daily uneaten and consumed carbon was then calculated using the assumption of 5% wastage (Equations 32 & 33).

$$\boldsymbol{OM_C} = \text{Feed C} \times \text{Consumed} \quad \textbf{(32)}$$

$$\boldsymbol{OM_U} = \text{Feed C} \times \text{Uneaten} \quad \textbf{(33)}$$

The amount of the daily carbon used by milkfish for growth (Equation 34) was calculated from the difference of the ABW from two consecutive days (body weight increase), multiplied by the number of fishes and the fish body carbon content(Table 3-6). (where t=day between the duration of culture)

$$\boldsymbol{OM_G} = (\text{ABW}_t - \text{ABW}_{t-1}) \times \text{Count}_{t-1} \times \text{Body C} \quad \textbf{(34)}$$

From theory, the routine metabolism rate for milkfish at the salinity of 35 ppt was calculated at 171.7 mgO_2/kg-hr and was converted to 1.54 gC/kgfish-day (Swanson 1998). The stoichiometry reaction for milkfish respiration showed that the amount of carbon in glucose used for respiration is equal to the amount of carbon excreted as CO_2. Equation 35 shows the relationship of respired and excreted carbon, (where BM is the biomass in kilograms from day t-1).

$$\boldsymbol{OM_R} = \boldsymbol{OM_E} = \text{RMR} \times \text{BM} \quad \textbf{(35)}$$

Finally, the amount of carbon in the feacal material was then calculated using the consumed (ingested) carbon subtracted by the excreted carbon, carbon used for respiration and carbon used for growth (Equation 36).

$$\boldsymbol{OM_F} = OM_C - OM_E - OM_R - OM_G \quad \textbf{(36)}$$

$$\boldsymbol{OM_P} = \boldsymbol{OM_U} + \boldsymbol{OM_F} \quad \textbf{(37)}$$

The daily generation of particulate carbon was then calculated through the summation of uneaten carbon and carbon in feacal material (Equation 37). The summation of daily particulate carbon for the whole duration of the experiment was then used for the calculation of the organic matter flux with the area and the total days of culture. This carbon flux was later used with the probability density

function to describe the dispersion of the organic matter in the experiment area. This procedure on estimating the carbon flux from cage culture study can also be used to different fish species.

3.3.2.b. Nitrogen balance

The nitrogen waste generated from milkfish cage culture was estimated using the box model. The nitrogen box balance model is showed in Figure 3.7.

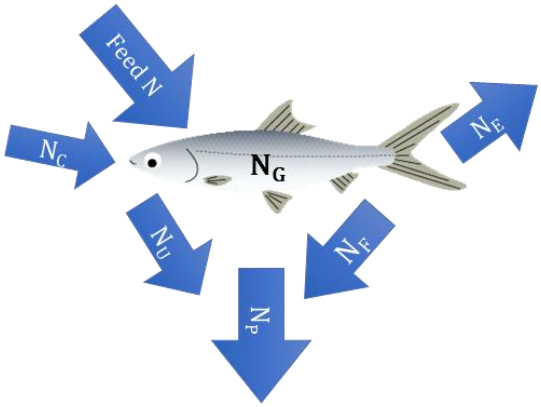

Figure 3.7. Schematic diagram of the milkfish nitrogen balance.

where:

N_C = Consumed Nitrogen (g)
N_U = Uneaten Nitrogen (g)
N_G = Nitrogen used for Growth (g)
N_E = Excreted Nitrogen = Dissolve Inorganic Nitrogen (DIN) (g)
N_F = Nitrogen in Feacal Matter (g)
N_P = Particulate Nitrogen = Particulate Organic Nitrogen (PON) (g)

Table 3-7. Feed and milkfish body nitrogen content (stable isotope data, Kodama Masashi unpublished)

	Feed N	Body N
Average	0.12	0.11
STD	0.0417	0.0155
Count	7	3

Based on Table 3-7, the nitrogen composition of feed is 12% which was used to calculate the daily consumed nitrogen and the daily uneaten nitrogen from the daily feed ration of 5% assumed feed wastage (Equation 38 & 39).

$$\boldsymbol{N_C} = \text{Feed N} \times \text{ Consumed} \quad \textit{(38)}$$

$$\boldsymbol{N_U} = \text{Feed N} \times \text{ Uneaten} \quad \textit{(39)}$$

Using the relationship from Figure 2.6, the daily excreted nitrogen was calculated using the daily biomass and the daily ABW (Equation 40).

$$\boldsymbol{N_E} = 1{,}493.6 \times (\text{ABW})^{-0.468} \times \text{ BM} / 1000 \quad \textit{(40)}$$

The amount of daily nitrogen used for growth was calculated using the ABW from two consecutive days and the biomass from the previous day with the body nitrogen based on Table 3-7. The daily nitrogen calculation is shown in Equation 41.

$$\boldsymbol{N_G} = (\text{ABW}_t - \text{ABW}_{t-1}) \times \text{Count}_{t-1} \times \text{Body N} \quad \textit{(41)}$$

Finally, the daily nitrogen found in faecal material was estimated using the consumed nitrogen subtracted by the nitrogen used for growth and the excreted nitrogen (Equation 42).

$$N_F = N_C - N_G - N_E \quad \textit{(42)}$$

The daily faecal nitrogen was summated and reported as nitrogen flux. However, for this study the results from the nitrogen balances were not used for the model but instead will be used for the future development of the model set-up for milkfish farming.

3.3.3 Organic matter dispersion

To estimate the organic matter flux distribution, a particle dispersion model was employed using probability density function. The goal of this analysis is to estimate the diffusivity coefficient of the experiment site using the relative spatial concentration of AVS and the amount of carbon flux at the center of the cage where it was assumed to have the maximum value.

Integrating the probability density function (Equation 9) over the area of the cage, gives the Equation 43. Parametrizing this equation using dimensional analysis and using the relationship of σ and diffusivity coefficient (E_x), Equation 44, yielded the Equation 45.

$$\int_{x-l/2}^{x+l/2}\int_{y-w/2}^{y+w/2} f(x,y)\,dxdy = \frac{1}{4}\left(\text{erf}\left(\frac{x-v_x+l/2}{\sigma_x\sqrt{2}}\right)-\text{erf}\left(\frac{x-v_x-l/2}{\sigma_x\sqrt{2}}\right)\right)\left(\text{erf}\left(\frac{y-v_y+w/2}{\sigma_y\sqrt{2}}\right)-\text{erf}\left(\frac{y-v_y-w/2}{\sigma_y\sqrt{2}}\right)\right) \quad \textbf{(43)}$$

$$\sigma_x = \left(\frac{h}{u}\right)\sigma_u \qquad \sigma_y = \left(\frac{h}{u}\right)\sigma_w \quad \textbf{(44)}$$

$$\frac{C(x,y)}{Co} = \frac{1}{A\,4}\left(\text{erf}\left(\frac{x-v_x+l/2}{\sigma_u\sqrt{2}}\cdot\frac{u}{h}\right)-\text{erf}\left(\frac{x-v_x-l/2}{\sigma_u\sqrt{2}}\cdot\frac{u}{h}\right)\right)\left(\text{erf}\left(\frac{y-v_y+w/2}{\sigma_w\sqrt{2}}\cdot\frac{u}{h}\right)-\text{erf}\left(\frac{x-v_y-w/2}{\sigma_w\sqrt{2}}\cdot\frac{u}{h}\right)\right) \quad \textbf{(45)}$$

where:

C_O = mass rate (g/day)
A = Area of the cage (m^2)
$C(x,y)$ = carbon flux at any x and y distance relative to the cage (g/m^2-day)
σ_u = std current east-west direction relative to the cage (m/s)
σ_w = std current north-south direction relative to the cage (m/s)
h = distance from bottom of the cage to the seabed (dispersion height) (m)
u = sinking rates (Table 3-8 Values) (m/s)
l = length of the cage east-west direction (m)
w = width of the cage north-south (m)

Table 3-8. Feed sinking rate and feacal material mass fraction with varying sinking rates.

Sinking rate (cm/s)	Mass Fraction (%)
Uneaten Feed	
10	
Feaces	
4	15
3	70
2	15

The experiment site has the average depth of 12m (surface to seabed), with the depth of the cage at 4m, thus the dispersion height is at 8m (h). It was also assumed that the current standard deviation in north-south direction is equal to the east-west direction thus $\sigma_u = \sigma_w$.

Solving for the diffusivity coefficient σ_u requires the spatial distribution of AVS concentration. However, there is no data for AVS concentration at the center of the cage. The AVS concentration at the center of the cage in every AVS sampling date should be estimated and the relative concentration of the sampling points should be calculated to define the distribution of the carbon flux. The AVS concentration from the experiment data is shown in Table 3-9 and Table 3-10.

Table 3-9. Trial 3 AVS data with corresonding coordinates in each sampling point.

X	7.5	17.0	31.4	55.3
Y	5	7.9	12.3	19.6
Days	0m	10m	25m	50m
28	1.017	0.389	0.070	0.080
55	0.894	0.196	0.116	0.044
83	0.683	0.229	0.179	0.087

Rows X and Y are the coordinates in east-west and north-south direction relative to the center of the cage. The same coordinates were used to calculate for the carbon flux concentration using the assumed value of diffusivity coefficient.

Table 3-10. Trial 1 AVS data with corresonding coordinates in each sampling point.

X	2.5	7.3	12.1	26.4	52.8
Y	2.5	4	5.4	9.8	17.1
Days	0m	5m	10m	25m	50m
21	0.100	0.074	0.091	0.043	0.057
34	0.090	0.034	0.036	0.049	0.037
49	0.016	0.071	0.051	0.014	0.035
63	0.021	0.029	0.016	0.019	0.009
77	0.140	0.058	0.037	0.035	0.017
91	0.074	0.115	0.057	0.033	0.061
105	0.219	0.141	0.049	0.102	0.056
119	0.100	0.108	0.061	0.057	0.064
133	0.149	0.057	0.054	0.086	0.071
147	0.158	0.131	0.173	0.057	0.077
161	0.179	0.081	0.033	0.024	0.037
175	0.152	0.068	0.184	0.066	0.038
189	0.246	0.086	0.038	0.035	0.042

The maximum carbon flux concentration is located at the center of the, C(0,0). With the assumed AVS concentration at (0,0), the flux distribution is defined by:

$$\frac{OM\ C(x,y)}{OM\ C(0,0)} = \frac{AVS\ C(x,y)}{AVS\ C(0,0)} \quad \textbf{(46)}$$

The variable parameters included in the estimation of the site's diffusivity coefficient were the AVS concentration at every sampling date at the cage center (0,0); the carbon fluxes at every sampling date with the assumption that the total carbon flux is the maximum concentration at the center

(Figure 3-8). Using Equation 45 with varying values of settling rates (u), the carbon flux concentration from each of the mass fraction was summated, and the total calculated flux was compared to the carbon flux concentration based on the AVS distribution in Equation 46, through the square of residual method (Equation 47). The limits for evaluating the SRR are the number coordinate pairs x and y from the center of the cage (limit 1 = (0,0). The effective distribution of carbon flux can only be observed within proximity to the cage thus only 4 sampling points were considered. The sum of the square of residual (SSR) was set to the most minimum value using Excel Solver (multiple regression analysis and iteration) , and the diffusivity coefficient was calculated.

$$\mathrm{SSR} = \sum_{1}^{4} \left(OM\ C(x,y) - OM\ C(x,y)_{\mathrm{equation}} \right)^2 \qquad \textbf{(47)}$$

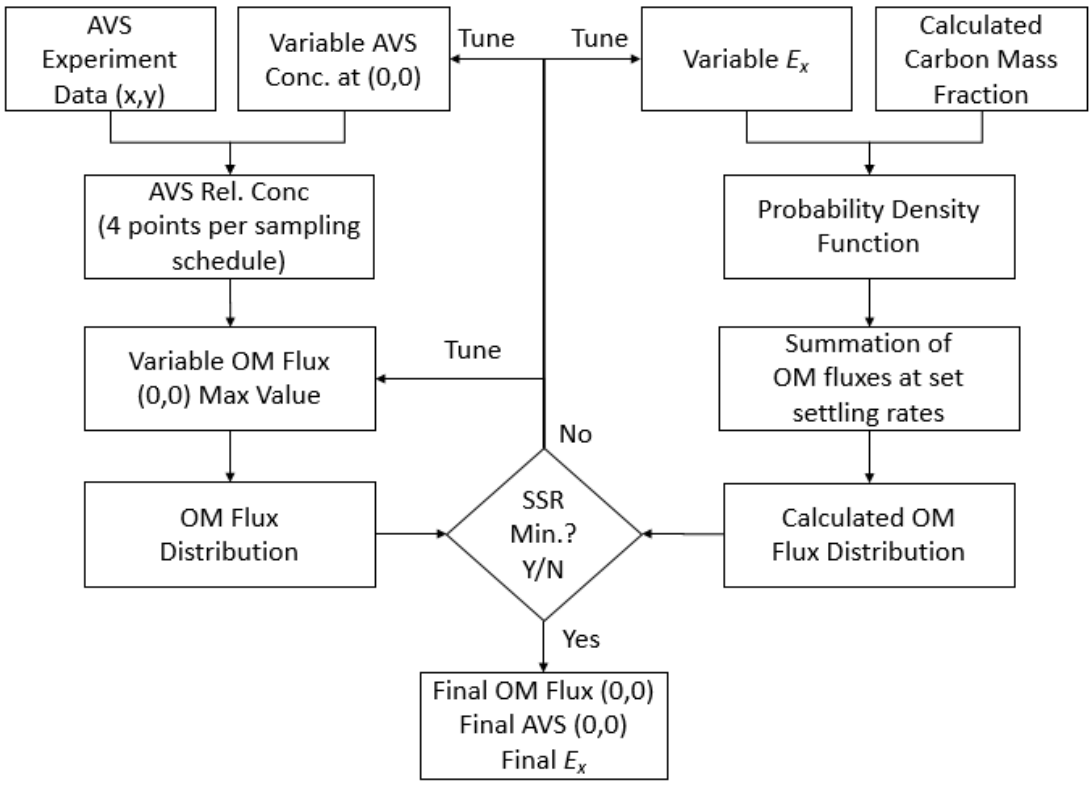

Figure 3.8. Iteration flowchart for the estimation of diffusivity coefficient E_x.

After the diffusivity coefficient σ_u was estimated, the carbon flux distribution was then recalculated using the mass rate (from the carbon balance) and the area of the cage in each mass fraction of settling rates. The resulting carbon flux from each mass fraction was totaled at each coordinate and a distribution graph was obtained. Only Trials 1 and 3 were considered for the particle dispersion model since these are the only experiment trials which have available AVS data. The calculated diffusivity coefficient from each of the trials were compared and were used for the simulation through the model setup for milkfish farming.

3.3.4 Hydrogen sulfide production

Based on the results of the organic matter flux calculated through probability density function, the amount of readily degradable organic matter was calculated based on Equation 21. The readily degradable organic matter was assumed to react with the sediment oxygen demand through the assumption of the dissolved oxygen concentration in the upper region of the diffusive boundary layer at thickness of 0.3 mm. The dissolved oxygen concentration was assumed to be 6 gO_2/m^3 and through the diffusion transport flux equation (Equation 23), the resulting sediment oxygen demand is at 1.71 g C/m2-day. This SOD was subtracted from the calculated distribution of the organic matter flux and the difference was used to calculated for the sulfate degradation (Equation 48). The readily degradable organic was graphed to illustrate the distribution from east-west direction.

$$OM_{anaerobic} = OM_D - OM_{O_2\,degradation} \quad \textbf{(48)}$$

$$OM_{SO_4} = 0.6\, OM_{anaerobic} \quad \textbf{(49)}$$

It was found that the sulfate degradation was 60% of the total anaerobic degradation Equation (49) (Fossing et al. 2004). Using this relationship, the organic matter that undergoes sulfate degradation was computed and through the sulfate degradation reaction (Equation 26), the amount of the hydrogen sulfide was calculated.

The computed hydrogen sulfide flux was then converted to the AVS concentration using the diffusion flux of H_2S from Equation 27, with the assumption that H_2S concentration at the surface of the seabed is negligible (C_{iH2S} = 0)(Figure 3.9). The resulting AVS concentration was then converted into dry weight (Equation 50) through the bulk density of the sediment which was computed based on the dry sediment density of 2.04 g/cm^3 and the moisture content of 58.16% (experiment data).

The AVS concentration at the furthest point from cage was then averaged and was considered as the background concentration which is defined as the natural AVS increase in the experiment site without sulfate degradation caused by organic matter flux from the marine cage culture. It was assumed that the background concentration is the average of the concentration found in the furthest sampling point (50m) in each sampling schedule. The point wherein the SOD and organic matter flux is equal (no anaerobic degradation occurs) was determined and showed in the graph of the distribution of AVS concentration with the background concentration.

$$C_{H2S}\frac{gH_2S}{m^3}\times\frac{cm^3}{1.46\ g\ wet\ sed}\times\frac{m^3}{100^3cm^3}\times\frac{1000mgH_2S}{gH_2S}\times\frac{1g\ wet\ sed}{(1-0.5816)g\ dry\ sed}\times\frac{32.065mgS}{34.065mg\ H_2S}=AVS\frac{mgS}{g\ dry} \quad \textbf{(50)}$$

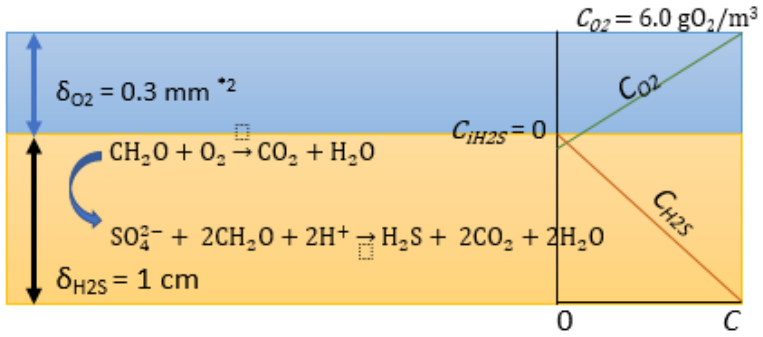

Figure 3.9. Mechanism for estimating the evolution of hydrogen sulfide. Blue layer shows the diffusive boundary layer in the water seabed inrface and orange layer for the upper layer of the sediment.

The estimated AVS concentration from the organic matter flux was compared to the experiment data through coefficient of determination (R^2) and t-test to test for the goodness of fit. This procedure of estimating the production of H_2S was later used for the simulation for the model set-up for milkfish farming.

Chapter 4 - RESULTS AND DISCUSSION

The results of this study were divided into two parts, (1) growth curve derivation and (2) estimation of the production of sediment AVS. Both the growth curve and the procedures for the AVS estimation will be used for the model simulation, in addition, for the comparison of the calculated AVS from the experiment data, the interpolated growth of Trials 1 and 3 will be used. The only purpose of Trial 2 and 4 for this study is to serve as additional data for the generalization of milkfish growth curve. The generalized growth curve was later used to predict the daily growth of milkfish where growth is a function of the duration of culture, temperature, fish density and feed rate.

From the daily interpolated ABW values and using carbon box model, the calculated carbon flux was corresponded to the sampling schedules of sediment AVS. At each of the sampling schedules, the relative AVS and carbon flux concentration was computed. The relative concentration of both this component was used to estimate the diffusivity coefficient based on the probability density function, which varies between both trials. The variation of the diffusivity coefficients was affected by the distance of the sampling points of the AVS data. This can be accounted, since the closer the points being analyzed for diffusion, the lower the diffusivity coefficient is.

Based on the calculated diffusivity coefficients from both trials, the amount of the actual carbon flux at each point was recalculated. The calculated carbon flux was then, divided into readily degradable carbon flux and through the assumptions from the nutrient flux model for Aarhus Bay (Fossing et al. 2004), the AVS concentration was calculated at the points similar to the sampling points from the experiment. Since sediment degradation is dependent on the dissolved oxygen concentration on the upper region of the diffusive boundary layer, the thin water layer between the seabed and the water column), the dissolved oxygen concentration was assumed. These resulting AVS concentration was then assessed for the goodness of fit using coefficient of determination and t-test to check if the procedure is feasible for the estimation.

4.1 Proposed milkfish growth equation

Verhulst logistic equation was used to propose a generalized growth curve for milkfish and it was illustrated by the equation:

From Equation 29

$$u(t) = \frac{Ku_{(0)}}{u_{(0)} + (K - u_{(0)})\exp(-rt)} \quad \textbf{(51)}$$

where:

$u(t)$ = average body weight of fish in t days (grams)
K = maximum body weight coefficient (grams)
$u_{(0)}$= initial weight at t= 0; stocking weight
r = intrinsic growth rate (%/day)
t = duration of culture (day)

Using Equation 51 and the data on each experiment trial (duration and ABW); K, r and $u_{(0)}$, were calculated using regression analysis. The resulting constants were tabulated in Table 4-2 and using the constants calculated with Equation 51, calculated ABW versus actual data was shown (Table 4-3).

Table 4-1. Average body weight data corresponded to the duration of culture.

Trial 1			Trial 2			Trial 3			Trial 4	
Duration (days)	ABW (g)		Duration (days)	ABW (g)		Duration (days)	ABW (g)		Duration (days)	ABW (g)
0	33.91		0	19.45		0	61.05		0	50.82
21	41.71		31	50.76		28	138.72		28	135.48
50	65.04		63	97.01		55	273.98		56	275.94
77	101.60		92	159.47		83	390.94		84	413.97
105	136.00		117	222.06						
133	203.72		148	291.64						
161	266.54		178	342.28						

Table 4-2. Calculated maximum weight (K), intrisic growth rate (r) and initial average body weight through regression analysis.

	Trial 1	Trial 2	Trial 3	Trial 4
K	411.97	398.50	496.46	531.04
r	0.019	0.026	0.040	0.042
u(0)	26.97	23.83	57.35	50.44

The results of the constants from regression analysis shows that the calculated values using Equation 51 were at a good fit with high coefficient of determination of 1 (R^2=1) for all trials. This proves that these constants can best describe the growth behavior of each trial. In Figure 4.1, The *K* value is at the highest in Trial 4 where the final actual ABW was also at its highest compared to the other trials. It also follows that; Trial 4 also has the highest intrinsic growth rate *r* among all the trials. While, Trial 3 has the highest initial ABW, the *K* value was lower compared to Trial 4 since the final ABW was also lower. From this analysis, it can be concluded that the final ABW of each trial is a determining factor in the estimation of *K* and *r*.

Table 4-3. Results of calculated average body weight using the constants from each trial.

Trial 1				Trial 2				Trial 3				Trial 4		
Duration (days)	Actual ABW(g)	Calculated ABW(g)		Duration (days)	Actual ABW(g)	Calculated ABW(g)		Duration (days)	Actual ABW(g)	Calculated ABW(g)		Duration (days)	Actual ABW(g)	Calculated ABW(g)
0	33.91	26.97		0	19.45	23.83		0	61.05	57.35		0	50.82	50.44
21	41.71	39.31		31	50.76	49.03		28	138.72	143.09		28	135.48	135.88
50	65.04	64.48		63	97.01	96.03		55	273.98	271.38		56	275.94	281.33
77	101.60	98.44		92	159.47	159.23		83	390.94	391.68		84	413.97	417.85
105	136.00	144.75		117	222.06	222.14								
133	203.72	199.02		148	291.64	293.03								
161	266.54	254.28		178	342.28	341.36								
189	299.17	303.04												

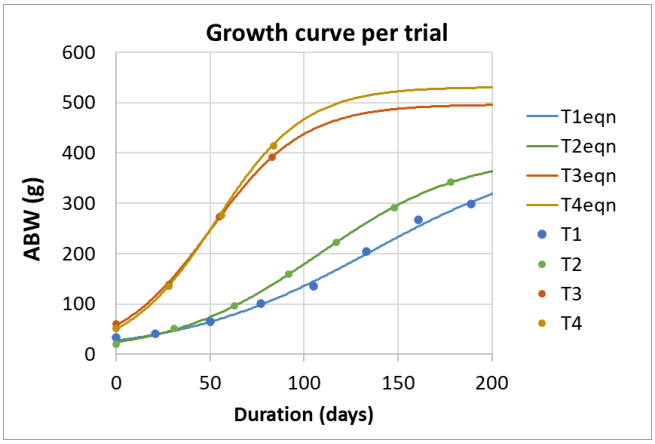

Figure 4.1. Graph in comparison of ABW experiment data and the calculated values. (TNeqn signifies the trial number)

By definition, *K* as the maximum body weight that the fish can attain, and the intrinsic growth *r* are directly affected by multiple physical factors like temperature, fish density and feed rate

(Equations 30 & 31). Therefore, the relationship of these factors needs to be established to best explain *K* and *r*.

Table 4-4 shows the fish density, temperature, and feed rate from each trial. The density of fish was calculated from the final amount of harvest (biomass) divided by the volume of the cage. The temperature was taken from average temperature recorded by the chlorophyll logger as was average for the whole duration of each experiment trials. While the daily feed rate was calculated using the daily feed ration divided by the daily biomass from the results of linear interpolation on growth and survival of fish. Using the daily feed rate, the average feed rate was calculated for the whole experiment duration.

Table 4-4. Physical parameters used for the estimation of K and r.

	Trial 1	Trial 2	Trial 3	Trial 4
Density (fish/m^3)	35.60	25.06	27.73	11.22
Temp (˚C)	28.24	28.7	29.83	29.61
Feed rate (%)	3.09	4.37	4.16	4.33

Since Trials 1 and 2 were executed during the colder months, it has lower average temperature compared to Trials 3 and 4. It is also apparent that the lowest fish density can be observed in Trial 4 compared to other trials. The density in Trial 4 was pre-decided since there is a difficulty in securing milkfish juveniles during this run. It can also be observed that the feed rate percentage in Trial 2 has the highest value. However, based on Table 4-2, the *K* value for Trial 2 is at its lowest among the trials. This shows that the feed ration was the highest among the 3 trials, but still milkfish has undergone stunted growth. This might be caused by the lower initial ABW which can also affect the values of *K*. Nevertheless, the data from Trial 2 was included in the estimation of the *K* and *r* values.

Using Equations 30 and 31, the *K* and *r* were estimated using regression analysis. The results of the regression analysis were tabulated in Table 4-5. In this table, the estimation of the coefficients

for the value of K, it showed that the unconstrained value has negative correlation with fish density and feed rate. The negative correlation of the fish density can be explained through feed behavior of fish. As the density of fish increases, feed competition increases resulting to less feed consumption and higher stress due to space restriction. This is also true in many population studies wherein the carrying capacity of an area depends on the available space wherein the population can grow. However, Table 4-5 also showed that feed rate has negative correlation with *K.* This showed otherwise and was caused by the higher value of feed rate in Trial 2. The maximum weight of the fish in the cage should have a positive correlation with the feed rate, thus C was set to positive or equal to 0. So thus, the resulting regression for K was concluded to be affected only by temperature and fish density. In addition, the results for the estimation of the intrinsic growth rate *r* showed that temperature and feed rate have positive correlation while density has negative correlation.

Table 4-5. Results of coefficients of K and r using linear regression analaysis

	K		r
	Uncons *	C≥ 0	Uncons *
A	-5.89	-3.75	-0.00075
B	28.77	19.01	0.00169
C	-57.78	0.00	0.00039

** Unconstrained*

Using the calculated constants from Table 4-5, Equations 30 and 31 can be written as:

$$K = 19.01T - 3.75\rho_c \quad \textbf{(52)}$$

$$r = \frac{1.69T + 0.39fr - 0.75\rho_c}{1000} \quad \textbf{(53)}$$

where:

ρ_c = fish density (fish/m^3)
T = temperature (˚C)
fr = average feed rate (%)

Using Equations 52 and 53, *K* and *r* were recalculated using the values in Table 4-4 and compared to the results from the regression analysis of each trial and was shown in Figures 4.2 and 4.3. The coefficient of determination of both *K* and *r* estimation was 0.68 and 0.66, respectively. This shows that the correlation for both estimations using density, temperature and feed rate can best

demonstrate the values. Moreover, since the feed rate has a direct effect on the growth of milkfish, it can be concluded that the intrinsic growth increases as the feed ration was increased.

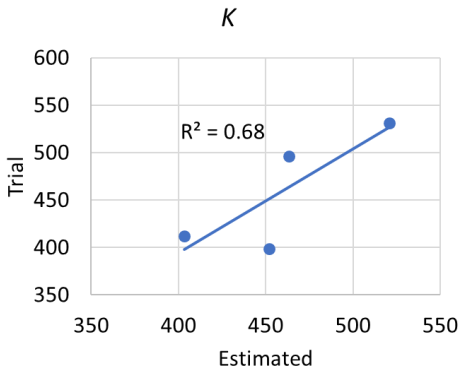

Figure 4.2. Comparison of calculated K through density and temperature from the K calculated per trial.

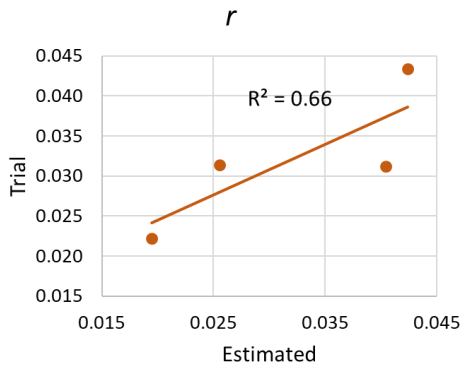

Figure 4.3. Comparison of calculated r through density, feed rate and temperature from the r calculated per trial.

The proposed generalized growth curve for milkfish using the trials in this study can be written as the following equation:

$$u(t) = \frac{u_{(0)}(19.01T - 3.75\rho_c)}{u_{(0)} + (19.01T - 3.75\rho_c - u_{(0)})\, e^{(-t\,(1.69T + 0.39fr - 0.75\rho_c)/1000)}} \quad \textbf{(54)}$$

where:

$u(t)$ = body weight in t days (g)
$u_{(0)}$ = initial body weight (g)
t = days of culture
r = intrinsic growth rate (/day)
K = infinite body weight (g)
ρ_c = fish density (fish/m3)
T = temperature (˚C)
fr = average feed rate (%)

In most fish growth curves, the infinite or maximum growth was defined only by a single variable and usually labeled as the asymptotic weight (Ricker 1979). In similar procedure, the regression analysis done per trial have similar results as the conventional curve estimation. In this case, certain environmental factors were included to best explain the asymptotic weight (see Equation 3). The point of inflection (POI) of the proposed growth moves closer to the origin as the initial weight increases. Since logistics growth are population growth curves, the point of origin was assumed at the lowest value close to zero and the point where the maximum growth rate is at ½ of the asymptotic weight. For the case of milkfish juveniles, linear regression was the most conventional procedure used to estimate growth. However, as the juveniles grow, consumption efficiency and growth rate were expected to decrease. The determination of the point when this decrease happens should be of utmost importance to aid farmers when to harvest the stocks and not lose the economic value of the stocks . It should also be noted that prolonging the duration of culture would drive the cost of production higher.

Several factors can also be included in the proposed growth equation especially the factors that can cause stress to the fish. Physical factors such as salinity, turbidity, net mesh size, types of feed and age of fish are most common parameters for milkfish cage operations. In addition, water quality such as dissolved oxygen, nitrates, phosphates, and sulfides concentration can also have direct effect on fish growth (Holmer et al. 2002).

However, the proposed growth curve only included density, temperature and feed rate which was considered as factors that have greater effects on the growth of milkfish. In addition, this proposed growth curve is only feasible for fish densities below 67 indv/m^3. At this density, the curve will result into decreasing ABW predictions since *K* value will be negative. However, according to the standards set for intensive milkfish farming in marine pens, the density should be 35-40 indv/m^3 and in marine cages greater than 30 indv/m^3. For semi-intensive milkfish farming in marine cages, the suggested density is at 20-30 indv/m3, the same density was suggested for freshwater cages.

Based on the standards set for milkfish farming, the usage of this proposed growth curve is applicable as a guide for milkfish aquaculture production and can estimate the growth with the suggested density standards. This proposed growth curve was used as the principal model for the model setup for milkfish farming which was discussed in the following chapters.

4.2 Estimation on the production of sediment acid volatile sulfides

The procedure for the estimation of the sediment organic matter degradation to produce AVS in marine milkfish culture to produce AVS is shown in the following flow chart (Figure 4.4).

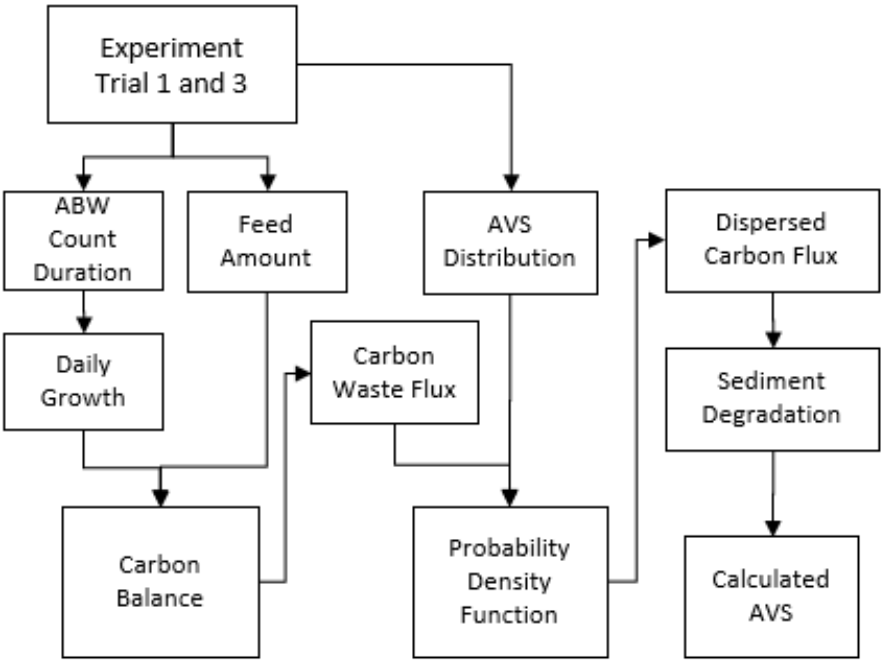

Figure 4.4. Schematic diagram for th estimation of AVS from Trials 1 and 3.

Experiment Trials 1 and 3 data on ABW and the number of fish was linearly interpolated between sampling schedules to generate the daily ABW and fish count. From these generated data, daily biomass was computed and was corresponded to the daily feed given based on the computed daily ration which was decided at the start of every sampling schedule. Trial 1 has constant daily feed ration every 28 days but in Trial, an additional 5% of the biomass was adjusted every 14 days from the

sampling schedule. Based on the assumption of 5% feed wastage, the consumed feed was calculated and using the stable isotope ratio of the feed, carbon and nitrogen inputs were estimated (Table 4-6 and 4-7). Through material box model, carbon and nitrogen waste was calculated. The accumulation of particulate waste was then corresponded to the sediment AVS sampling schedules. The relative distribution of the carbon waste flux and AVS concentration was then used in probability density function to estimate the diffusivity coefficient of the culture site. The estimated diffusivity coefficient was the used to recalculate the carbon flux to elucidate its dispersion. From the estimated dispersed carbon flux, sediment degradation reactions based on nutrient flux model for Aarhus Bay were employed to calculate the AVS concentration and distribution. The calculated AVS was then compared to the AVS data through t-test.

Table 4-6. Excerpt from Trial 3 calculated daily average body and count through linear interpolation, and the amount of daily feed ration divided into consumed and wasted.

Day	ABW (g)	Count	Biomass (kg)	Feed Ration (kg)	Consumed (kg)	Uneaten (kg)
0	61.05	17,039.0	1,040.23			
1	63.82	17,027.5	1,086.76	72.82	69.18	3.64
2	66.60	17,016.0	1,133.23	72.82	69.18	3.64
3	69.37	17,004.5	1,179.63	72.82	69.18	3.64
4	72.15	16,993.0	1,225.97	72.82	69.18	3.64
5	74.92	16,981.5	1,272.25	72.82	69.18	3.64
20	116.53	16,809.0	1,958.73	78.01	74.11	3.90
21	119.30	16,797.5	2,003.98	78.01	74.11	3.90
22	122.08	16,786.0	2,049.17	78.01	74.11	3.90
23	124.85	16,774.5	2,094.30	78.01	74.11	3.90
24	127.62	16,763.0	2,139.37	78.01	74.11	3.90
25	130.40	16,751.5	2,184.37	78.01	74.11	3.90
40	198.84	16,712.1	3,322.96	139.14	132.18	6.96
41	203.85	16,711.7	3,406.60	139.14	132.18	6.96
42	208.85	16,711.3	3,490.23	139.14	132.18	6.96
43	213.86	16,710.9	3,573.86	150.73	143.19	7.54
44	218.87	16,710.5	3,657.49	150.73	143.19	7.54
45	223.88	16,710.1	3,741.11	150.73	143.19	7.54
60	294.87	16,694.2	4,922.55	183.10	173.95	9.16
61	299.04	16,691.9	4,991.58	183.10	173.95	9.16
62	303.22	16,689.5	5,060.59	183.10	173.95	9.16
63	307.40	16,687.1	5,129.58	183.10	173.95	9.16
64	311.57	16,684.8	5,198.55	183.10	173.95	9.16
65	315.75	16,682.4	5,267.50	183.10	173.95	9.16
79	374.23	16,649.4	6,230.74	205.98	195.68	10.30
80	378.41	16,647.1	6,299.39	205.98	195.68	10.30
81	382.59	16,644.7	6,368.03	205.98	195.68	10.30
82	386.76	16,642.4	6,436.65	205.98	195.68	10.30
83	390.94	16,640.0	6,505.24	205.98	195.68	10.30

Table 4-7. Excerpt from Trial 1 calculated daily average body and count through linear interpolation, and the amount of daily feed ration divided into consumed and wasted.

DOC	ABW(g)	Count	Biomass (kg)	Feed Ration (kg)	Consumed (kg)	Uneaten (kg)
0	33.91	3,674.00	124.60			
1	34.29	3,671.62	125.89	5.00	4.75	0.25
2	34.66	3,669.24	127.17	5.00	4.75	0.25
3	35.03	3,666.86	128.44	5.00	4.75	0.25
4	35.40	3,664.48	129.72	5.00	4.75	0.25
5	35.77	3,662.10	130.99	5.00	4.75	0.25
30	48.95	3,615.32	176.96	6.10	5.80	0.31
31	49.75	3,614.36	179.82	6.10	5.80	0.31
32	50.56	3,613.39	182.68	6.10	5.80	0.31
33	51.36	3,612.43	185.54	6.10	5.80	0.31
34	52.16	3,611.46	188.39	6.10	5.80	0.31
35	52.97	3,610.50	191.25	6.10	5.80	0.31
36	53.77	3,609.54	194.10	6.10	5.80	0.31
55	71.81	3,596.36	258.24	9.40	8.93	0.47
56	73.16	3,596.25	263.11	9.40	8.93	0.47
57	74.52	3,596.14	267.97	9.40	8.93	0.47
58	75.87	3,596.04	272.83	9.40	8.93	0.47
59	77.22	3,595.93	277.69	9.40	8.93	0.47
60	78.58	3,595.82	282.55	9.40	8.93	0.47
85	111.43	3,592.57	400.32	12.80	12.16	0.64
86	112.66	3,592.39	404.71	12.80	12.16	0.64
87	113.89	3,592.21	409.10	12.80	12.16	0.64
88	115.11	3,592.04	413.49	12.80	12.16	0.64
89	116.34	3,591.86	417.89	12.80	12.16	0.64
90	117.57	3,591.68	422.28	12.80	12.16	0.64
121	174.70	3,581.00	625.59	17.10	16.25	0.86
122	177.12	3,580.50	634.16	17.10	16.25	0.86
123	179.53	3,580.00	642.73	17.10	16.25	0.86
124	181.95	3,579.50	651.30	17.10	16.25	0.86
125	184.37	3,579.00	659.87	17.10	16.25	0.86
151	244.11	3,570.50	871.58	25.50	24.23	1.28
152	246.35	3,570.25	879.53	25.50	24.23	1.28
153	248.59	3,570.00	887.48	25.50	24.23	1.28
154	250.84	3,569.75	895.43	25.50	24.23	1.28
155	253.08	3,569.50	903.37	25.50	24.23	1.28
156	255.32	3,569.25	911.32	25.50	24.23	1.28
185	294.51	3,561.14	1,048.79	28.60	27.17	1.43
186	295.68	3,560.86	1,052.86	28.60	27.17	1.43
187	296.84	3,560.57	1,056.92	28.60	27.17	1.43
188	298.01	3,560.29	1,060.99	28.60	27.17	1.43
189	299.17	3,560.00	1,065.05	28.60	27.17	1.43

Tables 4-6 and 4-7 shows the daily interpolated ABW and number of fish including the feed ration and calculated biomass. These parameters were used to calculate for the carbon and nitrogen waste derived from Trials 1 and 3.

4.2.1 Particulate carbon and nitrogen accumulation

4.2.1.a.Carbon waste

The equations used in the carbon box model for the estimation of carbon waste from milkfish cage culture were Equations 32, 33, 34, 35, 36, and 37 (Chapter 3).

Table 4-8. Excerpt from Trial 3 interpolated values.

Day	ABW(g)	Count(pcs)	BM(kg)	Consumed (kg)	Uneaten (kg)
0	61.05	17039.0	1040.23		
1	63.82	17027.5	1086.76	69.179	3.64
2	66.60	17016.0	1133.23	69.179	3.64

Based on Table 3-6 (Chapter 3), the carbon content in feed and milkfish body was at 45% and 36%, respectively. These carbon content percentages were assumed to be consistent for both trials for the purpose of estimation since there are no data available data on the exact stable isotope ratio for each material and so, it is important that certain assumptions need to be made.

Using Equations 32 and 33, the uneaten carbon (OM_U) and consumed carbon (OM_C) were calculated using the values from Table 4-8. (number subscripts signifies day number):

$\boldsymbol{OM_{C\,1}}$ = Feed C × $Consumed_1$ = 69.179 kg × 0.45 = **31.13 kg C**

$\boldsymbol{OM_{U1}}$ = Feed C × $Uneaten_1$= 3.64 kg × 0.45 = **1.64 kg C**

Given the carbon content in the body of milkfish, the carbon used for growth (OM_G) was calculated between Day 0 and 1 using Equation 34:

$\boldsymbol{OM_{G1}}$ = (ABW_1 – ABW_0) × $Count_0$ × Body C

= (63.82 – 61.05) × 17,039 × 0.36 ÷ 1000 = **17.02 kg C**

To calculate the amount of carbon respired (OM_R) and excreted (OM_E), the amount of oxygen needed for the milkfish respiration was taken from theory as the routine metabolism rate for milkfish. The amount of oxygen needed for respiration was converted to glucose based on milkfish respiration reaction and the resulting value is 1.545 gC/kg fish-day (RMR). This value signifies the glucose needed

for the milkfish metabolism and excretion on a daily basis. The denominator of the unit also signifies the biomass of the milkfish. Using this data, the OM_R and OM_E were calculated through Equation 35.

$$\boldsymbol{OM_{R1}} = \boldsymbol{OM_{E1}} = \text{RMR} \times BM_1 = (1.545 \text{ g C})/(\text{kg}-\text{day}) \times 1040.23 \text{ kg} \div 1000 = \mathbf{1.61 \text{ kg C}}$$

The objective of using this box model, is to estimate the amount of carbon in the feacal material of the milkfish. With the known amounts consumed carbon (OM_C), excreted carbon (OM_E), respired carbon (OM_R) and carbon used for growth (OM_G), the amount of feacal carbon (OM_F) was calculated using Equation 36.

$$\mathbf{OM_{F1}} = OM_{C1} - OM_{E1} - OM_{R1} - OM_{G1}$$
$$\mathbf{OM_{F1}} = 31.13 - 1.61 - 1.61 - 17.02 = \mathbf{10.90 \text{ kg C}}$$

The total particulate carbon waste was computed using the uneaten carbon (OMU) and the feacal carbon and was illustrated by Equation 37.

$$\mathbf{OM_{P1}} = OM_{F1} + OM_{U1} = 10.90 + 1.64 = \mathbf{12.54 \text{ kg C}}$$

The daily amounts of each component were computed using the above procedure and were totaled. The percent distribution of the carbon budget was then computed in both Trials 1 and 3 (Table 4-9 & 4-10; Figure 4-5 & 4.6).

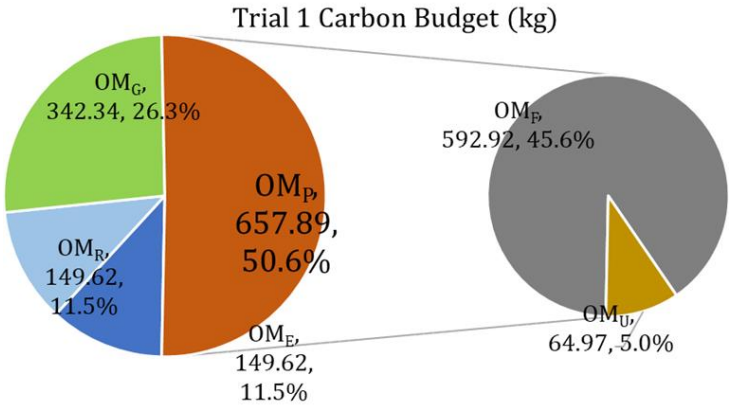

Figure 4.5. Trial 1 carbon budget in amounts and percentages.

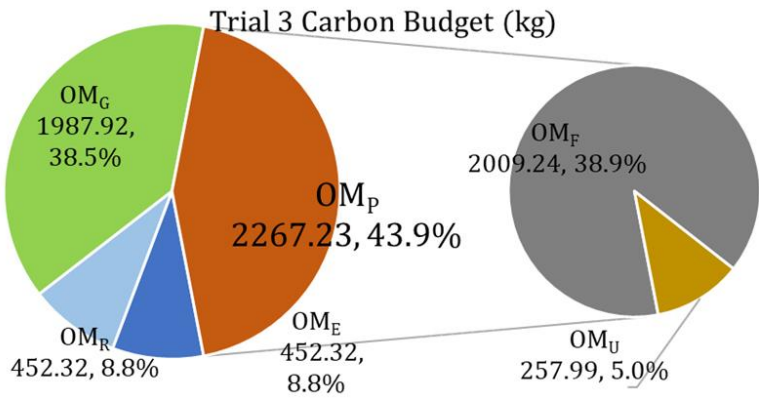

Figure 4.6. Trial 3 carbon budget in amounts and percentages.

Table 4-9. Excerpt of calculated Trial 3 daily amount of carbon budget parameters.

Day	OM_C (kgC)	OM_U (kgC)	OM_E (kgC)	OM_R (kgC)	OM_G (kgC)	OM_F(kgC)	OM_P (kgC)
0							
1	31.13	1.64	1.61	1.61	17.02	10.90	12.54
2	31.13	1.64	1.68	1.68	17.00	10.77	12.41
3	31.13	1.64	1.75	1.75	16.99	10.64	12.27
4	31.13	1.64	1.82	1.82	16.98	10.50	12.14
5	31.13	1.64	1.89	1.89	16.97	10.37	12.01
20	33.35	1.76	2.96	2.96	16.80	10.64	12.39
21	33.35	1.76	3.03	3.03	16.79	10.51	12.27
22	33.35	1.76	3.10	3.10	16.77	10.38	12.14
23	33.35	1.76	3.17	3.17	16.76	10.25	12.01
24	33.35	1.76	3.24	3.24	16.75	10.13	11.88
25	33.35	1.76	3.31	3.31	16.74	10.00	11.75
40	59.48	3.13	5.01	5.01	30.14	19.33	22.46
41	59.48	3.13	5.13	5.13	30.14	19.07	22.20
42	59.48	3.13	5.26	5.26	30.14	18.81	21.95
43	64.44	3.39	5.39	5.39	30.14	23.51	26.90
44	64.44	3.39	5.52	5.52	30.14	23.25	26.65
45	64.44	3.39	5.65	5.65	30.14	23.00	26.39
60	78.28	4.12	7.50	7.50	25.11	38.17	42.29
61	78.28	4.12	7.61	7.61	25.10	37.96	42.08
62	78.28	4.12	7.71	7.71	25.10	37.75	41.87
63	78.28	4.12	7.82	7.82	25.10	37.54	41.66
64	78.28	4.12	7.93	7.93	25.09	37.33	41.45
65	78.28	4.12	8.03	8.03	25.09	37.12	41.24
79	88.06	4.63	9.52	9.52	25.04	43.97	48.61
80	88.06	4.63	9.63	9.63	25.04	43.76	48.40
81	88.06	4.63	9.73	9.73	25.03	43.55	48.19
82	88.06	4.63	9.84	9.84	25.03	43.35	47.98
83	88.06	4.63	9.95	9.95	25.03	43.14	47.77
TOTAL	**4,901.80**	**257.99**	**452.32**	**452.32**	**1,987.92**	**2,009.24**	**2,267.23**

Table 4-10. Excerpt of calculated Trial 1 daily amount of carbon budget parameters.

Day	OM_C (kgC)	OM_U (kgC)	OM_E (kgC)	OM_R (kgC)	OM_G (kgC)	OM_F(kgC)	OM_P (kgC)
0							
1	2.14	0.11	0.19	0.19	0.49	1.26	1.37
2	2.14	0.11	0.19	0.19	0.49	1.26	1.37
3	2.14	0.11	0.20	0.20	0.49	1.25	1.37
4	2.14	0.11	0.20	0.20	0.49	1.25	1.36
5	2.14	0.11	0.20	0.20	0.49	1.25	1.36
30	2.61	0.14	0.27	0.27	1.05	1.02	1.16
31	2.61	0.14	0.27	0.27	1.05	1.01	1.15
32	2.61	0.14	0.28	0.28	1.05	1.01	1.14
33	2.61	0.14	0.28	0.28	1.05	1.00	1.13
34	2.61	0.14	0.29	0.29	1.05	0.99	1.13
35	2.61	0.14	0.29	0.29	1.05	0.98	1.12
36	2.61	0.14	0.30	0.30	1.05	0.97	1.11
55	4.02	0.21	0.39	0.39	1.75	1.48	1.69
56	4.02	0.21	0.40	0.40	1.75	1.47	1.68
57	4.02	0.21	0.41	0.41	1.75	1.45	1.66
58	4.02	0.21	0.41	0.41	1.75	1.44	1.65
59	4.02	0.21	0.42	0.42	1.75	1.42	1.63
60	4.02	0.21	0.43	0.43	1.75	1.41	1.62
85	5.47	0.29	0.61	0.61	1.59	2.66	2.95
86	5.47	0.29	0.62	0.62	1.59	2.65	2.93
87	5.47	0.29	0.63	0.63	1.59	2.63	2.92
88	5.47	0.29	0.63	0.63	1.59	2.62	2.91
89	5.47	0.29	0.64	0.64	1.59	2.61	2.89
90	5.47	0.29	0.65	0.65	1.59	2.59	2.88
121	7.31	0.38	0.95	0.95	3.12	2.28	2.67
122	7.31	0.38	0.97	0.97	3.12	2.26	2.64
123	7.31	0.38	0.98	0.98	3.12	2.23	2.62
124	7.31	0.38	0.99	0.99	3.12	2.21	2.59
125	7.31	0.38	1.01	1.01	3.12	2.18	2.57
151	10.90	0.57	1.33	1.33	2.88	5.35	5.92
152	10.90	0.57	1.35	1.35	2.88	5.32	5.90
153	10.90	0.57	1.36	1.36	2.88	5.30	5.87
154	10.90	0.57	1.37	1.37	2.88	5.27	5.85
155	10.90	0.57	1.38	1.38	2.88	5.25	5.82
156	10.90	0.57	1.40	1.40	2.88	5.23	5.80
185	12.23	0.64	1.61	1.61	1.49	7.50	8.15
186	12.23	0.64	1.62	1.62	1.49	7.49	8.13
187	12.23	0.64	1.63	1.63	1.49	7.48	8.12
188	12.23	0.64	1.63	1.63	1.49	7.47	8.11
189	12.23	0.64	1.64	1.64	1.49	7.45	8.10
TOTAL	**1,234.49**	**64.97**	**149.62**	**149.62**	**342.34**	**592.92**	**657.89**

Figure 4-5 and 4-6 show the carbon budget from Trials 1 and 3. It can be observed that the percent of carbon used for growth is higher in Trial 3 than in Trial 1. This signifies that the milkfish in Trial 3 exhibits high efficiency in feed consumption. This can be caused by slightly higher average temperature during the whole experiment duration and a lower fish density. Based on the proposed growth these factors have high influence in the growth and feeding behavior of the milkfish. In addition, the duration of culture in Trial 1 was 189 days while in Trial 3, it was only 83 days. Since the milkfish Trial 3 grow faster than the Trial 1, the percent of excreted carbon, respired carbon and particulate waste was lower compared to Trial 1. Similarly, in a view the carbon footprint of any species, the longer the species exist, the waste produced per individual through also increases based on the waste generated that goes to the environment. Moreover, as the species ages, its effectivity to assimilate the food ingested decreases also leading to less nutrient absorption. In the case of milkfish, the faster it can reach the marketable size (economical since) the shorter is the duration of culture needed. From these trials, it can be observed that the conditions in Trial 3 is far better than the conditions in Trial 1 in terms of growth efficiency and duration of culture. However, the total amount of particulate carbon generated from the culture was 2,267.23 kg compared to the Trial 1 which was 657.89 kg only. The higher is the number of fish being cultured in an area, it is highly expected that the waste generated will also be higher.

The particulate carbon estimated in this chapter were divided into mass fraction and were used for the calculation of the diffusivity coefficient in the study area.

4.2.1.b.Nitrogen waste

Particulate and dissolved waste nitrogen was computed for future modeling considerations, more specifically on the fate of particulate nitrogen which served as the deregulating factor on the nitrate sediment degradation as part of the anaerobic degradation mechanism. Nitrate degradation allows the production of ammonia which on higher concentrations can increases the sediment oxygen demand. In this study the nitrogen waste was estimated using Equations 38, 39, 40, 41 and 42.

Nitrogen waste was estimated analogous to the carbon waste estimation. The values in Tables 4-6 and 4-7 were used to estimate the consumed and uneaten nitrogen component of feed for both trials. In addition, the based-on Table 3-7 (Chapter 3), it was shown that the feed and milkfish body nitrogen composition were 12% and 11% respectively. For the purpose of illustrating the computations done for the estimation, the first 2 days of Trial 3 data was used.

Table 4-11. Excerpt from Trial 3 interpolated values.

Day	ABW(g)	Count(pcs)	BM(kg)	Consumed (kg)	Uneaten (kg)
0	61.05	17039.0	1040.23		
1	63.82	17027.5	1086.76	69.179	3.64
2	66.60	17016.0	1133.23	69.179	3.64

Using equations 38 and 39, the consumed (N_C) and uneaten nitrogen (N_U) was calculated. (*number in subscript signifies the day number*)

$\boldsymbol{N_{C1}}$ = Feed N × $Consumed_1$ = 0.12 × 69.179 kg = **8.301 kg N**

$\boldsymbol{N_{U1}}$ = Feed N × $Uneaten_1$ = 0.12 × 3.64 kg = **0.437 kg N**

Based on the equation derived from theory (Sumagaysay-Chavoso 2003). The excreted nitrogen (N_E) was calculated (Equation 40).

$\boldsymbol{N_{E1}} = 1{,}493.6 \times (ABW_0)^{-0.468} \times BM_0 \div (1000)^2$

$= 1{,}493.6 \times (61.05)^{-0.468} \times 1040.23 \div (1000)^2$ = **0.227 kg N**

With the milkfish body composition of 12% nitrogen, the nitrogen used for growth (N_G) was calculated using Equation 41.

$\boldsymbol{N_{G1}} = (ABW_1 - ABW_0) \times Count_0 \times$ Body N

$= (63.82 - 61.05) \times 17{,}039 \times 0.11 \div 1000$ = **5.199 kg N**

Finally, based on the nitrogen box model the feces nitrogen (N_F) was calculated using the Equation 42.

$\boldsymbol{N_{F1}} = N_{C1} - N_{G1} - N_{E1} = 8.301 - 5.199 - 0.227$ = **2.876 kg N**

The particulate nitrogen (N_P) was then calculated using summation of the uneaten nitrogen (N_U) and the feces nitrogen (N_F).

$$\boldsymbol{N_{P1}} = N_{F1} + N_{U1} = 2.876 + 0.437 = \mathbf{3.312\ kg\ N}$$

This procedure was then repeated for the remaining days until the whole duration of the culture was reached. The daily calculated nitrogen components were then totaled and tabulated in Tables 4-12 & 4-13 for both trials. The nitrogen budget for the whole experiment duration was shown.

Table 4-12. Excerpt of calculated Trial 3 daily amounts of nitrogen budget parameters.

Day	NC (kg)	NU(kg)	NE (kg)	NG (kg)	NF (kg)	NP (kg)
0						
1	8.301	0.437	0.227	5.199	2.876	3.312
2	8.301	0.437	0.232	5.196	2.874	3.311
3	8.301	0.437	0.237	5.192	2.872	3.309
4	8.301	0.437	0.242	5.189	2.871	3.308
5	8.301	0.437	0.247	5.185	2.869	3.306
20	8.893	0.468	0.312	5.132	3.449	3.917
21	8.893	0.468	0.316	5.129	3.449	3.917
22	8.893	0.468	0.319	5.125	3.448	3.916
23	8.893	0.468	0.323	5.122	3.448	3.916
24	8.893	0.468	0.327	5.118	3.448	3.916
25	8.893	0.468	0.330	5.115	3.448	3.916
40	15.862	0.835	0.411	9.210	6.241	7.076
41	15.862	0.835	0.417	9.209	6.236	7.071
42	15.862	0.835	0.422	9.209	6.230	7.065
43	17.183	0.904	0.428	9.209	7.546	8.451
44	17.183	0.904	0.433	9.209	7.541	8.446
45	17.183	0.904	0.439	9.208	7.536	8.440
60	20.873	1.099	0.510	7.672	12.692	13.790
61	20.873	1.099	0.514	7.671	12.689	13.788
62	20.873	1.099	0.517	7.670	12.686	13.785
63	20.873	1.099	0.521	7.669	12.684	13.782
64	20.873	1.099	0.525	7.668	12.681	13.780
65	20.873	1.099	0.529	7.666	12.678	13.777
79	23.482	1.236	0.578	7.651	15.252	16.488
80	23.482	1.236	0.581	7.650	15.250	16.486
81	23.482	1.236	0.585	7.649	15.248	16.484
82	23.482	1.236	0.588	7.648	15.246	16.481
83	23.482	1.236	0.592	7.647	15.243	16.479
TOTAL	**1,309.162**	**68.903**	**34.650**	**607.420**	**667.093**	**735.996**

Table 4-13. Excerpt of calculated Trial 1 daily amounts of nitrogen budget parameters.

Day	NC (kg)	NU(kg)	NE (kg)	NG (kg)	NF (kg)	NP (kg)
0						
1	0.570	0.030	0.036	0.150	0.384	0.414
2	0.570	0.030	0.036	0.150	0.384	0.414
3	0.570	0.030	0.036	0.150	0.384	0.414
4	0.570	0.030	0.036	0.150	0.384	0.414
5	0.570	0.030	0.037	0.150	0.384	0.414
30	0.695	0.037	0.042	0.320	0.333	0.370
31	0.695	0.037	0.043	0.320	0.333	0.369
32	0.695	0.037	0.043	0.320	0.332	0.369
33	0.695	0.037	0.044	0.320	0.332	0.369
34	0.695	0.037	0.044	0.320	0.332	0.368
35	0.695	0.037	0.044	0.320	0.332	0.368
36	0.695	0.037	0.045	0.319	0.331	0.368
55	1.072	0.056	0.052	0.536	0.484	0.541
56	1.072	0.056	0.052	0.536	0.484	0.540
57	1.072	0.056	0.053	0.536	0.483	0.540
58	1.072	0.056	0.053	0.536	0.483	0.539
59	1.072	0.056	0.054	0.536	0.482	0.539
60	1.072	0.056	0.054	0.536	0.482	0.538
85	1.459	0.077	0.065	0.486	0.908	0.985
86	1.459	0.077	0.066	0.486	0.908	0.985
87	1.459	0.077	0.066	0.485	0.907	0.984
88	1.459	0.077	0.067	0.485	0.907	0.984
89	1.459	0.077	0.067	0.485	0.907	0.984
90	1.459	0.077	0.067	0.485	0.906	0.983
121	1.949	0.103	0.083	0.953	0.914	1.016
122	1.949	0.103	0.083	0.953	0.913	1.016
123	1.949	0.103	0.084	0.953	0.913	1.015
124	1.949	0.103	0.085	0.952	0.912	1.015
125	1.949	0.103	0.085	0.952	0.912	1.015
151	2.907	0.153	0.099	0.881	1.927	2.080
152	2.907	0.153	0.099	0.881	1.926	2.079
153	2.907	0.153	0.100	0.881	1.926	2.079
154	2.907	0.153	0.100	0.881	1.926	2.079
155	2.907	0.153	0.101	0.881	1.925	2.078
156	2.907	0.153	0.101	0.881	1.925	2.078
185	3.260	0.172	0.109	0.457	2.695	2.866
186	3.260	0.172	0.109	0.456	2.694	2.866
187	3.260	0.172	0.110	0.456	2.694	2.866
188	3.260	0.172	0.110	0.456	2.694	2.866
189	3.260	0.172	0.110	0.456	2.694	2.865
TOTAL	**329.198**	**17.326**	**13.500**	**104.605**	**211.093**	**228.419**

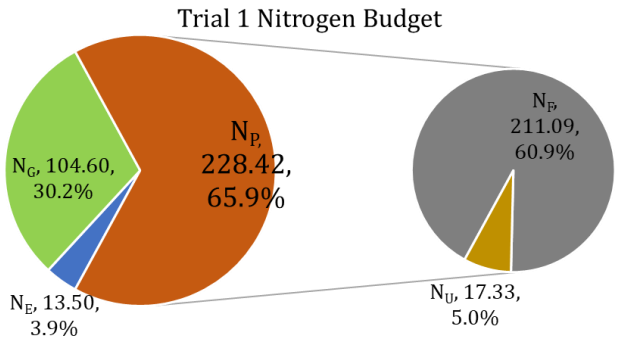

Figure 4.7. Pie chart of the distribution of nitrogen budget in kg for Trial 1.

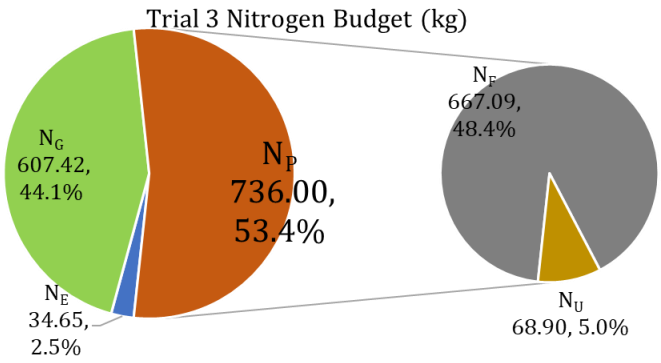

Figure 4.8. Pie chart of the distribution of nitrogen budget in kg for Trial 3.

Similar to the results of carbon budget for both trials, Trial 3 has lower particulate nitrogen waste percentage compared to Trial 1. This confirms that the Trial 3 experimental milkfish have higher consumption efficiency than those in Trial 1. This can also be explained by the final harvest weight which are 299.17g and 390.94g, respectively for Trial 1 and Trial 3. Moreover, the duration of culture in Trial 1 is 189 days and for Trial 3 it was only 83 days. Since Trial 1 exhibited a slower growth rate, the prolonged duration of culture has resulted to more feed wastage percentage compared to the shorter culture duration. If milkfish growth rate is high, the milkfish stocks can be harvested in a shorter period. Though the percentage of nitrogen waste is higher Trial 1, the amount of particulate nitrogen waste was only at 228.42 kg N compared to Trial 3 which was at 736 kg N. This is logical since the number of fish cultured in Trial 3 is around 5 times more than Trial 1.

Furthermore, it was assumed that the quality of feeds was the same in both experiment trials and this can also cause the difference of the growth rate if physical factors are excluded. In order to isolate the issue on fish nutrition, an accurate feed approximate analysis is necessary to have the basis of both carbon and nitrogen content of the feed to be used for the estimation. It was also assumed that the milkfish body nitrogen content was constant between two trials which may also cause differences on the nitrogen and carbon used for growth. The differences between the ratio of carbon and nitrogen in feeds can also affect the resulting stable isotope ratio of the body of milkfish. However, these analyses were more considered in nutrition studies and least considered in environmental studies. As many factors may affect the assimilation efficiency of milkfish, the procedure done using the box models in this study can be used as representative procedure for the estimation of the waste derived from marine milkfish cage culture.

4.2.2 Waste dispersion with probability density function

4.2.2.a.Estimation of diffusivity coefficient

The calculated particulate carbon waste as uneaten feed at every sediment sampling day was divided into mass fraction based on the settling rate from theory (Stucchi et al. 2005). The particulate uneaten was separated from the mass fraction and was assumed to have a sinking rate of 0.1 m/s.

Table 4-14. Trial 1 particulate carbon amounts distributed to corresponding sampling days and settling rates.

	Total OMU (g/m2-day)	Total OMF (g/m2-day)	OMF Mass Ratio			Total OMP (g/m2-day)
			0.15	0.7	0.15	
Day	0.1 m/s		0.04 m/s	0.03 m/s	0.02 m/s	
21	4.50	49.02	7.35	34.32	7.35	53.52
34	4.88	46.18	6.93	32.32	6.93	51.06
49	5.07	43.31	6.50	30.31	6.50	48.37
63	5.77	46.21	6.93	32.35	6.93	51.98
77	6.26	46.90	7.03	32.83	7.03	53.16
91	7.07	56.09	8.41	39.26	8.41	63.16
105	7.66	61.82	9.27	43.28	9.27	69.49
119	8.57	66.35	9.95	46.44	9.95	74.92
133	9.29	68.38	10.26	47.87	10.26	77.67
147	10.59	83.22	12.48	58.25	12.48	93.81
161	11.67	94.29	14.14	66.00	14.14	105.95
175	12.79	111.41	16.71	77.99	16.71	124.20
189	13.75	125.49	18.82	87.84	18.82	139.24

Table 4-15. Trial 3 particulate carbon amounts distributed to corresponding sampling days and settling rates.

	Total OMU (g/m2-day)	Total OMF (g/m2-day)	OMF Mass Ratio			Total OMP (g/m2-day)
			0.15	0.7	0.15	
Days	0.1 m/s		0.04 m/s	0.03 m/s	0.02 m/s	
28	11.31	68.31	10.25	47.82	10.25	79.62
55	16.42	104.16	15.62	72.91	15.62	120.58
83	20.72	161.38	24.21	112.97	24.21	182.11

The distribution of the carbon flux to the sediment sampling schedule was done to compare the accumulation of particulate waste to the increasing AVS concentrations based on the experiment data. Tables 4-14 & 4-15 were used separately for the estimation of diffusivity coefficient of the study site. The final particulate flux for Trials 1 and 3 are, 139.24 and 182.11 g/m^2-day, respectively. The main difference between the two trials is that Trial 1 sediment sampling points included a 5-meter distance from the north-east edge of the cage while Trial 3 does not have. Since Trial 1 has a shorter range of data points from the origin to be analyzed, it should be expected that the resulting diffusivity coefficient will be lower compared to Trial 3.

As mentioned in the previous chapter, the maximum carbon flux should be expected at the center of the cage and similarly the AVS concentration at the center should also be at maximum. However, the sediment AVS concentration at the center of the cage was not taken, therefore, to estimate the diffusivity coefficient it is necessary that the AVS concentration should be considered as a variable parameter.

Table 3-10 (AVS data) and Table 4-14 were used to estimate the diffusion in Trial 1. Table 3-10 was then revised to Table 4-16 with the assumed AVS concentration at the center of the cage. AVS values from 25m and 50m sampling points were not included in the estimation since the values did not exhibit significant increase compared to those points proximate to the cage but will serve as the background concentration (AVS increase without organic matter loading from the culture cage). This background concentration will be included on the final calculation of the estimated AVS increase. Table 4-17 shows the calculated relative AVS concentration to the assumed values at the center of the cage (0,0).

Table 4-16. Trial 1 AVS data and assumed used for calculating the relative AVS concentration.

X	0	2.5	7.3	12.1
Y	0	2.5	4	5.4
Days	Assumed	0m	5m	10m
21	0.180	0.100	0.074	0.091
34	0.111	0.090	0.034	0.036
49	0.148	0.016	0.071	0.051
63	0.047	0.021	0.029	0.016
77	0.167	0.140	0.058	0.037
91	0.183	0.074	0.115	0.057
105	0.282	0.219	0.141	0.049
119	0.183	0.100	0.108	0.061
133	0.184	0.149	0.057	0.054
147	0.336	0.158	0.131	0.173
161	0.212	0.179	0.081	0.033
175	0.334	0.152	0.068	0.184
189	0.281	0.246	0.086	0.038

Table 4-17. Trial 1 AVS data relative to the assumed AVS value.

X	0	2.5	7.3	12.1
Y	0	2.5	4	5.4
Days	Assumed	0m	5m	10m
21	1.00	0.55	0.41	0.50
34	1.00	0.81	0.30	0.32
49	1.00	0.11	0.48	0.34
63	1.00	0.45	0.61	0.34
77	1.00	0.84	0.34	0.22
91	1.00	0.41	0.63	0.31
105	1.00	0.77	0.50	0.17
119	1.00	0.55	0.59	0.33
133	1.00	0.81	0.31	0.30
147	1.00	0.47	0.39	0.51
161	1.00	0.84	0.38	0.15
175	1.00	0.46	0.20	0.55
189	1.00	0.88	0.31	0.13

The ratio in Table 4-17 were used to calculate for the distribution carbon flux at specified sampling day using the relationship established by Equation 46.

$$\frac{OM\ C(x,y)}{OM\ C(0,0)} = \frac{AVS\ C(x,y)}{AVS\ C(0,0)}$$

The carbon flux at the center of the cage was assumed and was considered as variable parameter *OM C(0,0).* In this case, for the purpose of calculation, the variable carbon flux was assumed to be close to the total carbon flux calculated which is 139.24 g/m^2-day. Based on the Equation 45, if the value in the left side were divided by the highest concentration, C_0/A will be cancelled, and the remaining factors

will only be the probability function distribution which is dimensionless. It also follows that at any assumed value of OM *C(0,0)*, because of the calculations' relative nature, the ratio was expected unchanged.

From the calculated total particulate carbon flux in Table 4-14, the ratio of the particulate carbon flux for each sampling day was calculated relative to the final particulate carbon flux (139.24 g/m^2-day). The ratio for each sampling was then used for the assumed variable particulate carbon flux. This proves that any assumed value for OM C(0,0) will always result to the same ratio as of the AVS concentration ratio.

Table 4-18 shows the distribution of carbon flux corresponded to the sampling days using the ratio in Table 4-17 and the assumed particulate carbon flux. Since the maximum flux at the center is not yet known, this distribution was used only for the estimation of diffusivity coefficient. The X and Y rows indicate the sampling points' distance from the center of the cage relative to its cage's orientation. The values in Table 4-18 were later compared to the values calculated using the probability density function with the diffusivity coefficient set as the variable parameter.

Table 4-18. Trial 1 total particulate carbon flux results relative to the maximum value at 0,0 and the AVS ratio.

X	**0**	**2.5**	**7.3**	**12.1**
Y	**0**	**2.5**	**4**	**5.4**
Day 21	53.52	29.67	22.11	27.01
34	51.06	41.53	15.51	16.46
49	48.38	5.35	23.13	16.69
63	51.99	23.37	31.94	17.54
77	53.16	44.54	18.32	11.84
91	63.16	25.65	39.82	19.70
105	69.49	53.85	34.70	12.01
119	74.92	41.09	44.18	25.00
133	77.68	62.83	23.95	22.93
147	93.81	44.15	36.65	48.21
161	105.96	89.40	40.32	16.31
175	124.21	56.61	25.14	68.49
189	139.24	122.02	42.64	18.63

From the probability density function (Equation 45), for the prediction of diffusivity coefficient E_x, Equation 55 was generated.

$$\frac{C(x,y)}{C(0,0)} = \frac{\left(\text{erf}\left(\frac{x+l/2}{\sigma_u\sqrt{2}}\cdot\frac{u}{h}\right)-\text{erf}\left(\frac{x-l/2}{\sigma_u\sqrt{2}}\cdot\frac{u}{h}\right)\right)\left(\text{erf}\left(\frac{y+w/2}{\sigma_u\sqrt{2}}\cdot\frac{u}{h}\right)-\text{erf}\left(\frac{x-w/2}{\sigma_u\sqrt{2}}\cdot\frac{u}{h}\right)\right)}{\left(\text{erf}\left(\frac{l/2}{\sigma_u\sqrt{2}}\cdot\frac{u}{h}\right)-\text{erf}\left(\frac{-l/2}{\sigma_u\sqrt{2}}\cdot\frac{u}{h}\right)\right)\left(\text{erf}\left(\frac{w/2}{\sigma_u\sqrt{2}}\cdot\frac{u}{h}\right)-\text{erf}\left(\frac{-w/2}{\sigma_u\sqrt{2}}\cdot\frac{u}{h}\right)\right)} \quad \textbf{(55)}$$

where:

$C(x,y)$ = carbon flux at any x and y distance relative to the cage (g/m^2-day)
$\sigma_u = \sigma_w$ =standard deviation of current x and y axis (m/s)
h = distance from bottom of the cage to the seabed (dispersion height) (m)
u = sinking rates (see Table 3-8) (m/s)
l = length of the cage east-west direction (m)
w = width of the cage north-south (m)

As previously mentioned, the maximum concentration C_0 and cage area cancel each other if the ratio was taken. The remaining parameters were the dispersion height, sinking rates, length and width of the cage, and the sampling point coordinates. To calculate for the distributed carbon flux *C(x,y)*, the values from Table 4-4 of OM_U and OM_P were used as *C(0,0).* The computed *C(x,y)* were then totaled and tabulated as the calculated particulate organic flux distribution. The current standard deviation was first assumed and was set as variable parameter. Then using the mass fraction in different sinking rates *u* (0.1, 0.04, 0.03, and 0.02 m/s) (Table 4-4), the distance from cage bottom to seabed *h* = 8m, length *l* = 5m, width *w* = 5m and the given sample coordinates (x,y), the total particulate organic flux distribution was calculated (Table 4-19).

Table 4-19. Trial 1 total particulate carbon flux calculate using probability density function.

X Y	0 0	2.5 2.5	7.3 4	12.1 5.4
Day 21	53.52	44.44	24.57	8.76
34	51.06	42.04	23.14	8.26
49	48.37	39.55	21.70	7.74
63	51.98	42.30	23.16	8.26
77	53.16	43.04	23.50	8.38
91	63.16	51.37	28.11	10.03
105	69.49	56.58	30.98	11.05
119	74.92	60.82	33.25	11.86
133	77.67	62.80	34.27	12.23
147	93.81	76.24	41.71	14.88
161	105.95	86.29	47.25	16.86
175	124.20	101.69	55.84	19.92
189	139.24	114.36	62.89	22.43

The calculated flux distribution (Table 4-19) through probability function was then compared to the flux distribution calculated through the AVS relative concentration, using the sum of square of the residual (SSR) as per defined by Equation 47. The SSR was set to minimum using the Excel Solver and the variables AVS concentration at (0,0) at each sampling day, carbon flux value relative to AVS, and the current standard deviation were estimated. The flowchart of the estimation is shown in Figure 4.9. The items in bold letters are the variable parameters.

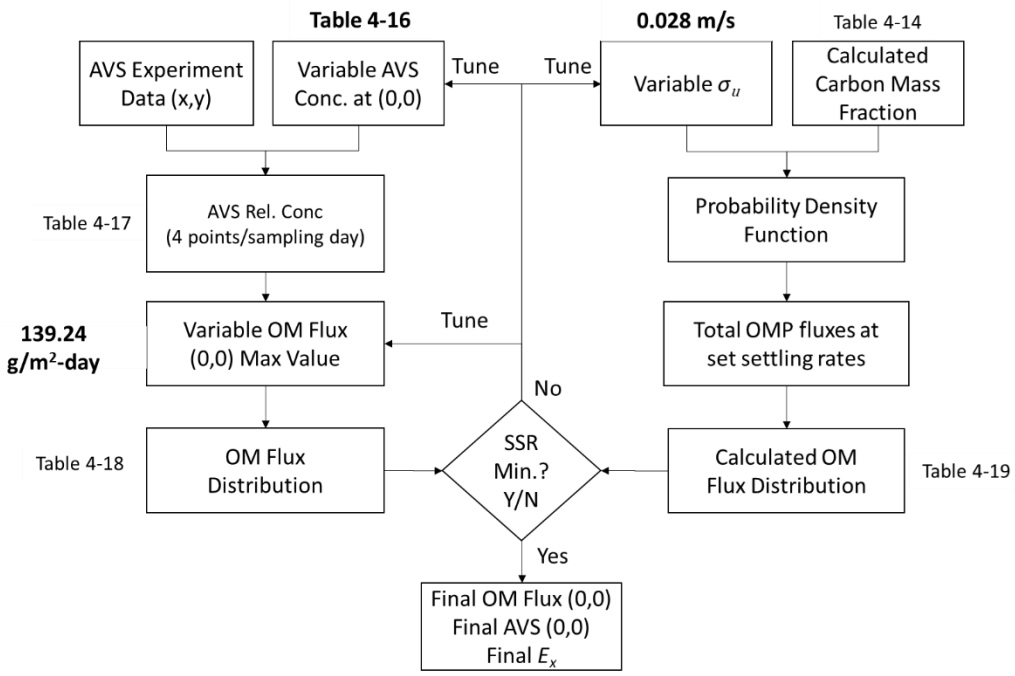

Figure 4.9. Schematic diagram and designated tables and results of the procedure for estimating σ_u for Trial 1.

In Figure 4.9, the previous tables presented earlier in this chapter was place into each step of estimation they were used. The assumed AVS concentration at cage center and the variable total carbon flux would not be of importance since the ratio of the concentrations were the ones only used. On the hand, the current σ_u was estimated at 0.028 m/s for Trial 1. This value represents how the AVS concentration was distributed on the seabed given the carbon flux and with the data on spatial AVS distribution. This current standard deviation was later discussed and used in this chapter to solve for the distribution of the carbon flux using the integrated carbon flux and the area of the cage.

Similar analysis was done for Trial 3 and Table 4-15 was used as the particulate carbon mass fraction and served as the baseline for the estimation of diffusion. The constants used for the estimation were h = 8m, l = 15m, and w = 10m, which are the distance from cage bottom to seabed, length of the cage, and width of the cage. The assumed particulate carbon flux at the center of the cage (0,0) was 182.11 g/m^2-day. Figure 4.10 shows the flowchart of the estimation of current standard deviation for Trial 3.

Table 4-20. Trial 3 assumed and experiment AVS data.

Days	C(0,0) Assumed	C(7.5,5)	C(17.0,7.9)	C(31.4,12.3)
28	1.6910	1.0173	0.3893	0.0703
55	1.4237	0.8941	0.1963	0.1163
83	1.1607	0.6830	0.2290	0.1792

Table 4-21. Trial 3 relative AVS concentration for the assumed value.

Days	C(0,0) Assumed	C(7.5,5)	C(17.0,7.9)	C(31.4,12.3)
28	1.0000	0.6016	0.2302	0.0416
55	1.0000	0.6280	0.1379	0.0817
83	1.0000	0.5885	0.1973	0.1544

Table 4-22. Trial 3 calculated total particulate carbon flux relative to the assumed maximum value and AVS relative concentration.

Days	C(0,0)	C(7.5,5)	C(17.0,7.9)	C(31.4,12.3)
28	79.621	47.898	18.328	3.309
55	120.575	75.721	16.623	9.848
83	182.106	107.161	35.937	28.112

Table 4-23. Trial 3 total pariculate carbon flux using the probability density function.

Days	C(0,0)	C(7.5,5)	C(17.0,7.9)	C(31.4,12.3)
28	79.621	50.310	12.559	0.351
55	120.576	76.379	19.139	0.536
83	182.107	116.446	29.593	0.830

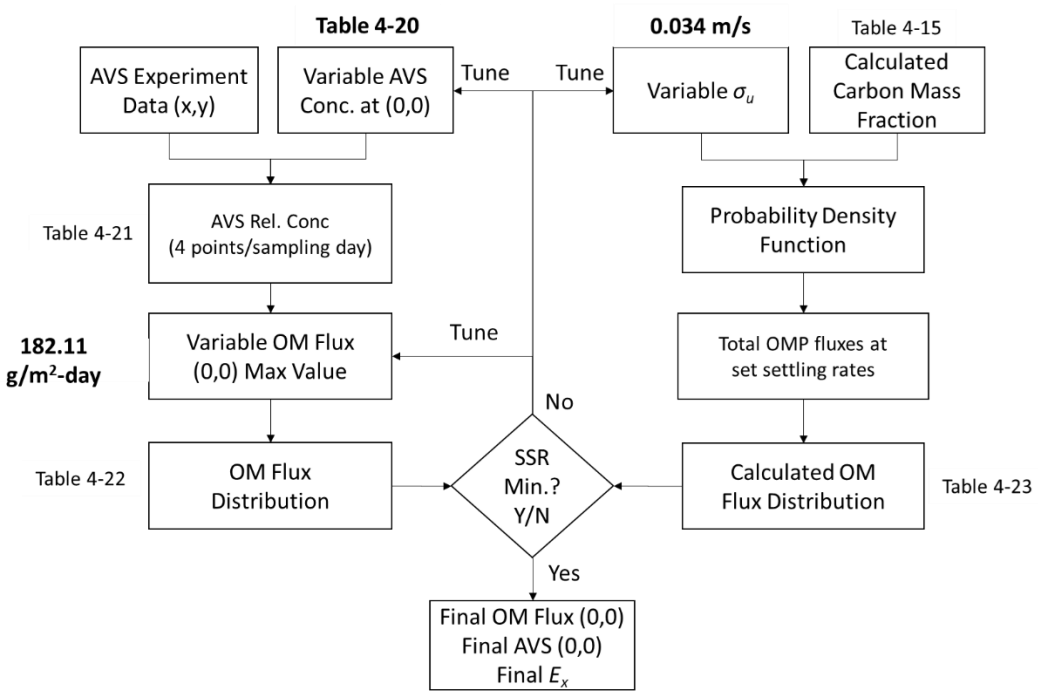

Figure 4.10. Schematic diagram and designated tables and results of the procedure for estimating σ_u for Trial 3.

The estimated current standard deviation for Trial 3 was 0.034 m/s which is almost twice the value from Trial 1 at 0.028 m/s. This difference was expected since Trial 1 sampling points were closer (5m data point) to the cage compared to Trial 3 (Ott and Mann 2000). This shows that the distance being considered for diffusion affects the estimation of diffusivity coefficient. And since it was assumed that the diffusion in east-west direction was equal to the north-south, though the cage was not properly aligned in east west direction, this shows that the diffusion coefficient can be used radially from the center of the cage. Calculating the diffusivity coefficients from the given current standard deviation, using the equation $\sigma = \sqrt{\frac{2hE}{u}}$ and the mass averaged sinking rates, the calculated diffusivity coefficient was 0.082 m^2/s and 0.156 m^2/s for Trial 1 and 3, respectively. These estimated values of diffusivity coefficients were similar to the values of salmon aquaculture site in Scotland with values 0.108 m^2/s major axis and 0.278 m^2/s minor axis, and sea bream site in Eastern Mediterranean with values 0.108 m^2/s and 0.353 m^2/s (Cromey and Black 2005). In many modeling studies, the diffusivity coefficient were assumed using Richardson's 4/3 rule (Kishi, Uchiyama, and Iwata 1994) and

through the use of drifter technology (Okubo et al. 1983). Both procedures can represent the diffusion behavior of the study site; however, the verification of its accuracy is often problematic since most of these diffusion studies assumes the particle behavior as constant. It is known that feed and feacal material in aquaculture has variable settling rates thus the dispersed carbon flux also varies. Often the data available for confirming the diffusivity of the study site is too broad and generalized especially on aquaculture production where data on the amount of feed given was usually summarize by the farmer. However, in this study, the amount of the carbon flux sources were calculated in detail through carbon box model. In addition, since the organic matter sediment degradation has high impact on sulfide concentration, it was believed that the above-mentioned procedure has high accuracy on illustrating the diffusion of the study area compared to known literatures.

The estimated diffusivity coefficients from this chapter were used to calculate for the amount carbon flux dispersed in the study area and discussed in the next chapter.

4.2.2.b.Distribution of organic matter flux

The total calculated particulate carbon flux and current standard deviation from Trial 1 and 3 were 139.24 g/m^2-day and 182.11 g/m^2-day, and 0.028 m/s and 0.034 m/s, respectively. Using the probability density function (Equation 45), the distribution of particulate carbon flux for Trial 1 was calculated through east-west direction setting y = 0. Moreover, the particulate carbon flux was divided to mass fraction based on the settling rate of feed and feacal material and was given by Table 4-24. The total feacal material divided into mass fraction is 125.49 gC/m^2-day.

$$\frac{C(x,y)}{Co} = \frac{1}{A\,4}\left(\mathrm{erf}\left(\frac{x - v_x + l/2}{\sigma_u\sqrt{2}}\cdot\frac{u}{h}\right) - \mathrm{erf}\left(\frac{x - v_x - l/2}{\sigma_u\sqrt{2}}\cdot\frac{u}{h}\right)\right)\left(\mathrm{erf}\left(\frac{y - v_y + w/2}{\sigma_w\sqrt{2}}\cdot\frac{u}{h}\right) - \mathrm{erf}\left(\frac{x - v_y - w/2}{\sigma_w\sqrt{2}}\cdot\frac{u}{h}\right)\right)$$

where:

C_0/A = based on Table 4-24
u = based on Table 4-24
E_x = 0.082 m2/s
h = 8 m
l = 5 m
w = 5 m

Table 4-24. Trial 1 total particulate carbon flux with mass fraction in varying sinking rates.

Total OMU (g/m2-day)	OMF Mass Ratio (g/m2-day)			Total OMP (g/m2-day)
0.1 m/s	0.04 m/s	0.03 m/s	0.02 m/s	
13.75	18.82	87.84	18.82	139.24

The calculated carbon flux from each mass fraction was then totaled on each of points along east-west direction and distributions graph were drawn.

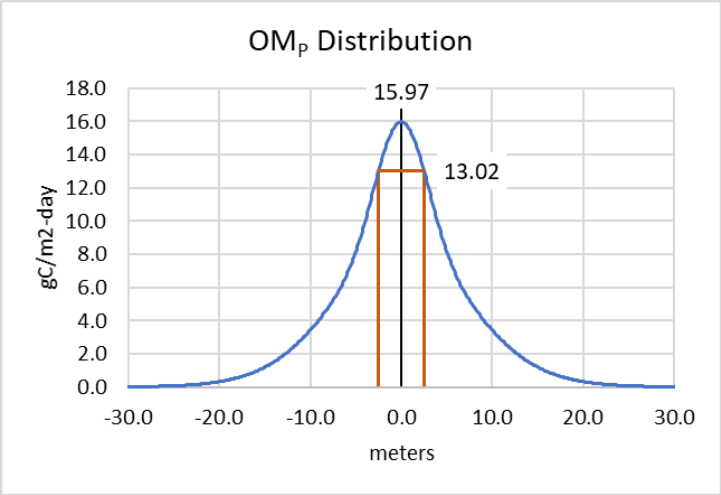

Figure 4.11. Resulting particulate carbon flux distribution through probability density function for Trial 1.

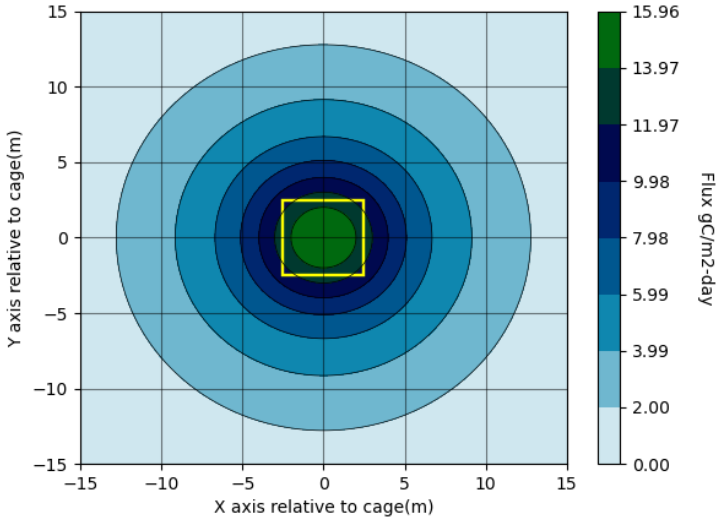

Figure 4.12. Trial 1 contour diagram of the particulate carbon flux, yellow square signifies the cage area.

Figure 4.11 shows that the maximum particulate carbon flux at the center of the cage is 15.97 gC/m^2-day and 13.02 gC/m^2-day at the edge. The orange line indicates the edge of the cage projected to the seabed which is the first sediment sampling point for AVS analysis and later be discussed on the next chapters. Figure 4.12 shows the contour distribution when the north-south axis was also considered in the calculation. The graphs show that high concentration of particulate carbon flux is located within the cage area as illustrated by the square shape. Moreover, the flux concentration greater than 2 gC/m^2-day reached around 13 meters relative to the center of the cage. Past 13 meters, particulate carbon flux was found to be less than 2 gC/m^2-day. In sediment degradation, aerobic degradation depends greatly in the sediment oxygen demand which also indicates the accumulation of organic material (Bowman and Delfino 1980). In Chesapeake Bay, SOD ranges 1.5 - 3.1 g O_2/m^2-day which are also dependent on dissolved oxygen concentration in the upper layer of the diffusive boundary layer. The amount of organic matter where total degradation through aerobic process were also discussed in the following chapter. In addition, the point where there is no noticeable increase in AVS concentration were also discussed in the next chapters.

In cases where there is prevailing current, the center of the distribution moves to the direction of that current, however, the distribution will remain unchanged. This can be explained since the probability function assumes the distribution in accordance with the standard deviation of the current and not based on the magnitude of the current itself. The greater the current standard deviation is, wider is the area of the carbon flux dispersion and the higher the prevailing current is, the farther the center of diffusion will be relative to the cage center.

Table 4-25. Trial 3 total particulate carbon in mass fraction with different sinking rates.

Total OMU (g/m2-day)	OMF Mass Ratio (g/m2-day)			Total OMP (g/m2-day)
0.1 m/s	0.04 m/s	0.03 m/s	0.02 m/s	
20.72	24.21	112.97	24.21	182.11

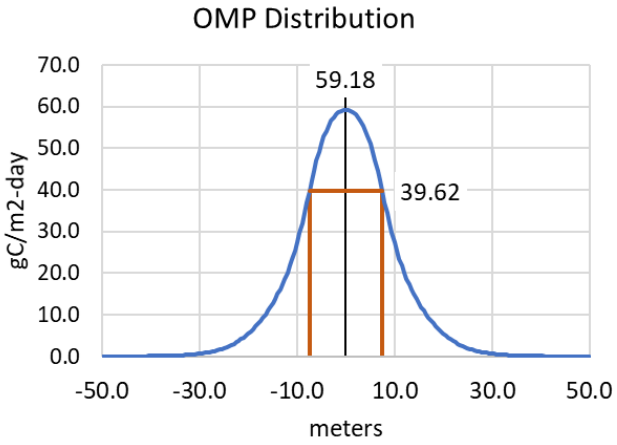

Figure 4.13. Trial 3 total particulate carbon flux distribution through probability density function evaulated at x-east-west direction.

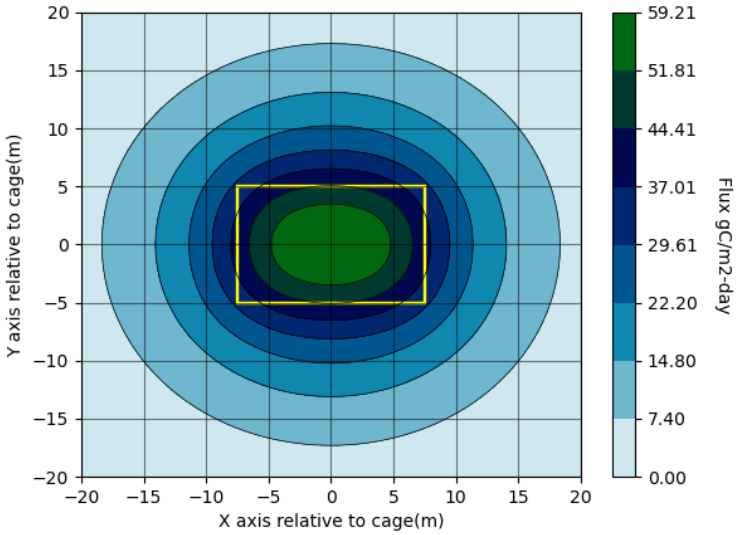

Figure 4.14. Trial 3 total particulate carbon flux distribution contour graph.

Similar analysis was made to the calculated total particulate carbon and current standard deviation in Trial 3 which are 182.11 gC/m^2-day and 0.034 m/s, respectively. Using h = 8m, l = 15m and w = 10 width settling rates and particulate carbon flux as variables (Table 4-25), the distribution graph created. The total feacal amount is 161.385 gC/m^2-day which was divided to the mass fraction at different settling rates. Figure 4.13 shows the maximum flux at the center of the cage was at 59.18

gC/m^2-day and 39.62 gC/m^2-day at the edge of the cage. In Figure 4.14, it can be observed that the maximum particulate flux was concentrated within 3 meters from the center of the cage in all direction. Particulate carbon flux greater than 7.4 gC/m^2-day reached around 13 meters away from the cage. It was also observed that around 60% of the total particulate carbon flux can be found with the bottom area of the cage as marked by the yellow rectangle.

Comparing the Trial 1 and 3 particulate carbon flux distribution, since Trial 1 has lower current standard deviation, the extent of waste dispersion is limited around the cage area while in Trial 3, the particulate carbon flux reached farther away from the center of the cage. Moreover, the dimension of the cage also affected the dispersion since in Trial 3, the contour shows a longer distance of dispersion in east-west direction compared to the north-south direction.

The estimated distribution of particulate carbon fluxes in both experiments were used for the estimation of the AVS concentration using the sediment degradation reactions and conditions from theory of nutrient flux model for Aarhus Bay (Fossing et al. 2004).

4.2.3 Estimation of acid volatile sulfide production

4.2.3.a.Carbon flux to hydrogen sulfide conversion

The analysis of the fate of particulate carbon flux to the evolution of hydrogen sulfide was analyzed using the flow chart in Figure 4.15.

Organic matter degradation includes two processes, aerobic and anaerobic degradation. Not all organic matter derived from aquaculture can be easily degraded. Easily degradable particulate carbon is considered labile since it decomposes on a time scale of days to weeks and it decomposes rapidly in water column or on the sediments. While slow degradable particulate carbon is considered refractory since it decomposes on a time scale of months and even years primarily in the sediments and it may contribute to sediment oxygen demand after deposition for a long time (McCormick 2001).

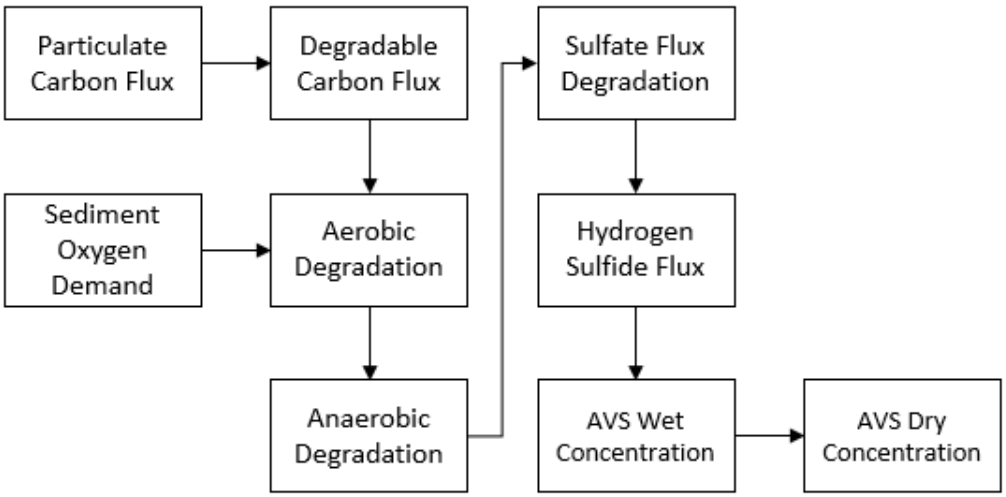

Figure 4.15. Flowchart of particulate carbon flux conversion to AVS concentration.

In aerobic degradation, the concentration of dissolved oxygen in the upper part of the diffusion boundary layer is needed to estimate the available oxygen flux that would react with the organic carbon degradation. For the sake of estimation, the dissolved oxygen concentration was assumed at 6.0 g O_2/m^3. This concentration was then converted to oxygen flux using the diffusion transport flux equation and oxygen diffusivity equation (Equations 24 and 25).

$$Flux_{O_2} = D_{O_2} \frac{C_{O_2}}{\delta} \quad \textbf{(24)}$$

$$D_{O_2} = (11.7 + 0.344T + 0.00505T^2) \times 10^{-6}\ cm^2 s^{-1\ *\ 2} \quad \textbf{(25)}$$

The average temperature for the whole experiment duration of Trial 1 is 28.24˚C. Calculating for the diffusivity of O_2 through Equation 25 and simplifying to match the flux unit resulted to, 2.29×10^{-4} m^2/day. Solving for the O_2 flux using Equation 24 and the assumption of the diffusive boundary layer thickness of 0.3mm resulted to, 4.57 gO_2/m^2-day. This value is higher compared to the values estimated from theory since the concentration of oxygen was assumed at 6 gO_2/m^3. At this concentration, the culture area was found to be in pristine and healthy condition based on the location and history of the experimental site.

Using the stoichiometry of sediment aerobic degradation, the sediment oxygen demand was converted to its carbon flux equivalent.

$$OM_{O_2\,degradation} = 4.57\frac{gO_2}{m^2 - day} \times \frac{\frac{12gC}{molC}}{\frac{32gO_2}{molO_2}} \times \frac{molC}{molO_2} = \mathbf{1.71}\frac{\boldsymbol{gC}}{\boldsymbol{m^2 - day}}$$

This value of SOD was used as the amount of carbon flux that undergoes aerobic degradation. The remaining unreacted carbon flux undergoes sulfate degradation and produce hydrogen sulfide.

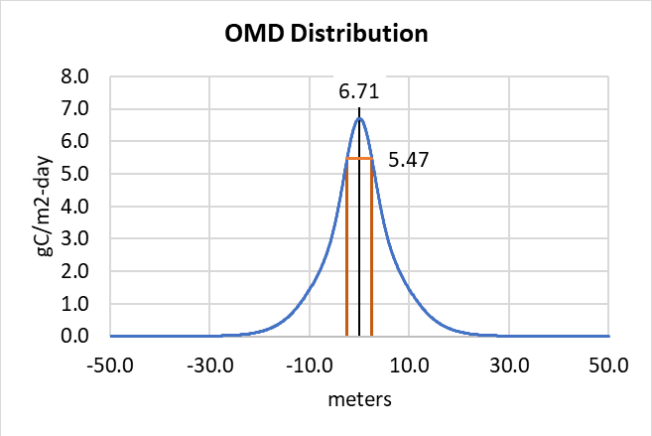

Figure 4.16. Trial 1 readily degradable particulate carbon flux distribution.

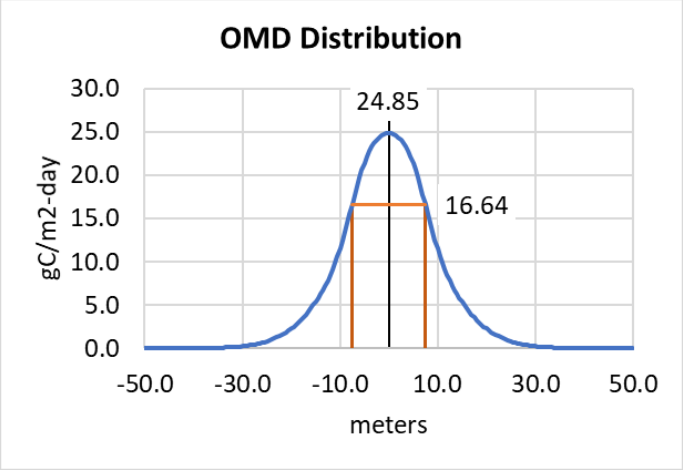

Figure 4.17. Trial 3 readily degradable particulate carbon flux distribution.

Results from the estimation of particulate carbon flux distribution in Trials 1 and 3 were converted to degradable particulate carbon flux through the ratio from Equation 21 and a new distribution graph was created (Figures 4.15 and 4.16).

$$\frac{OM_D}{OM_P} = 0.42 \quad \textbf{(21)}$$

The maximum readily degradable carbon in Trials 1 and 3 are 6.71 and 24.85 gC/m^2-day. Subtracting the amount of carbon reacted through aerobic degradation resulted to 5.01 and 23.22 gC/m^2-day. These amounts will undergo aerobic degradation, however, only 60% will react to sulfate and produce hydrogen sulfide (Fossing et al. 2004). With this relationship, carbon flux that would react with sulfate were converted to 3.0 and 13.93 gC/m^2-day for Trials 1 and 3, respectively. These amounts were then used for the estimation of AVS concentration on the last sampling day of each trial. Moreover, the amounts dispersed in the area were also converted to sulfate degradation. In cases where the amount of SOD is greater than the particulate carbon flux, resulting to negative values for anerobic degradation, the hydrogen sulfide production was assumed to be zero or non-existent. In addition, the point where there was no hydrogen sulfide production was also marked. This is the point where farmers can decide where to place the next culture cage as to prevent accumulation of organic waste from other culture cages.

For Trial 1, the maximum carbon flux that undergoes sulfate degradation is 3.0 gC/m^2-day. Through the sulfate degradation reaction, the production of hydrogen sulfide was calculated.

$$\begin{aligned} AVS_{H_2S} &= OM_{SO_4} \times \frac{MW_{H_2S}}{MW_C} \times \frac{1 mol H_2S}{2 mol C} \\ &= 3.0 \frac{gC}{m^2 - day} \times \frac{34.065\ gH2S/mol H_2S}{12\ gC/molC} \times \frac{1 mol H_2S}{2 mol C} \\ &= \mathbf{4.26 \frac{g H_2 S}{m^2 - day}} \end{aligned}$$

The hydrogen sulfide flux was then converted to hydrogen sulfide concentration using the Equations 27 and 28.

$$Flux_{H_2S} = D_{H_2S}\frac{C_{\delta H_2S}}{\delta} \quad \textit{(27)}$$

$$D_{H_2S} = (8.74 + 0.264T + 0.004T^2) \times 10^{-6}\ cm^2 s^{-1\ *2} \quad \textit{(28)}$$

The resulting diffusivity of hydrogen sulfide at 28.24˚C is 1.68 × 10 $^{-4}$ m^2/day. The thickness of the sediment layer δ was assumed at 1cm. Since the sedimentation rate (cm/day) was not known, based on the sampling procedure for AVS measurements which uses 1cm of the uppermost layer of the sediment, this assumption was made. It is not clearly identified at what depth does sulfide degradation starts, however with the presence of organic matter that could undergo aerobic degradation it can be briefly assumed that all hydrogen sulfide produced can be found within that upper 1cm layer. In addition, the refractory organic matter which would take years before undergoing sulfate degradation may be found under that 1cm layer. With this assumption, the concentration of hydrogen sulfide can be calculated using Equation 27.

$C_{\delta H2S}$ = $Flux_{H2S}$ × δ / D_{H2S} = 4.26 gH_2S/m^2-day × 0.01 m / 1.68 × 10 $^{-4}$ m^2/day

= **253.57 gH_2S/m^3**

The computed hydrogen sulfide concentration was based on wet sediment. Given the dry sediment density at 2.04 g/cm3 and the sediment moisture content at 58.16% (experiment data), the calculated wet hydrogen sulfide concentration was converted to dry sulfide concentration.

$$\mathbf{253.57}\ \frac{\boldsymbol{gH_2S}}{\boldsymbol{m^3}} \times \frac{cm^3}{1.46\ g\ wet\ sed} \times \frac{m^3}{100^3 cm^3} \times \frac{1000 mg H_2S}{gH_2S} \times \frac{1g\ wet\ sed}{(1-0.5816) g\ dry\ sed} \times \frac{32.065 mgS}{34.065 mg\ H_2S} = \mathbf{0.391}\ \frac{\boldsymbol{mgS}}{\boldsymbol{g\ dry\ sediment}}$$

The AVS background concentration for Trial 1 is 0.046 mgS/g dry. Adding the background concentration to the calculated amount resulted to 0.441 mgS/g dry (Figure 4.18).

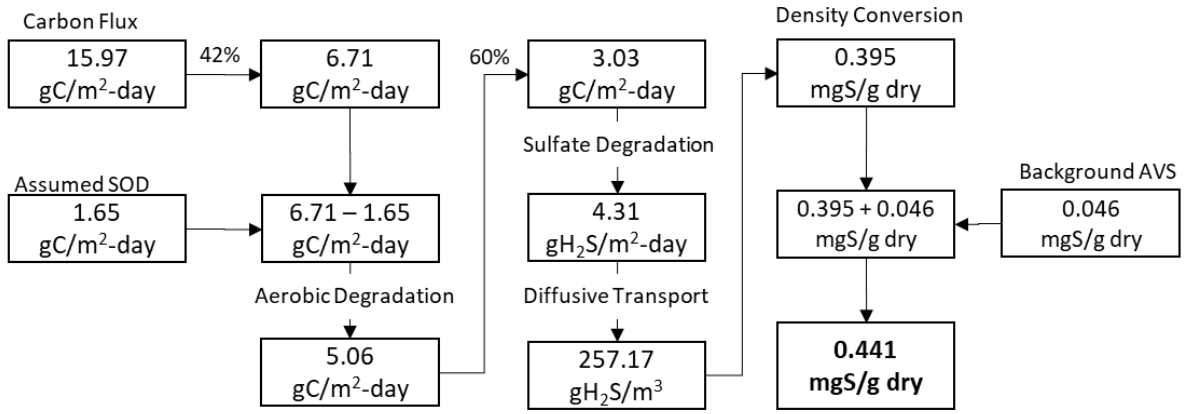

Figure 4.18. Trial 1 flowchart for the conversion of readily degradable particulate cabon flux to AVS concentration.

The final calculated AVS concentration represents the amount of AVS at the center of the cage in Trial 1. Similar calculation procedure was made to all distributed carbon flux, and as mentioned earlier in this chapter, in cases where SOD is higher than the carbon flux, the resulting AVS was set to the background AVS concentration.

In the case of Trial 3 where 59.18 gC/m^2-day is the particulate flux at the center of the cage and the average temperature is 29.83˚C, the evolution of AVS was calculated (Figure 4.19).

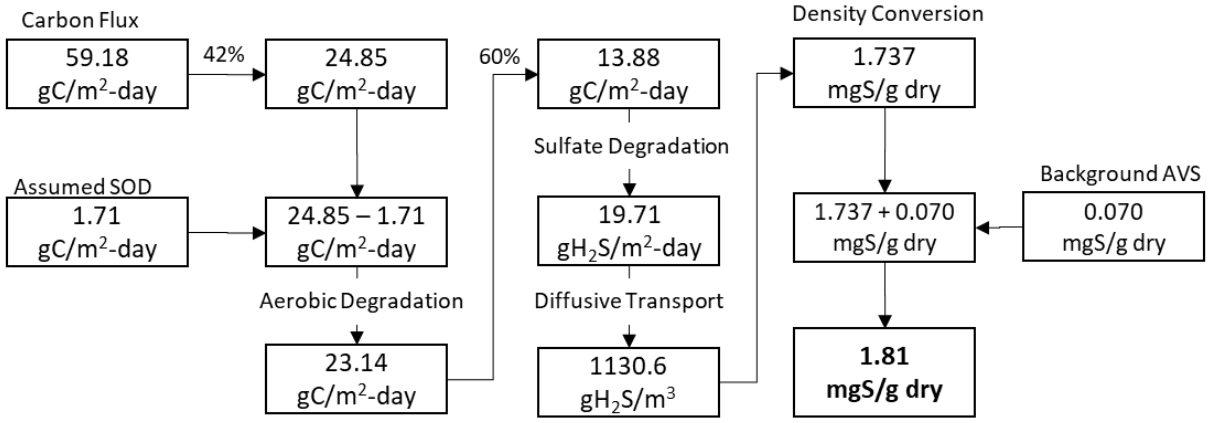

Figure 4.19. Trial 3 flowchart for the conversion of readily degradable particulate cabon flux to AVS concentration.

Figure 4.19 shows that the maximum AVS concentration in Trial 3 is 1.81 mgS/g dry. Based in the procedure, SOD has a small effect on the sediment degradation due to the large amount of carbon flux. Only 7.9% of the readily degradable carbon flux was degraded aerobically. However, in Trial 1, since the carbon flux Is lower, 28.12% of the readily degradable carbon flux was degraded with O_2. This signifies that the larger the carbon flux is, the lower is the effect of aerobic degradation which favors the production of hydrogen sulfide (Rickard and Morse 2005).

Converting the carbon fluxes into degradable carbon from both trials resulted to 6.71 and 24.85 kgC/m^2-year, which is similar to a study done in Seto Inland Sea which ranges from 2 to 57 kgC/m2-year. In addition, the maximum AVS concentration found in Tashima Area at the highest carbon flux was found to be around 1.6 mgS/g dry, which is low considering that the carbon flux is at 57 kgC/m^2-year (Pawar et al. 2002). This can be explained through the seasonal variations in Seto Inland Sea where the amount of the diffused oxygen is high during cold seasons. And since there is high amount of oxygen in the sediment, the capacity of the sediment to undergo aerobic degradation is increased thus limiting the production of hydrogen sulfide. In the case of tropical regions, the amount of available oxygen in the sediment is constant all year round since the temperature variations is around ± 2˚C, thus the capacity of the sediment for aerobic degradation does largely not vary.

The procedure to estimate the AVS evolution from organic waste was used for the model-setup for milkfish cage aquaculture. For this model requires a measurable parameter for such estimation, the dissolved oxygen concentration was included as a variable factor together with the standard deviation of the water current.

4.2.3.b.Comparison of estimated and experiment AVS data

The amount of the estimated degradable carbon flux at each of the AVS sampling coordinate points based on sampling day were tabulated in Tables 4-26 and 4-27, for Trials 1 and 3, respectively.

Table 4-26. Trial 1 calculated degradable particulate carbon flux at given x and y coordinates corresponded to AVS sampling day. Values in zeroes are very small and negligible carbon fluxes.

Days	(0,0)	(2.5,2.5)	(7.3,4.0)	(12.1,5.4)	(26.4,9.8)	(52.8, 17.1)
21	2.43	1.71	0.75	0.30	0.01	0.00
34	2.43	1.67	0.71	0.28	0.01	0.00
49	2.39	1.61	0.66	0.26	0.01	0.00
63	2.63	1.76	0.71	0.28	0.01	0.00
77	2.76	1.83	0.72	0.28	0.01	0.00
91	3.20	2.14	0.86	0.34	0.01	0.00
105	3.50	2.35	0.95	0.37	0.01	0.00
119	3.84	2.55	1.02	0.40	0.01	0.00
133	4.06	2.68	1.05	0.41	0.01	0.00
147	4.78	3.19	1.28	0.50	0.01	0.00
161	5.34	3.58	1.45	0.57	0.01	0.00
175	6.08	4.13	1.71	0.67	0.01	0.00
189	6.71	4.59	1.92	0.76	0.01	0.00

Table 4-27. Trial 3 calculated degradable particulate carbon flux at given x and y coordinates corresponded to AVS sampling day. Values in zeroes are very small and negligible carbon fluxes.

Day	(0,0)	(7.5,5)	(17.5,9)	(31.4,12.3)	(55.3,19.6)
28	11.51	5.78	1.18	0.05	0.00
55	17.23	8.73	1.80	0.07	0.00
83	24.85	13.04	2.78	0.11	0.00

The zero values in Tables 4-26 and 4-27, implies that the amount of degradable carbon flux at these points were low. These low values were expected since the further the point is from the center, the less is the amount of carbon flux and, in the case of Trial 1, estimated diffusivity coefficient is low.

In the previous chapter, it was discussed that the DO concentration needs to be assumed to calculate for the SOD. Values in Tables 4-26 and 4-27 which are less than the SOD resulted to zero AVS production. However, there is a natural increase of AVS concentration that needs to be accounted and that is the background concentration which was taken from the average AVS of the farthest sampling point. Instead of having zero AVS, the background concentration was added to compensate to these natural AVS increase. Trials 1 and 3 have AVS background concentration at 0.046 and 0.070 mgS/g dry.

From the previous chapter, the procedure for estimating the AVS concentration was then used to calculate the production of AVS at each sampling point and were tabulated in Tables 4-28 and 4-29 for each trial.

Table 4-28. Trial 1 calculated AVS from the degradabable carbon distribution evaluated at AVS sampling points using probability density function.

Days	(0,0)	(2.5,2.5)	(7.3,4.0)	(12.1,5.4)	(26.4,9.8)	(52.8, 17.1)
21	0.107	0.050	0.046	0.046	0.046	0.046
34	0.107	0.048	0.046	0.046	0.046	0.046
49	0.104	0.046	0.046	0.046	0.046	0.046
63	0.123	0.055	0.046	0.046	0.046	0.046
77	0.133	0.060	0.046	0.046	0.046	0.046
91	0.168	0.085	0.046	0.046	0.046	0.046
105	0.191	0.101	0.046	0.046	0.046	0.046
119	0.217	0.117	0.046	0.046	0.046	0.046
133	0.234	0.126	0.046	0.046	0.046	0.046
147	0.290	0.166	0.046	0.046	0.046	0.046
161	0.334	0.197	0.046	0.046	0.046	0.046
175	0.393	0.240	0.051	0.046	0.046	0.046
189	0.441	0.276	0.068	0.046	0.046	0.046

Table 4-29. Trial 1 calculated AVS from the degradabable carbon distribution evaluated at AVS sampling points using probability density function.

Day	C(0,0)	C(7.5,5)	C(17.0,7.9)	C(31.4,12.3)	(55.3,19.6)
28	0.8055	0.3758	0.0702	0.0702	0.0702
55	1.2346	0.5971	0.0763	0.0702	0.0702
83	1.8073	0.9201	0.1504	0.0702	0.0702

It can be observed that most of the calculated values from Trial 1 is the background concentration. As what was mentioned from the previous chapter, the degradable carbon flux for this trial is low and SOD concentration played a major role in particulate carbon degradation. In addition, with diffusivity of 0.082 m^2/s, the amount of dispersed carbon flux is limited around the cage area. A distribution graph was made to show the difference between the estimated and experiment data on days 21, 77, 133, and 189. Figure 4.20 shows that the estimation has a good correlation with the lower values of AVS concentration, while it has overestimated the AVS concentration at the center of the cage on day 189. The distribution graph also showed that there is no AVS production at around 12m away from the cage center based on the sediment sampling points. However, considering only the distance relative to the cage and the carbon flux at day 189 (Figure 4.21), the distance wherein no AVS production was found past 9.1m. Since this distance is based on the cage orientation and the horizontal axis is where the length of the cage was set, it can be used radially to identify the distance

to where the carbon flux has no sulfate degradation on both directions. This distance can also aid farmers where to place the next culture cage to prevent high organic matter accumulation coming from series of multiple cages. Projecting the edge of the cage to the sediment, at this point, the AVS concentration is 0.344 mgS/g dry. In practical use, since it is difficult to get samples exactly at the cage center, this concentration can also be an aide for ease of monitoring the sediment quality.

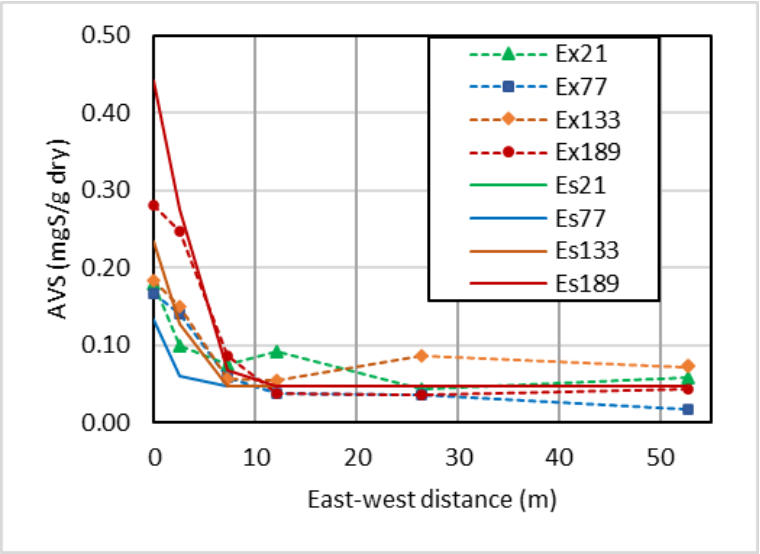

Figure 4.20. Trial 1 AVS distribution of experiment (Ex) and estimated (Es) values at day 21, 77, 133 and 189.

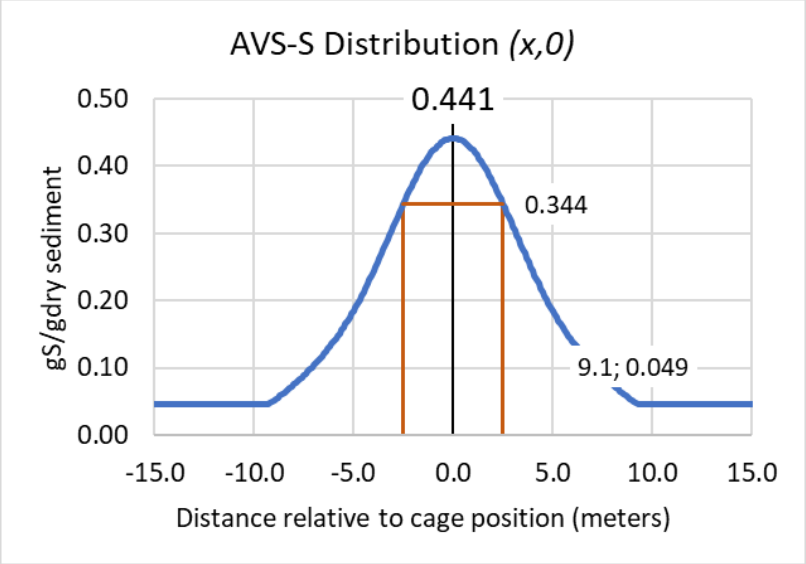

Figure 4.21. Trial 1 final AVS concentration and distribution with background concentration.

To test for the goodness of fit of the estimated AVS concentration with the experiment data, the coefficient of determination (R^2) was computed, and F-test was done. The assumed values at the center of the cage were not included for the following analysis.

Table 4-30. Trial 1 AVS F-test results.

	Actual	Calculated
Mean	0.074	0.061
Variance	0.003	0.002
Observations	65	65
df	64	64
F	1.337	
P(F<=f) one-tail	0.124	
F Critical one-tail	1.513	

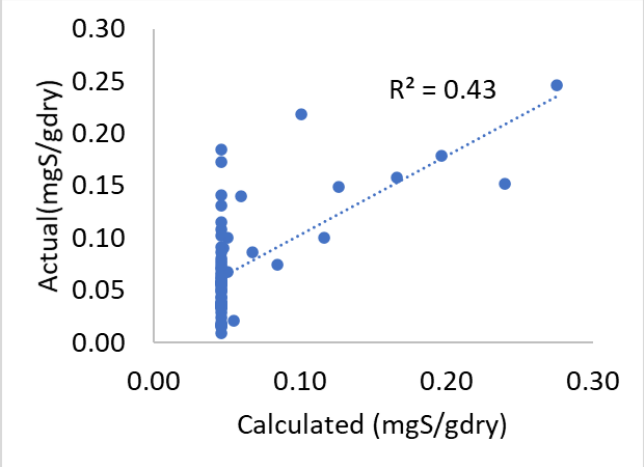

Figure 4.22. Trial 1 comparison of experiment and estimated AVS concentrations.

Figure 4.22 shows that the coefficient of determination (R^2) is 0.432. This shows that the estimated AVS concentration is moderately correlated with the experiment values. It can also be observed that most of the points were clustered on the lower AVS concentration which is mostly the background concentration from the calculated values. This is where the diffusivity coefficient matters the most, since most of the particulate carbon settled near the cage, the increase of AVS concentration on the points further away from the cage was not compensated. In addition, as a rule for estimating the diffusivity coefficient, the smaller is the area being analyzed for dispersion, the lesser the diffusion (Okubo et al. 1983; Yanagi et al. 1982). Since the sediment sampling points increments were close to

the cage, the resulting current standard deviation is also low (0.028 m/s), thus resulting to points cluster at low AVS concentration.

In Table 4-30, F-test results shows that the variances of both actual and calculated values were equal. Since the F-critical one-tail is greater than the F value (1.513 > 1.337), it can be concluded that the actual AVS data and the calculated AVS are not significantly different.

In the case of Trial 3, at day 28, the calculated AVS concentrations were underestimated, however, most of the points in days 55 and 83 were observed with moderate correlation (Figure 4.23). It can also be observed in Figure 4.24, that the actual AVS and calculated AVS values has a better correlation compared to Trial 1 with R^2= 0.59.

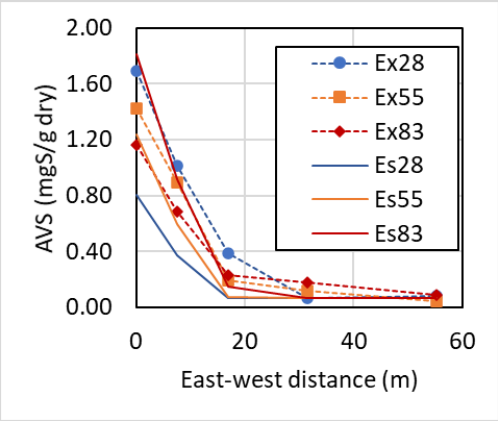

Figure 4.23. Trial 3 AVS distribution of experiment (Ex) and estimated (Es) values.

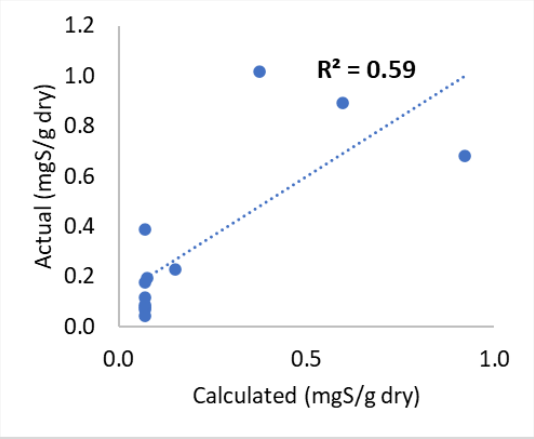

Figure 4.24. Trial 3 comparison of experiment and estimated AVS concentrations.

Table 4-31. Trial 3 AVS F-test results

	Actual	Calculated
Mean	0.332	0.218
Variance	0.117	0.076
Observations	12	12
df	11	11
F	1.533	
P(F<=f) one-tail	0.245	
F Critical one-tail	2.818	

Using F-test to check for the variance between the actual and calculated AVS values, it was found that they are not statistically different with F-critical one-tail greater than F-value (2.82 > 1.53). This proves that the current standard deviation of 0.0342 m/s in Trial 3, through the dispersed particulate carbon, was able to compensate for the increase of AVS concentration not only near the cage, but also in its vicinity. Though day 28 was underestimated, most of the calculated AVS values were close to the actual values. Based also in Figure 4-24, there are fewer points in cluster at low AVS concentrations compared to the results in Trial 1, which proves that the particulate carbon from the cage were able to disperse until the 25m sampling point. Considering the final carbon flux at day 83, the maximum AVS concentration is 1.807 mgS/g dry (Figure 4.25). It can also be observed that the concentration at the edge of the cage is 1.191 mg/S g dry and the distance to where the organic matter flux has no effect on hydrogen sulfide production at 21.5m away from the cage center.

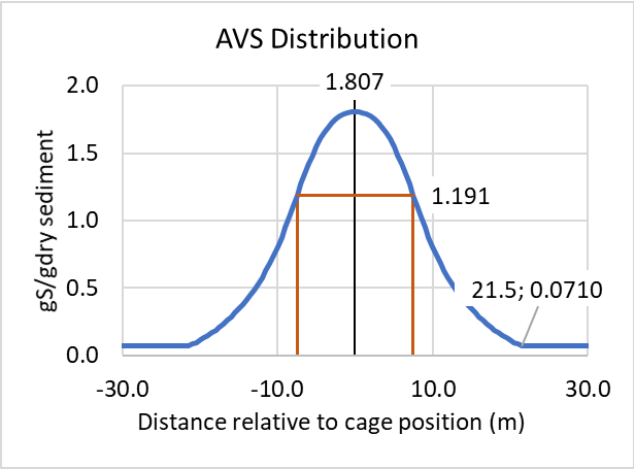

Figure 4.25. Trial 1 final AVS concentration and distribution with background concentration.

4.3 Milkfish feed and faeces sinking rates

The sinking rates mass ratio discussed from the previous chapter were based on salmon theoretical data. For the estimation of diffusivity coefficient of the experiment site, milkfish feed and faecal sinking rates are necessary.

An experiment was conducted to measure the sinking rates of milkfish feed pellet and faecal material using a graduated glass cylinder (Kodama 2012). Feed and feces were collected from the experimental tanks and was poured on the water surface in the cylinder. The time taken by the settling material to reach the bottom of the cylinder were then recorded and the sinking rates were averaged and calculated.

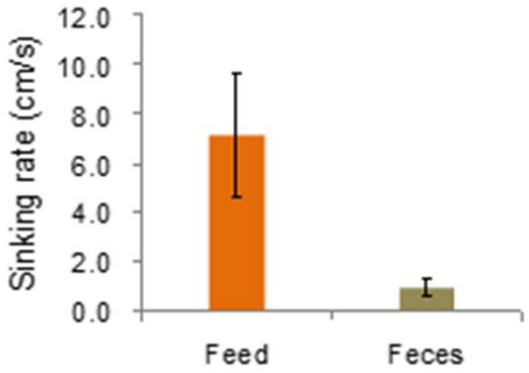

Figure 4.26. Milkfish feed and faeces sinking rates

Figure 4.26 shows the results of the sedimentation experiment. The milkfish feed sinking rate was 7.1 ± 2.5 cm/s (n=10) and the milkfish faeces sinking rate was 0.9 ± 0.3 cm/s (n=9). These results were lower compared to the assumed sinking rates of salmon studies which are 10 cm/s for the feed and 2-4 cm/s for the faeces.

Using the particulate carbon flux of Trials 1 and 3, with 139.24 and 182.11 g/m^2-day respectively, using the probability density function and assigning the feed sinking rate at 7.1 cm/s and the faecal material at 0.9 cm/s, the diffusivity coefficients were calculated. The current standard

deviations were 0.008 and 0.0104 m/s for Trials 1 and 3, respectively. Compared to the estimated current standard deviation using salmon feed and faeces sinking rates, these estimated values are 4 times lower. The reason for these variations is caused by the lower sinking rates of milkfish feed and faeces. Since the AVS relative concentration is constant, to compensate to the particulate carbon flux distribution, when the sinking rates are minimal, particle diffusion also slows down. It follows that, since the current standard deviation is low, the probability of the particulate carbon at the center of the cage is also high. In fact, the calculated AVS concentration at the center of the cage at day 189 is higher at 0.673 mgS/g dry (Figure 4.27) compared to 0.441 mgS/g dry (Figure 4.21) computed from the salmon sinking rates. Similarly, the distribution shows the distance where there is no AVS generation was found at 9.1 meters away from the center of the cage on both estimations.

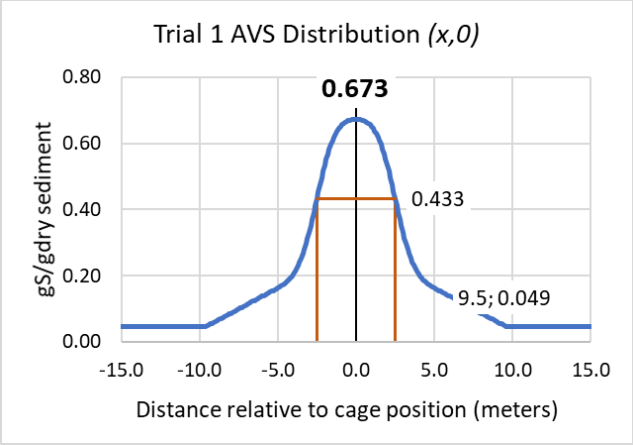

Figure 4.27. Trial 1 AVS distribution at day 189 using the calculated diffusivity coefficient with milkfish feed and faeces

The variations of the diffusion behavior can also be accounted on the feed pellet diameter used for salmon farming. Relationship between feed pellet diameter and settling velocity allow detailed estimation of diffusion of both feed and faeces (Cromey and Black 2005). In salmon farming, the mean feed pellet diameter was determined around 7 mm, while in milkfish farming the diameter can range from 3-4mm. This difference of feed sizes results to a slower diffusion rate in the case of milkfish wastes.

Table 4-32. Trial 1 calculated and data AVS statistical F-test with milkfish waste sinking rates

	Actual	Calculated
Mean	0.074	0.065
Variance	0.003	0.003
Observations	65	65
df	64	64
F	1.016	
P(F<=f) one-tail	0.475	
F Critical one-tail	1.513	

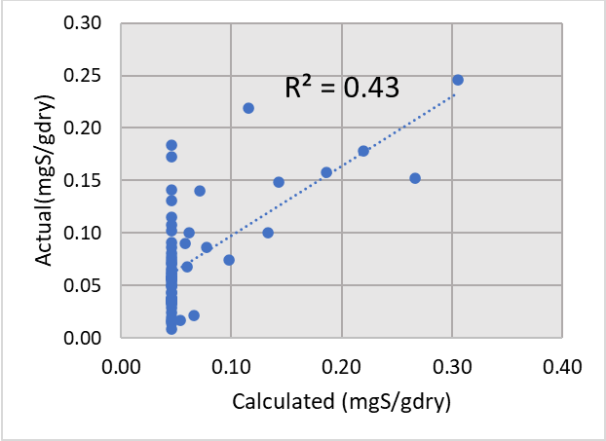

Figure 4.28. Comparison of computed AVS and data of Trial 1 using milkfish waste sinking rates

In Figure 4.28, the coefficient of determination (R^2) is 0.43 which is not different when compared to salmon waste sinking rates (R^2 = 0.43). The F-test (Table 4-32) also showed that F critical is greater than F (1.51 > 1.02) which means, the calculated and actual AVS data are not significantly different. Statistically the estimation of AVS generation for Trial 1 are not significantly different which means that the procedure for the estimation can be applicable to estimate the generation of AVS.

For Trial 3, at day 83, the calculated AVS concentration at the center of the cage was 1.81 mgS/g dry (Figure 4.29) which is equal compared to the previous estimation using salmon waste sinking rates. However, the distance where there is no AVS generation was found at 22 meters away from the cage center which is further by a meter from the previous estimation. Since the milkfish waste sinking rates were slower compared to salmon sinking rates, the distance of diffusion is higher. In Figure 4.30, it shows that R^2 value is 0.58 which is slightly lower than the previous which is 0.59.

This shows that the calculated values have relatively stronger correlation than that of the previous estimation. Moreover, based on the F-test results in Table 4-33, the difference between F-critical and F values (2.82 > 1.53) were found to be equal compared to the values in Table 4-31 (2.82 > 1.53). These statistic results illustrate that through the use of milkfish wastes sinking rates, the distribution of particulate carbon fluxes reflects the diffusion characteristic of the experiment site.

Table 4-33. Trial 3 calculated and data AVS statistical F-test with milkfish waste sinking rates

	Actual	Calculated
Mean	0.332	0.220
Variance	0.117	0.076
Observations	12	12
df	11	11
F	1.529	
P(F<=f) one-tail	0.246	
F Critical one-tail	2.818	

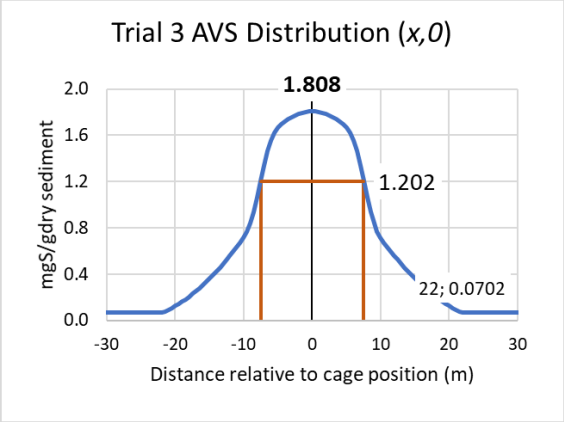

Figure 4.29. Trial 3 AVS distribution at day 83 using the diffusivity coefficient from milkfish waste sinking rates.

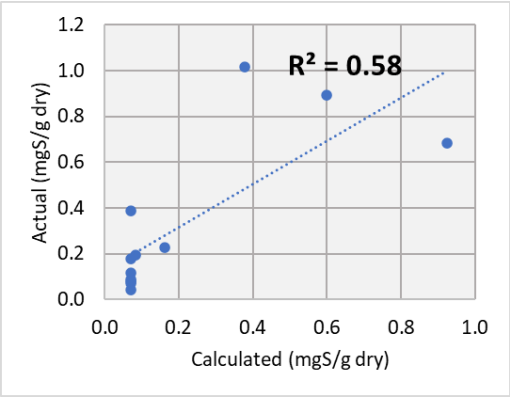

Figure 4.30. Comparison of computed AVS and data of Trial 3 using milkfish waste sinking rates.

In simulating the fate of particulate carbon waste for milkfish cage culture, 0.104 m/s current standard deviation of Trial 3was used since the estimation used the milkfish feed and feces and has higher coefficient of determination compared to Trial 1 and has fewer number of points where no hydrogen sulfide was generated. In both trials, it was also observed that there was small increase of AVS concentration on sampling points further away from the cage thus a lower current standard deviation can best illustrate the diffusion further away from the cage center in the experiment site. Moreover, this value falls within the average diffusivity coefficient on some salmon aquaculture sites found in theory (Chamberlain and Stucchi 2007; Cromey and Black 2005). Since the area exhibits stagnation with mean current velocity at 0.009 ± 0.46 cm/s, a lower diffusivity coefficient was feasible. In addition, instead of employing mass fraction for the milkfish faecal material, like in salmon waste sinking rates, it was assumed that all faecal material sinks at the rate of 0.9 cm/s and the milkfish feed pellet sinks at the rate of 7.1 cm/s. These sinking rate values limits the uncertainties in elucidating the generation of AVS from the particulate carbon flux distribution in the milkfish cage culture.

Chapter 5 - MODEL SET-UP FOR MILKFISH FARM

5.1 General calculation flow of the model

The model set-up for marine milkfish cage farming involved four sub-model processes, namely, (1) growth model, (2) carbon box model, (3) particle dispersion model, and (4) sediment degradation model. The detailed processes and inputs in each of the sub-models were discussed in the later part of this chapter.

Figure 5.1 shows the general calculation flow for the model-setup. The environmental criteria considered in the model-setup was the AVS concentration, which also served as the limiting factor to the number of fish to be cultured. The waste generated from the number of cultured fish should result to an AVS concentration that is lower than the set AVS criteria, if the criteria was not met, the simulation will tune the number of cultured fish until the criteria was satisfied. Moreover, in fish production, the marketable size of the fish to be harvested should be firstly identified before the initial stocking. This parameter is the harvest body weight and was considered as the economic criteria in the model-setup.

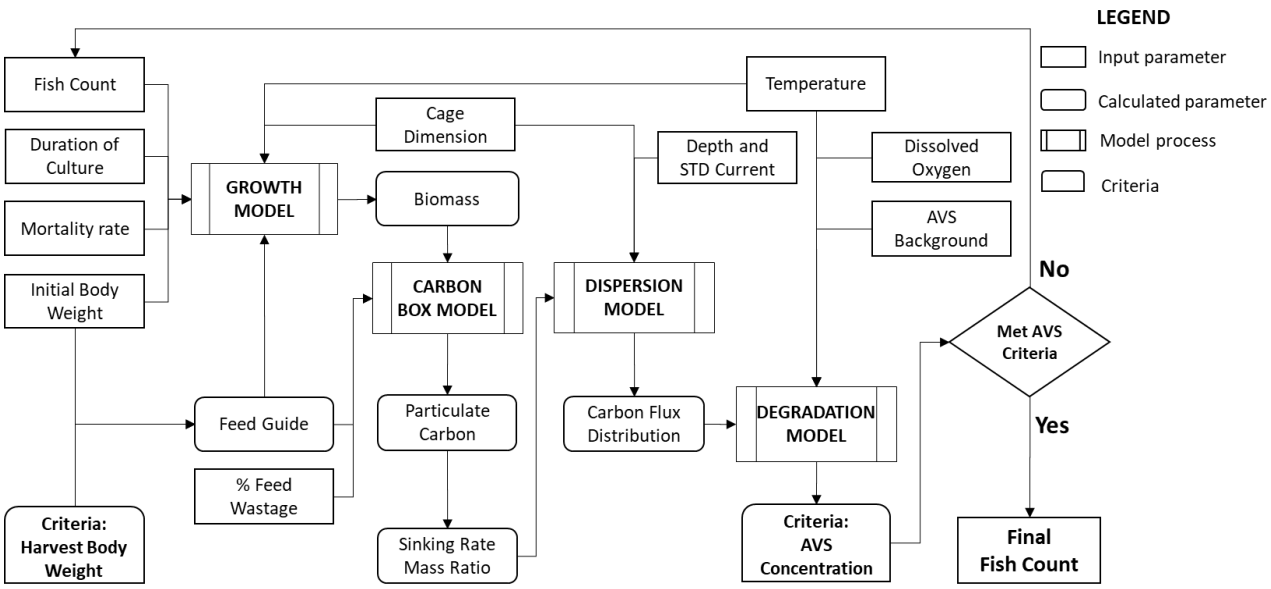

Figure 5.1. General model-setup flow chart for milkfish cage culture with fish count as a variable parameter.

The duration of culture and initial fish body weight should be identified for these parameters were used to determine the economic sustainability of the fish production, that is, to provide the capital outlay. These parameters are the key factors in determining the financial viability of the milkfish production.

Environmental factors such as temperature, dissolved oxygen, depth, current velocity standard deviation and initial AVS concentration should be also known before planning the milkfish cage production in the site. More importantly, cage dimensions should also be known before the start milkfish cage culture.

5.2 Parameters used in milkfish model set-up

5.2.1 Growth sub-model parameters

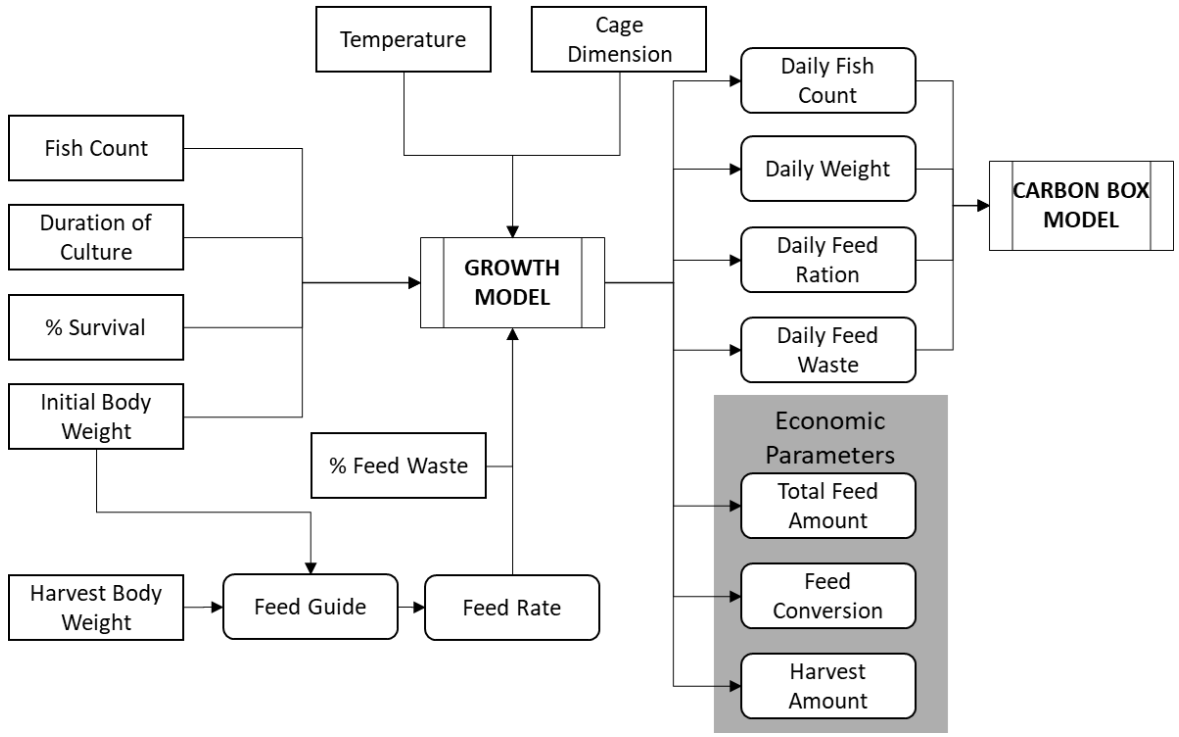

Figure 5.2. Milkfish growth sub-model calculation flow chart.

The goal of the growth sub-model is to forecast the daily weight increase of the milkfish based on the proposed logistics milkfish growth curve. Moreover, through the aide of the feed guide, the daily feed ration and daily feed wastage are also forecasted. As for the fish count, linear interpolation was employed to calculate the daily mortalities based on the estimate survival rate as was reported as daily fish count. The milkfish growth sub-model calculation flow procedure was shown in Figure 5.2. Economic parameters were also determined and served as the guide for economic viability. In the model set-up, the daily amounts calculated from the growth model were shown as inputs to the carbon box sub-model. These input parameters in the carbon box sub-model were discussed separately from the growth sub-model.

5.2.1.a.Input parameters for growth sub-model

Fish count

The number of the fish to be cultured served as the most important input and control parameter in making sure that the environmental criteria does not exceed the threshold limit. This parameter is also the final estimated result of the model set-up. This provides the farmers of the amount of capital needed for procuring the fingerlings for production. For the growth curve model, this parameter also limits the growth rate of the milkfish stocks since fish density was considered as a function for the growth estimation. Based on the theory of carrying capacity, the number of fish that can be cultured can also be considered as in its optimum once it was tuned by the model.

Initial body weight (grams)

As the number of stocks were required for fish production, the average initial body weight of milkfish should also be known. The common practice in milkfish farming was using fingerlings with 5-6 inches of total length, that is roughly around 20-35 grams of milkfish wet weight. This parameter affects the duration of culture needed to reach the harvest weight (marketable weight). In practical perspective, this factor depends on the available fingerlings from culture nurseries which are near the site of milkfish cage culture.

Duration of culture (days)

The duration of culture in days should also be known initially before the cage culture. This provides necessary information on the labor and feed expenses needed for the production. The days of culture is only the estimated days for which the production would attain the harvest body weight criteria. In the model set-up, final the days of culture can be less than the required days of culture to since the fish growth predicts the days required until the production reached limit of the environmental criteria. Commonly, duration days of culture ranges from 90-120 days.

Survival rate (%)

In milkfish production, the estimated survival rate for the whole culture duration is around 95%. This is to account for the unhealthy fish stocks which was included in the initial stocking. In practical sense, this estimated survival rate allows the farmer to estimate the number of fish stocks expected to be harvested and allows the calculation of the income from the production.

Temperature (˚C)

Temperature was considered as a function of the proposed growth curve, which illustrates the rainy and dry seasons in the Philippines. In rainy season, water temperature can reach 27˚C while in dry season, it can reach until 30˚C. It was found that a slight increase in temperature results to higher growth rate.

Cage dimensions (L × W x D)

The length, width and depth of the cage should also be known to calculate for the volume of the cage. Cage dimensions in meters, was also used to calculate for the density of fish per cage volume which also served as a factor for the milkfish growth. A high the fish density denotes higher feed competition between fish individuals and increased physical stress to the fish yielding lower growth rate. Temperature is directly proportional to the maximum attainable weight for milkfish while fish density is inversely proportional.

Feed waste, %

There are few studies in the literature on feed wastage generation. In the model-setup, 5% feed wastage was assumed to represent the worst-case scenario. Several factors can be considered from this parameter, namely, the feed quality which represents the consistency of the feed without the presence of feed powders, the handling of feeds during transportation, and most importantly the feeding management or the husbandry practices for the fish production. In practical sense, this parameter represents the uneaten feed which was fed directly to the milkfish cage.

Harvest body weight (grams)

As the criteria for fish production, the harvest body should be determined before the initial stocking which also serves as the target body weight for the model-setup. The harvest body weight served the factor for the marketable size of the milkfish. Commonly, the marketable size for milkfish ranges from 250-400 grams. The known value of this parameter allows the calculation of the feed rate through the linear interpolation of the maximum body weight and intrinsic growth rate in the feed guide, which are factors for the milkfish growth. In the model-setup, this criterion was set to be not less than the target harvest weight, thus it is expected that in some cases the set body weight in the criteria is less than estimated harvest body weight based on the duration of culture.

Feed guide

The percent feed rate for milkfish varies in ranges of the average body weight. As the cage culture progress, the growth rate of fish decreases. To account to these changes, a feed guide was necessary. In fish nutrition, as fish ages, the amount of feed intake changes from growth to metabolism. At early juvenile stages, most of feed intake goes to the growth of milkfish, and at the later stages, feed intake goes to metabolism and respiration. Table 5-1 shows the feed guide used in the model set-up. This feed guide was based on the common feed practices in milkfish cage culture. For most commercial feed manufacturer, there is a recommended feed guide for each type of feed which were based on the sizes of the milkfish. Feed type such as starter, grower, finisher, and brood

stock are commonly divided depending on the stages of milkfish juvenile growth since nutritional requirements varies with different stages. However, in the model set-up, these differences were not defined since all feeds were assumed with equal carbon and nitrogen content.

Table 5-1. Feed guide used in milkfish model-setup cage culture

ABW(g)	Feed Rate(%)
5-25	10-8
25-150	8-6
150-280	6-4
280-500	4-2

Feed rate (% average)

The average feed rate was calculated through the linear interpolation of growth based on the maximum attainable body weight (*K*). K was calculated through temperature and fish density based on the proposed growth curve. Using linear interpolation with the duration of culture, percent daily feed rates were calculated and averaged using the feed guide. The average feed rate was used as an input factor to calculate the intrinsic growth rate.

5.2.1.b.Output parameters for fish growth model

Total feed amount (kg)

Based on the feed guide, the daily feed amounts were calculated and summated, forecasting the amount of feed to be used for the whole duration of production. If the price of the feed per kilogram is known, the price of feed necessary for the production can be computed and a working capital can be planned.

Harvest amount (kg)

The harvest amount of fish or the total fish biomass is the product of the harvest body weight and the number of fish for the whole of production duration. By definition, this is the carrying capacity of the cage in the culture site. Since the aim of the model is to recommend a management scheme, the carrying capacity of the cage in the site should be determined given the environmental criteria

which in this case is the AVS concentration. As previously mentioned, the limiting factor for the AVS not to exceed the criteria was the number of cultured fish. Thus, the optimum carrying capacity of the cage in the production site is the total fish biomass to be harvested as what the model suggests.

Feed conversion ratio (kg feed/kg weight increase)

The feed conversion ratio is a parameter necessary for determining the efficacy of the feed. In most nutrition studies, feed conversion ratio is considered as the most important parameter. For milkfish aquaculture, the overall feed conversion ratio ranges from 2.0 to 3.0. In practical sense, if the ratio is 2.0, to gain 1kg of milkfish weight, 2kgs of feed is needed. The economic importance of this parameter is when there is a need to change the quality of feed in the fish production or to change the husbandry practices of the milkfish culture. In the model-setup since the feed rate varies with the average body weight, the ranges of the fish weight and the feed rate can be tuned to get the optimum feed conversion ratio. Nevertheless, the straightforward use of the feed guide was employed.

5.2.2 Carbon box sub-model parameters

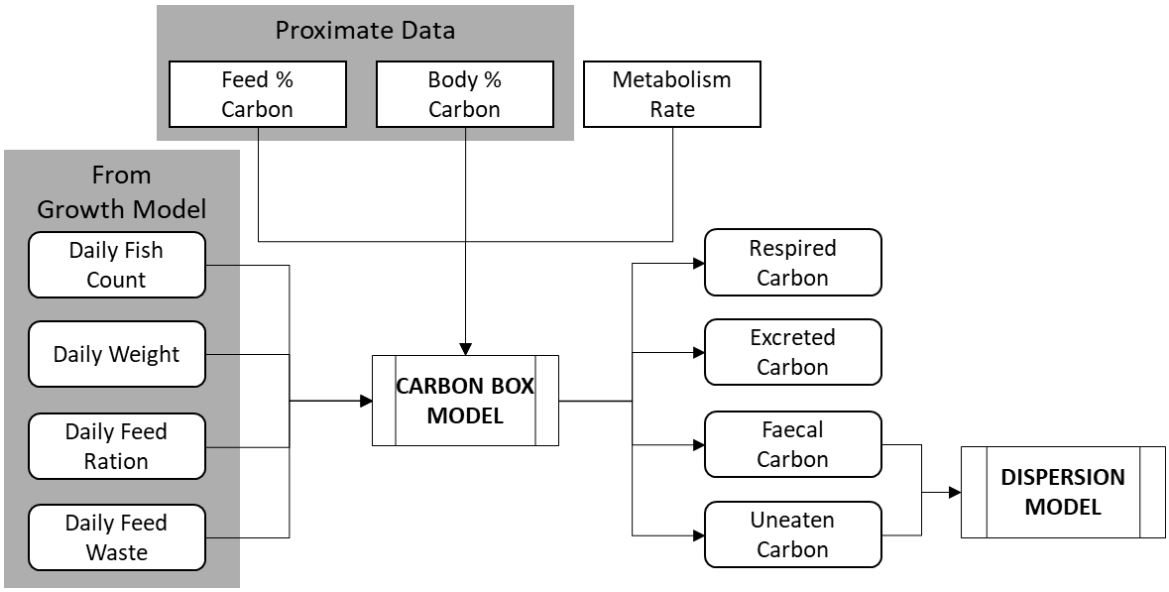

Figure 5.3. Carbon box sub-model calculation flow chart.

The goal of the carbon box sub-model is to calculate for the faecal carbon that resulted from the feed assimilation of milkfish. From the feed proximate analysis, the carbon content of the uneaten carbon can also be calculated. The faecal carbon and uneaten carbon were considered as the particulate waste and was regarded as the source of AVS production in the sediment through aerobic and anaerobic degradation. Daily carbon balance calculations were employed, and the total particulate waste were forecasted and converted to average carbon flux based on the horizontal area of the cage and the duration of culture. Figure 5.3 shows the calculation flow and the parameters for the carbon box sub-model. Faecal carbon and uneaten carbon were discusses under the particle dispersion and sediment degradation sub-model.

5.2.2.a.Input parameters for carbon balance

Daily fish count

The daily fish counts were forecasted using the estimated survival rate which was linearly interpolated and distributed based on the duration of culture from growth sub-model. In carbon box sub-model, the daily fish count was used to calculate for the daily biomass which was used for calculating the respired and excreted carbon.

Daily weight (grams)

Based on the proposed logistic growth curve for milkfish, daily average body weights were forecasted. The initial temperature and fish density were considered as averaged values and not the daily variations within the duration of culture. This parameter was used with the daily fish count to calculate for the daily biomass.

Daily feed ration and daily feed waste (kg)

Based on the feed guide, daily feed rations and feed waste with dependence on the average body weight were forecasted from the growth sub-model. The amount of feed consumed by the milkfish was calculated using the assumed feed rate wastage.

Fish body and feed carbon content (%)

These parameters are the result of carbon and nitrogen proximate analysis of milkfish feed and body. Based on the experiment results, the percent carbon in feed and fish body were 45% and 36% respectively. Given the forecasted amount of feed wastage, the uneaten feed carbon and the amount of consumed feed carbon can be estimated. The carbon content of feed and fish body were considered as the most important parameter for the carbon to proceed. In the absence of these data, calculations using apparent digestibility can also be employed, however since there are limited number of theories for milkfish feed digestibility, it is necessary that proximate analysis data should be employed.

Routine metabolism rate, RMR (gC/kg-day)

The routine metabolism rate is the amount of oxygen consumption rate of the milkfish used for metabolism and unstressed swimming activities. The amount of excreted and respired carbon can be estimated using the aerobic respiration of glucose with standard vertebrate species such as the milkfish. From oxygen consumption demand, the converted carbon consumption rate to maintain the milkfish metabolism is 1.55 gC/ kg-day. This parameter was assumed as the daily carbon demand of milkfish.

5.2.2.b. Output parameters for carbon balance

Respired carbon (kgC)

The amount of carbon needed for respiration was calculated using the respiration stoichiometry for vertebrate species. The respired carbon present in the reaction is in terms of glucose (sugar) which was converted to energy that provide the requirements for daily activities such as swimming and feeding. This implies that if the milkfish experiences physical or chemical stresses, the RMR value also increases which means that more energy is needed for milkfish to go on with its activities. This parameter has no direct effect on the immediate environment.

Excreted Carbon (kgC)

Based on the respiration stoichiometry, the amount of excreted carbon is equal to the amount of respired carbon. The excreted carbon exists in the form of carbon dioxide which can accelerate the activity of primary production through photosynthesis. In small amounts, this parameter was considered not harmful, however, in larger amounts, especially in tropical regions, this can instigate plankton bloom which has adverse effects to the fish itself. For future modeling studies this parameter can be used to elucidate the internal impacts on milkfish aquaculture.

5.2.3 Dispersion and sediment degradation sub-models

The particle dispersion and sediment degradation sub-models were discussed together in this in this chapter. The goal of the particle dispersion sub-model was to calculate the distribution of carbon flux, which was considered as an area source, while the goal of the sediment degradation sub-model is to calculate the evolution of carbon to AVS. Figure 5.4 shows the parameters involved in each sub-model.

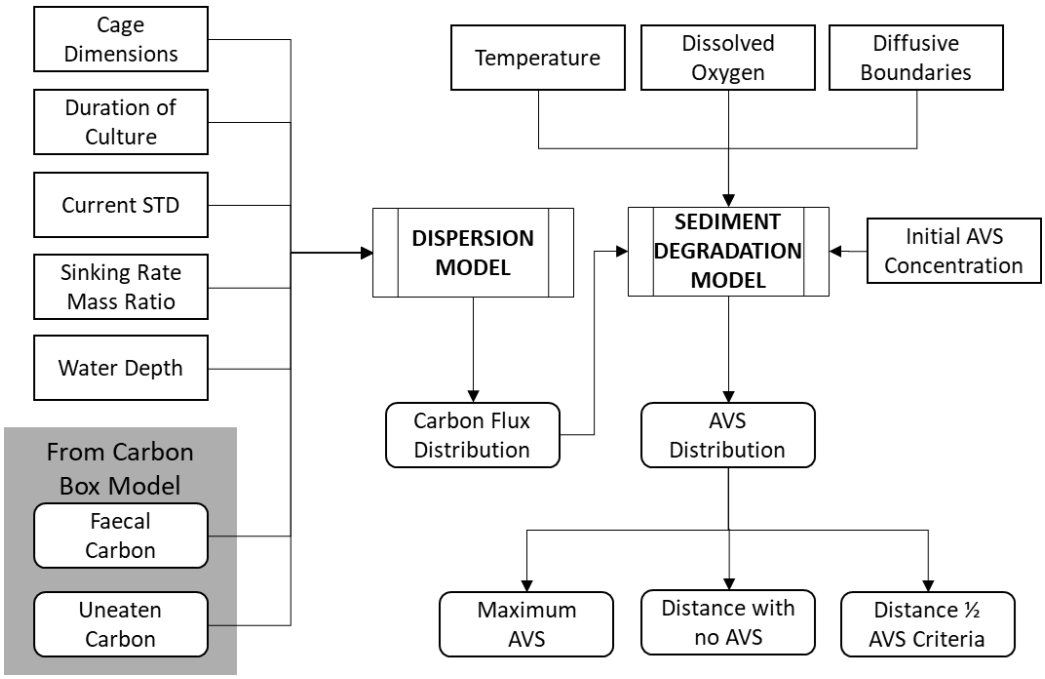

Figure 5.4. Dispersion and sediment degradation sub-model's calculation flow chart.

The particulate waste in the form of faecal carbon and uneaten carbon was converted through carbon flux and the distribution was estimated through the particle dispersion sub-model. The distributed carbon flux at each point from the center of the cage was used to calculate for the AVS generation. The distance where there is no AVS generation and the distance where half of the AVS criteria was also determined away from the center of the cage. Based on the general flow chart of the model-setup for milkfish culture. In the event where the maximum AVS concentration at the center of the cage exceeded the set AVS criteria, the model automatically tunes the number of fishes as the input parameter in the growth sub-model.

5.2.3.a.Input parameters for particle dispersion and sediment degradation sub-models

Faecal carbon (kgC)

Faecal carbon was considered as the main component of the particulate waste in the milkfish culture. Through carbon balance equations given the consumed, respired, excreted and growth carbon, the faecal carbon was estimated. In particle dispersion sub-model, it was converted into carbon flux with unit gC/m^2-day, using the duration and the horizontal area of the cage. All milkfish faeces was assumed to sink to the sea bottom and did not undergo decomposition in the water column.

Uneaten Carbon (kgC)

Uneaten carbon is the direct result of the feed carbon content and the estimated feed wastage rate. Compared to faecal carbon the amount of uneaten carbon is relatively small however, milkfish feed tends to sink faster than the faeces, this parameter has a reasonable effect on sediment degradation located just below the cage.

Cage dimensions and duration of culture

As mentioned previously, cage dimensions and duration of culture were used to calculate for the carbon flux for the whole duration of the milkfish cage culture. A larger cage and a longer duration of culture would result to a lower particulate carbon flux.

Current velocity standard deviation (m/s)

The diffusion of the particulate carbon flux was dependent on the probability density function. This parameter should be checked first before starting the cage culture. Data gathering and survey is necessary or if not available, historical data can be used. For the dispersion sub-model, this parameter was considered as a variable, however for the sake of simulation, this parameter was assumed based on the diffusivity coefficient calculated with milkfish feed and faeces sinking rate ratio and it was calculated at 0.0104 m/s.

Sinking rate mass ratio

The time it takes for the particulate wastes to settle to the seabed needs to be determined. Based on the experiment results, the milkfish sinking rate for feed pellet was found to be at 7.1 cm/s, while milkfish faeces was 0.9 cm/s. The accuracy of this data needs to be confirmed and more experimentation is needed. However, with the limited theories on milkfish feed and faecal material sinking rates, for the purpose of simulation these values were assumed.

Water depth (m)

The distance to how far the particulate waste will travel from the bottom of the cage to the seabed was needed for the particle dispersion sub-model. Water depth was considered also as an important parameter since a slight increase would result to higher particle dispersion causing lower carbon fluxes on the seabed directly below the center of the cage.

Temperature (˚C)

For the sediment degradation sub-model, oxygen and hydrogen sulfide diffusion were temperature dependent. It was assumed that the average temperature in the water column was equal to the seabed temperature thus this temperature is equal to the temperature used in the growth sub-model. However, if there is available data in the site for seabed temperature, it can be different from the water column temperature.

Dissolved oxygen (mg/L)

Dissolved oxygen plays an important role in sediment aerobic degradation. The concentration of dissolved oxygen was later converted to sediment oxygen demand. In sediment degradation reaction, the sediment oxygen demand was then converted to the aerobic carbon flux. This carbon flux indicates the amount of carbon that can be degraded aerobically. However, if the particulate carbon flux is high, the effect of aerobic degradation is minimal thus AVS generation was expected to be high. In practical usage, dissolved oxygen near the seabed should be known or if not available, it can be assumed that the dissolved oxygen constant all throughout the water column.

Diffusive boundary layers

The diffusive boundary layer between the water and sediment interface was assumed at 0.3mm based on theory. At this water-sediment interface the dissolved oxygen concentration diffuses at this distance to the sediment. For hydrogen sulfide diffusive boundary layer, 1 cm depth was assumed. As discussed from the previous chapters, this depth is the sediment thickness where AVS concentration was measured as per theory suggests. This depth accounts all the possible generated AVS in the absence of sedimentation rates.

Initial AVS concentration (mgS/g dry)

In the cage culture site, the initial sediment AVS is an important parameter before deciding to start milkfish production. Healthy sediment should have an AVS concentration below 0.2 mgS/g dry. To allow cage culture operations, initial sediment AVS concentration should be low enough to allow aerobic degradation. In many cases, sediment AVS analysis are not available for farmers, so an ocular inspection of the sediment health is necessary. If the sediment exhibits a dark thick black layer, these signifies that the AVS concentration is high. However, if the area was assumed to be pristine before the start of production, initial AVS concentration can be negligible. If sediment AVS concentration is greater than 0.2 mgS/g dry, the model predicts a lower number of fish to be cultured.

5.2.3.b.Output parameters for particle dispersion and sediment degradation sub-models

Carbon flux distribution (gC/m^2-day)

The carbon flux distribution served as an output parameter of dispersion sub-model and an input parameter to the degradation sub-model. It was calculated using the probability density function and considering the carbon flux as an area source. As an input to the degradation sub-model, the distributed carbon flux at each point moving away from the center of the cage was used to calculate for AVS generation. In points where carbon flux is lower than the SOD, it was presumed to have no AVS production.

AVS distribution (mgS/g dry)

The AVS concentration evolved from the particulate carbon flux distribution was calculated. If no AVS production was observed, the lowest AVS concentration is that of the initial. Since it was assumed that there was unidirectional current velocity in the aquaculture site, the seabed directly below the center of the cage was assumed to have the maximum concentration. If the maximum AVS concentration exceeded the AVS criteria, the model-setup tunes the number of fishes to be cultured. The AVS criteria set as a control parameter focuses on this point. The distance where no AVS generation was also calculated. In addition, the distance where half of the criteria was also determined to aid farmers to decide where to place the next cage with same dimensions to ensure that the environment criteria will not be exceeded when multiple cages were positioned close to each other.

5.3 Milkfish Cage Simulation

The milkfish cage model-setup was created using Microsoft Excel. The dashboard of the simulator was shown in Figure 5.5. The important variable input parameters were divided in to three groups namely, production or culture, cage dimensions and site parameters. The criteria considered were the AVS concentration and the harvest body weight (ABW).

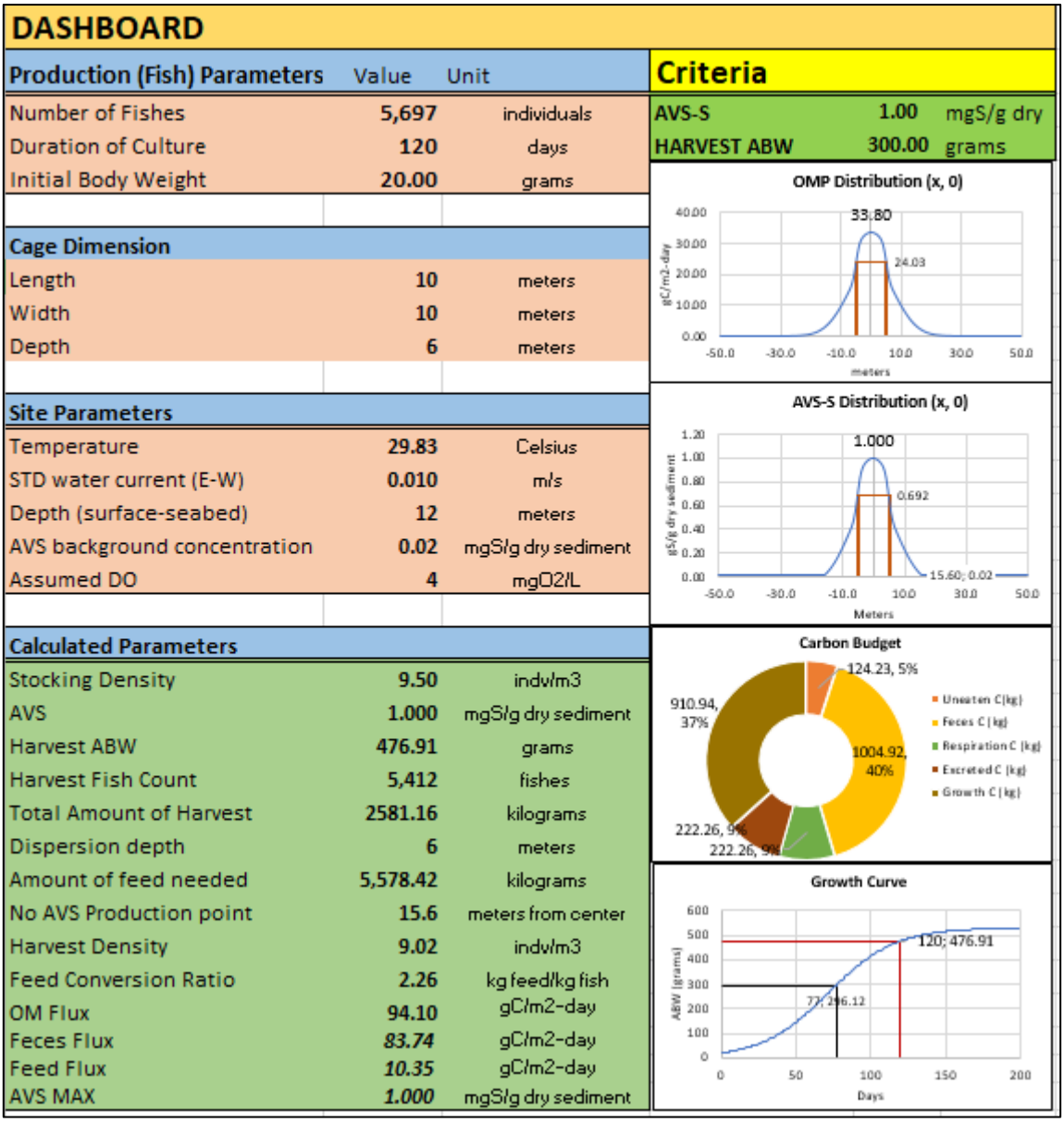

Figure 5.5. Milkfish model-setup dashboard.

The dashboard also shows the carbon flux and AVS distribution that would serve as basis for the extent of AVS generation. A pie chart of the carbon budget was included to give valuable information on the efficiency of the husbandry practices done with the milkfish culture. Moreover, the growth curve was also presented which can give an idea of which days the targeted harvest weight was reached. It also includes the peak where the duration of culture reached the maximum days and

the body weight at that point was also determined. For this example, the duration of culture and the target harvest body weight was both satisfied at a single point.

The usage of this program starts with setting the environmental and harvest criteria. Then, the production/culture parameters, cage dimensions and site parameters can be entered. For the initial conditions, the number of fish to be cultured can also be entered, nevertheless the model will compute for the exact number once the Excel Solver was run.

The economic sustainability can be computed based on the calculated parameters, more importantly, the number of fish to be cultured and harvested, amount of feed needed, and the number of cage units. Table 5-2 shows the unit price for the calculation of investment requirements and revenues from the milkfish cage culture for a 10 × 10 × 6m cage as suggested on the Milkfish Sea Cages Culture. The miscellaneous costs include the feed and milkfish fingerlings transportation cost to the cage culture area, cage maintenance cost and marketing expenses. The cage and nets can be used in 5 years with 2-3 cropping per year, thus continuous milkfish culture would yield more income for the farmers from the first cropping. The working capital includes fingerlings, feed, and labor costs. The fingerlings costs may vary from 5 to 8 PhP depending on the availability of juveniles.

Table 5-2. Basic unit prices for milkfish cage culture (Philippine Peso)

CAPITAL OUTLAY (average life span = 5 years)	
Bamboo cage frame with floats and mooring system	₱ 55,000.00
Net cage (10 × 10 × 6m)	₱ 59,750.00
Motorized boat (transportation of fingerlings and feeds)	₱ 25,000.00
Subtotal	₱ 139,750.00

WORKING CAPITAL (per crop)	Unit Price
Fingerlings (individuals)	₱ 5.00
Feeds (kg)	₱ 20.00
Maintenance (5% of capital outlay)	₱ 6,987.50
Family Labor (daily)	₱ 100.00
Marketing Expenses	₱ 66,334.00

SALES	Unit Price
Harvest Biomass (kg)	₱ 100.00

5.3.1 Single Cage Simulation

The simulation for a single net cage was run using the conditions of culture parameters, cage dimensions and site parameters presented in Figure 5.6. For the simplification of the model results, a two-dimensional figure was used. In this case the vertical coordinate (y-axis) was not considered.

The harvest criteria were set to 300g and the environmental AVS criteria was set to 0.20 mgS/ g dry. The model calculated for the number of fishes to be cultured which is 923 fishes with 382 kg of feed requirements. The expected harvest body weight is 300 grams in 73 days of culture based on the results of the growth curve. The harvest biomass (carrying capacity) of the cage was estimated at 230 kg of fish. In this scenario, the AVS criteria was found to be the limiting factor for controlling the number of fish to be cultured. Since the AVS criteria was set and 0.20, this is the maximum concentration attainable. The seabed located directly below the edge of cage has 0.11 AVS. In cases where seabed sampling needs to be employed, taking samples at the exact cage center has proven to be difficult, however, it easy easier to get sediment samples at the sides of the cage, thus this point was also considered. The figure also shows that at 4.2m away from the cage center, the AVS concentration is equal to the initial. This is the point where AVS production is zero. It was also shown that at 2.8m, the AVS is half of the criteria. If there is a plan to put another cage from production, the distance from center to center should be 5.3m as to control the AVS concentration below the criteria.

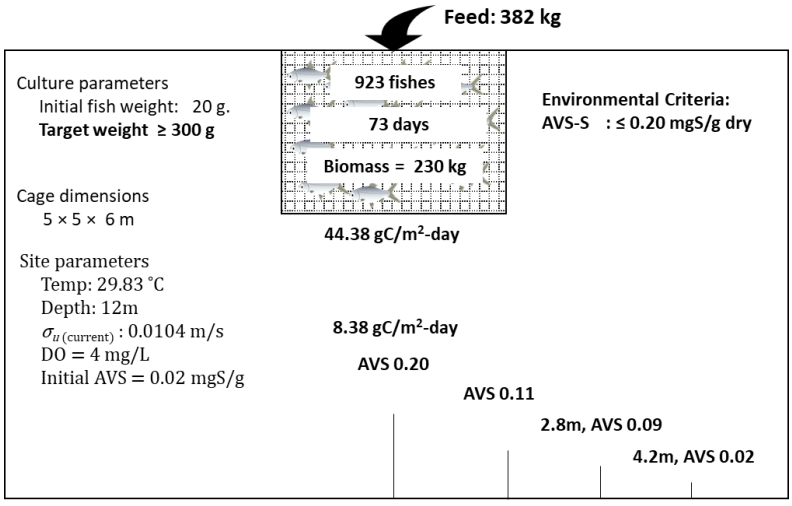

Figure 5.6. Simulation results for one 5x5x6m milkfish cage with set conditions.

Based on Table 5-2, the economic sustainability for single cage was analyzed. The capital outlay was suggested for the cage with dimensions of 10 × 10 × 6m thus it was assumed that the production will be 4 times the calculated biomass. The result of the simulation shows a biomass of 230 kg, thus for the larger cage, it will be 920 kg. Table 5-3 shows the summary of the expenses and the expected income from the 4-cage culture. The table shows a negative income on the first cropping, this implies that a 5 × 5 × 6m cage with AVS 0.20 as environment criteria is not economically viable. This also shows that the working capital is greater than sales which denotes that continues culture would still result to loses. As previously mentioned, the cage and net can be used for 5 years, however, if we remove the cage and net expenses for the next cropping, it will still result with negative income. This implies that in all forms of food production, the more cultured species and the bigger is the place of culture would result to higher income. However, since the limiting factor is the AVS criteria which is 0.20, the resulting number of stocks that can be culture is limited due to its effect on the sediment bottom. To increase the number of stocks, another possible criteria should be considered in the simulation.

Table 5-3. Economic analysis for single cage milkfish culture at AVS 0.20

WORKING CAPITAL (per crop)	Unit Price	Unit	
Fingerlings (individuals)	₱ 5.00	3692	₱ 18,460.00
Feeds (kg)	₱ 20.00	1528	₱ 30,560.00
Maintenance (5% of capital outlay)	₱ 6,987.50	(-)	₱ 6,987.50
Family Labor (daily)	₱ 100.00	72	₱ 7,200.00
Marketing Expenses	₱ 66,334.00	(-)	₱ 66,334.00
Subtotal			**₱ 129,541.50**

SALES	Unit Price	Unit	
Harvest Biomass (kg)	₱ 100.00	920	₱ 92,000.00

SALES	₱ 92,000.00	
CAPITAL OUTLAY		₱ 139,750.00
WORKING CAPITAL		₱ 129,541.50
INCOME	**-₱ 177,291.50**	

In the next simulation, the environmental AVS criteria was adjusted to 1.0 with the rest of the parameters were kept constant. Figure 5.7 shows the result of such simulation.

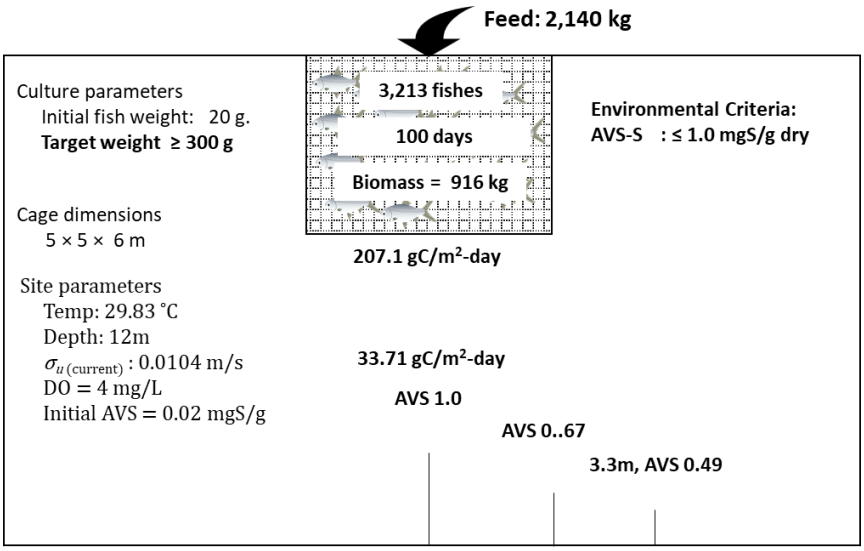

Figure 5.7. Simulation results for 5x5x6m cage with AVS 1.0 criteria

The results of the simulation with AVS 1.0 as criteria showed a harvest biomass of 916 kg with 3,213 stocking number of fishes and 100 days of culture. The AVS concentration at the edge of the cage was calculated at 0.67 and 3.3m away from the center is the half concentration of the criteria. The distance of the 2nd cage that can be place adjacent to this one without accumulation of AVS concentration is approximately 1.6m away.

Using the unit prices for the 10 × 10 × 6m cage, the resulting values were multiplied by 4.

Table 5-4. Economic analysis for 4 cages of 5 x 5 x 6m at AVS 1.0 criteria

Working Capital (per crop)	**Unit Price**	**Unit**	
Fingerlings (individuals)	₱ 5.00	12852	₱ 64,260.00
Feeds (kg)	₱ 20.00	8560	₱ 171,200.00
Maintenance (5% of capital outlay)	₱ 6,987.50	--	₱ 6,987.50
Family Labor (daily)	₱ 100.00	120	₱ 12,000.00
Marketing Expenses	₱ 66,334.00	--	₱ 66,334.00
Subtotal			**₱ 320,781.50**
Total Investment (Outlay + Working)			**₱ 460,531.50**

Sales	**Unit Price**	**Unit**	
Harvest Biomass (kg)	**₱ 100.00**	**3664**	**₱ 366,400.00**

Sales	₱ 366,400.00	
Capital Outlay		₱ 139,750.00
Working Capital		₱ 320,781.50
Net Income 1st crop	-₱ 94,131.50	
Net Income subsequent crop (till cage life span)	₱ 45,618.50	
1st year net income (2 crops/year)	-₱ 48,513.00	
Annual income after 1st year (2 crops/year)	₱ 91,237.00	
Income in 5 years	**₱ 316,435.00**	

The assumption of the 2 crops per year was specified to give an ample time for the sediment to naturally degrade the available organic matter without any marine cage waste accumulation. In nature AVS production will reach a point of equilibrium wherein in AVS generation is equal to the AVS degradation rate of reaction.

For continuous milkfish production for the 5-year lifespan of the cages, based on Table 5.4, the total income is 316,435 Philippine peso. The economic analysis also shows that to have an income on the first crop, the production should yield around 5 tons to compensate for the capital outlay. It was specified in the Milkfish Culture in Sea Cages flyer; the production estimate was given at around 9 tons and the amount of investment was estimated at 830,000 pesos. However, the estimates used in the flyer are based only on economic sustainability and environmental criteria were not included.

5.3.2 Multiple Cages Simulation

It was concluded from the results that a single net cage it was not economically sustainable. For the next simulation, four 5 × 5 × 6m net cages were position together to get a 10 × 10 × 6m net cage. AVS criteria was set to 1.0 and all conditions were set equal to the previous simulation. Figure 5.8 shows the simulation results for the multiple cages.

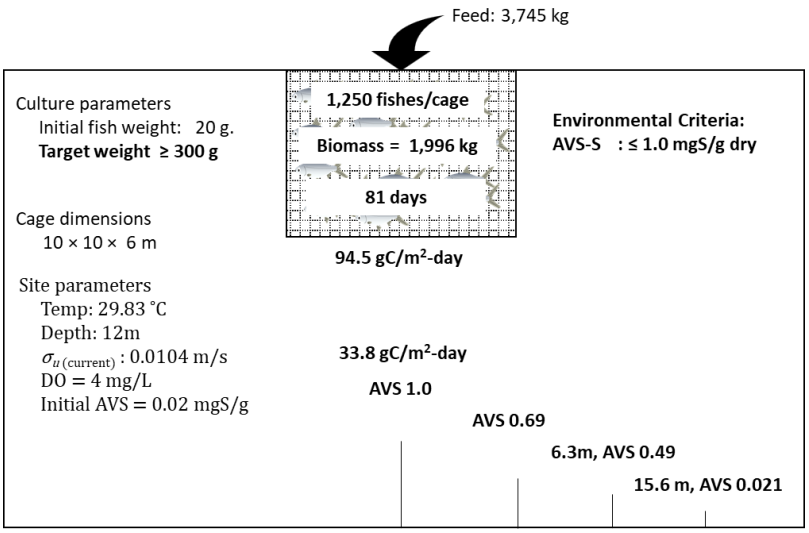

Figure 5.8. Simulation results for four 5 × 5 × 6m net cages taken as one cage.

In the figure, the resulting number of fish per cage is only 1,250 fishes. The amount of needed feed to reach a harvest body weight of greater than 300g is 3,745kg. Comparing the biomass from the single cage results, the value is almost doubled. However, since 4 cages were simulated, the biomass should be more than 4 times compared to the single cage for it to be considered economically feasible. It can also be observed that the particulate carbon flux at the center of the cage for single and multiple net cages was equal. This implies that the amount of carbon flux to reach 1.0 AVS is only 33.8 gC/m^2-day. In this scenario, the AVS concentration strongly controlled the number of fish to cultured leading to fewer stocks in each cage. For this scenario, an economic analysis is not necessary since it was expected to be not feasible.

Another multiple cage scenario can be simulated, but this time the AVS criteria was set to 2.0 mgS/g dry. This AVS condition is when the sediment is about to reach critical levels. In Japan aquaculture practices, the law states that sediment AVS should be below 2.0 mgS/g dry as this value is the critical limit. The AVS 2.0 criteria was expected to allow more numbers of fishes to be cultured allowing the balance between economic and environmental criteria. In the model, the AVS criteria was changed and the rest of the parameters were kept the same. Figure 5.9 shows the result of the simulation for four net cages taken as one 10 × 10 × 6m cage with AVS 2.0 criteria.

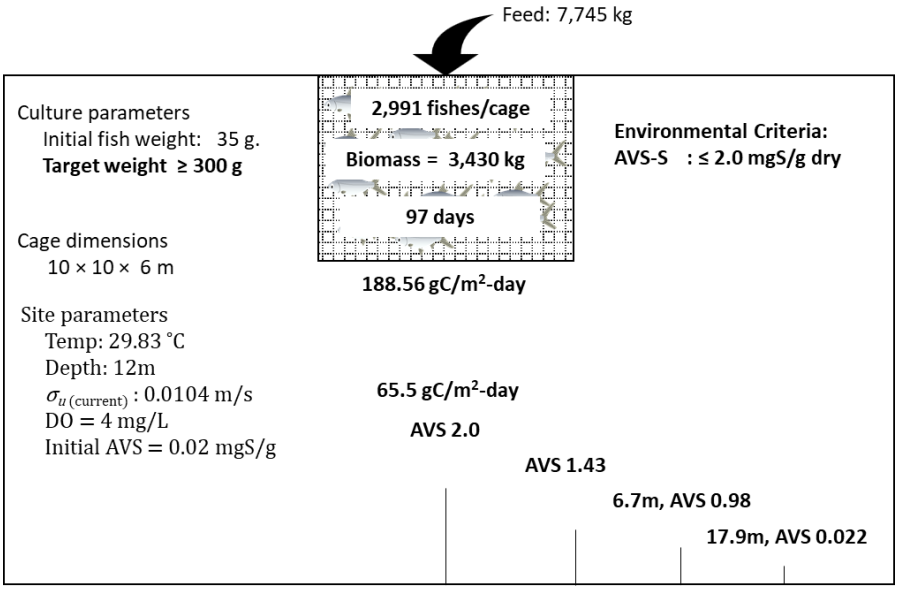

Figure 5.9. Simulation results for multiple net cages with AVS 2.0 criteria

In the figure, the total number of fishes to be cultured is 11,964 in 97 days of culture. The harvest biomass was 3,430kg which is lower compared to 4 times the single cage simulation with AVS 1.0. Judging by this premise it can be deducted that the income from AVS 2.0 criteria in multiple cages is lower compared to the previous economic analysis in single cage with AVS 1.0, thus economic analysis for this results is not necessary. And since the environmental criteria is higher, this culture management yields a more polluted sediment. Both economic and environmental sustainability were not satisfied in this simulation thus the AVS 2.0 with 4 cages taken as one is not recommended.

In summary of the simulation results, the recommended management for a 5 × 5 × 6m cages in the experiment site would be the 4 cages in square orientation with the distance of 1.6m between the cages. The stocking number of fishes would be approximately 12,900 individuals in 100 days ensuring optimum growth. Though the first cropping schedule would yield a negative income, the successive crops thereafter have an evident income, though it was comparably low to the suggested Milkfish Culture guide, the resulting management is both economically and environmentally sustainable.

The model-setup for milkfish cage culture can be used in a wide range of parameters and scenarios. More importantly this model can be a tool for establishing environmental criteria in tropical regions through regulating the number of cultured fish in each cage with considerations of its economic viability.

5.4 Index of Suitable Location

The model-setup for milkfish farm has been developed to predict the AVS production associated with milkfish marine cage culture given the rectangular cage dimensions. Based on the concept of index of suitable location (ISL) (Yokoyama et al. 2004) which is expressed as $ISL = DV^2$, where D is the water depth (m) and V is the time-averaged current velocity (m/s), different values of ISL were simulated using 10 × 10 × 6m cage, 29.63˚C temperature, 120 days of culture, initial ABW of

20g, harvest ABW of >300g and 0.02 mgS/g dry background AVS concentration. The AVS criteria were set to 0.2, 1.0, 2.0, and 3.0 and would serve as the zones of fish-cage environments i.e., healthy, polluted, cautionary and critical, respectively. The resulting stocking count and harvest biomass were recorded and correlated to establish a relationship which can serve as guide for farmers. Figure 5.10 shows the results of the simulation with different ISL values correlated with the harvest biomass (carrying capacity of the cage). Linear regression line was then fitted to the AVS 1.0 and 2.0 to determine the zones of fish-cage environments and was shown in Figure 5.11.

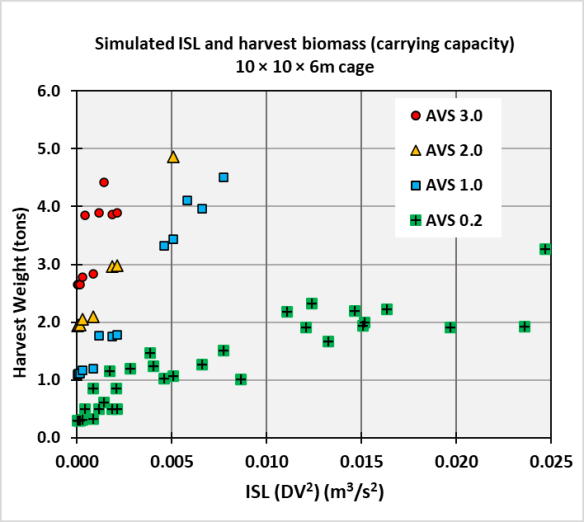

Figure 5.10. Simulation results for different depth and current velocity combinations with harvest weight.

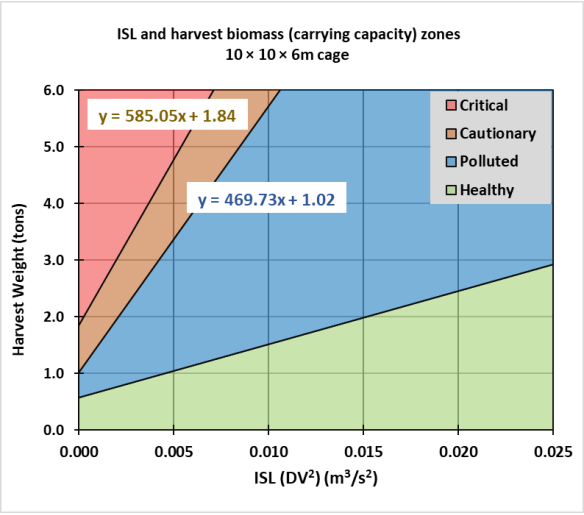

Figure 5.11. Fitted regression line in AVS 1.0 and 2.0 with determined zones of fish-cage environment.

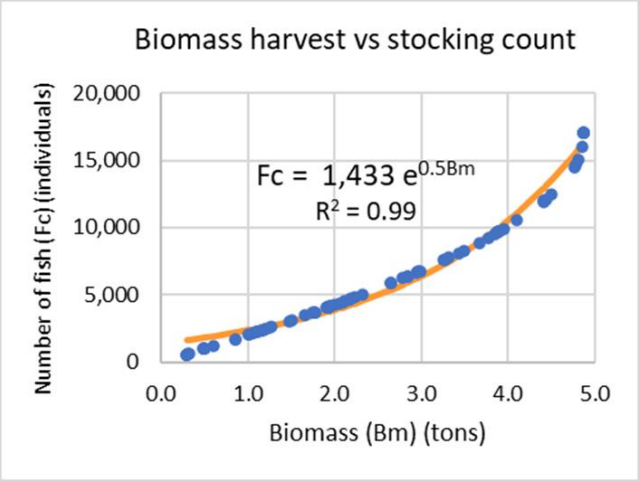

Figure 5.12. Biomass and stocking number of fish relationship.

In Figure 5.11, the AVS 1.0 and 2.0 data set was fitted with a linear regression line. However, the AVS 1.0 trendline will be given much preference to keep the sediments below cautionary zone. The trendline with AVS 0.20 was not considered since the number of fish to be stocked and the harvest biomass will yield a non-economically viable production thus is not economically sustainable.

In determining the maximum number of fish stocks to be stocked in a 10 × 10 × 6m cage for both economically and environmentally sustainable milkfish production, depth and instead of time-averaged current, current standard deviation is needed for the simulation.

For instance, the selected site for milkfish production has 14m depth and 0.024 m/s current standard deviation. This results to an ISL value of 0.082. Using the equation for polluted AVS zone in Figure 5.11, the harvest weight in tons is 4.81. Moreover, using equation in Figure 5.12, it can be calculated that the number of fish stocks to be stocked is 15,860 individuals. The exponential relationship of harvest biomass and the number of fish stocks was the result of the effect of the fish density on the growth of the fish. If the density effect were not considered the graph of Figure 5.12 would result to a linear trendline. The model-up setup for milkfish cage farming can also calculate optimal conditions for any cases and water parameters.

Chapter 6 - CONCLUSION

The model setup for milkfish cage culture has many limitations and uncertainties because the processes involved in each of the sub-model was simplified. Nevertheless, it was successful on the prediction of the number of fish to be cultured using the AVS criteria and the harvest criteria. The growth sub-model used for the set-up was based only on four different trial runs. To improve its prediction and accuracy, several trials can be added to tune the coefficients. In addition, several factors can also be included to the growth model such as age, mass index, salinity, dissolved oxygen, nutrient concentrations, and feed quality. These factors can also be sources of stress on fish in which the maximum weight *K* and intrinsic growth rate *r* can be affected. There are also many issues arising on which feed guide is effective. In most cases the feed guide was used with pellet size and nutritional content variations to optimize juvenile growth. These variations were not included in the model since it was assumed that the carbon and nitrogen of feed is the same on all trials.

The equations and parameter used for material balances were mainly based on existing theories more specifically on the routine metabolism rate of milkfish. The routine metabolism rate may also vary with temperature, salinity, and dissolved oxygen changes. These factors can also be incorporated with the carbon balances to have more accurate forecast of the faecal material. Most importantly, the carbon and nitrogen content of feed or the proximate analysis data should be known, without these data, the material balances would not be possible.

The statistical model to explain the particle dispersion contains several assumptions. Through the use of the relative AVS concentration, the diffusivity coefficient was estimated, however it was assumed that there was no decomposition of organic matter in the water column. Since the faecal material has a greater mass compared to the feed material, the AVS generation can be assumed to be solely dependent on the amount of settle faecal material. Fish faeces are often ejected as a gelatinous material which can easily decompose or break apart into finer grains and in some cases do not settle at all. The statistical approach on representing the behavior of particles may not explain the actual

dynamics on the diffusion of organic waste, for such theories are limited. Milkfish feed and faecal material sinking rates needs to be studied more especially on the mass ratio of the faeces. The assumed fee wastage of 5% may best represent the husbandry practices of the milkfish culture however as these waste feed settles; wild fish populations may be able to consume them resulting to less amount of feed waste that settles on the seabed. This speculation is highly possible since in tropical regions milkfish feed can be used as bait for local fisheries.

In the sediment degradation sub-model, the carbon flux distribution estimated through the probability function, resulted to a moderately correlated calculated AVS when compared to the actual AVS data. The results of statistical analysis of particle dispersion combined with the assumptions based on Aarhus bay nutrient and sediment flux model proved to be applicable on the evolution of AVS in milkfish cage culture. However, sedimentation rate is also necessary to forecast the daily evolution of AVS. Moreover, only the labile organic carbon was used for AVS calculations since it is readily degradable, which is the opposite of refractory organic carbon that decomposes slowly and contribute to the sediment oxygen demand years after deposition. The importance of refractory organic is to determine its effect on the quality of the water just above the sediment.

Finally, the carrying capacity in terms of optimum harvest biomass and number of fish to be cultured in a milkfish cage or series of milkfish cages in cluster was successfully estimated through the proposed sub-models. The equations derived for the estimation of the carrying capacity are dependent on cage dimensions, temperature, initial and final body weight, duration of culture and initial AVS concentration. These parameters can be easily acquired through simple data gathering procedures and careful planning. Variations on any of these parameters will result to a site-specific relationships on ISL and biomass, however the initial and harvest body weight of the fish has the most impact on the carrying capacity. At any given current velocity and depth, the number of fish to be cultured can be estimated and if the production requires a certain amount of harvest, the site that qualifies for such production demand can be successful selected.

6.1 Implications and future perspective of the study

Sediment quality are often overlooked and not being considered for environmental quality standards. This is because in aquaculture, the internal impacts which has a direct effect on the fish are often considered more important. However, local impacts may also play an important role on mass mortality incidents in cage farming. Most aquaculture sites were placed in estuarine and coves which exhibits low water exchange particulate waste accumulates rapidly in these sites. As wastes accumulates, the AVS production through sediment degradation also increases and hydrogen sulfide concentration may also increase in the water column, however, the lethal dose of hydrogen sulfides to the fish was not known. As hydrogen sulfide dissolves in water column, dissolved oxygen concentration also decreases leading to hypoxia and this may cause mass fish kills.

The model can also be improved by converting the cage rectangular dimensions into circular in which many big aquaculture firms are using. Radial dispersion analysis with probability function can be used for the conversion. For the case of fish nutrition, CNP feed ratios through proximate analysis can be employed and a material balance using phosphate can be done. Using CNP balances, a complete degradation model in both water and sediment can be done and would have more accurate predictions. Fish growth rate can also be a function of environmental stressors like temperature, dissolved oxygen, and nutrient concentrations. The rate of metabolism of fish can be accounted to these several factors which effects the amount of undigested carbon. For the particle dispersion model, since the daily carbon waste can be estimated, daily dispersion with daily current data can be employed. This would result to a less fine contour distribution and the maximum flux may not be located directly under the center of the cage. In addition, the Philippines has typhoon season thus, the sediment resuspension is highly anticipated on the typhoon paths and during these events, most of the accumulated carbon can be dispersed in a longer distance away from the cages. This negative AVS production can also be expected from the days of no cage culture activities and the rate of the negative overall AVS production should also be studied. Sedimentation rates in aquaculture was also

not taken into consideration thus the assumptions on the diffusive boundary layer. Careful data gathering on the exact sedimentation rates should also be studied.

Finally, the model set-up can be applicable to all aquaculture species, given the basic parameters discussed in previous chapters. Several tropical species like mangrove red snapper, grouper, pompano, and rabbit fish are getting popular because of the need to diversify production. Not only in tropical aquaculture, but also in temperate regions since temperature a is a function of both fish growth and sediment degradation. This model can also be used for creating an integrated multi-trophic aquaculture setup for tropical regions using seaweeds and benthic species to augment and reduce waste products from aquaculture.

List of tables

Table of figures

Bibliography

Allen, Herbert E., Gongmin Fu, and Baolin Deng. 1993. “Analysis of AVS and SEM for the Estimation of Potential Toxicity in Aquatic Sediments.Pdf.” *Environmental Toxicology and Chemistry* 12:1441–53.

Arndt, Sandra, B. B. Jørgensen, D. E. LaRowe, J. J. Middelburg, R. D. Pancost, and P. Regnier. 2013. “Quantifying the Degradation of Organic Matter in Marine Sediments: A Review and Synthesis.” *Earth-Science Reviews* 123:53–86.

Avnimelech, Yoram. 1999. “Carbon/Nitrogen Ratio as a Control Element in Aquaculture Systems.” *Aquaculture* 176:227–35.

Bagarinao, T. 1991. “Biology of Milkfish (Chanos Chanos Forsskal).” 94.

Ballester-Moltó, M., P. Sanchez-Jerez, J. Cerezo-Valverde, and F. Aguado-Giménez. 2017. “Particulate Waste Outflow from Fish-Farming Cages. How Much Is Uneaten Feed?” *Marine Pollution Bulletin* 119(1):23–30.

Bergheim, A. and T. Asgard. 1996. “Waste Production from Aquaculture.” *Aquaculture and Water Resource Management* 50–80.

Bowman, George T. and Joseph J. Delfino. 1980. “Sediment Oxygen Demand Techniques: A Review and Comparison of Laboratory and in Situ Systems.” *Water Research* 14:491–99.

Bravo, Francisco and Jonathan Grant. 2018. “Modelling Sediment Assimilative Capacity and Organic Carbon Degradation Efficiency at Marine Fish Farms.” *Aquaculture Environment Interactions* 10:309–28.

Chaikaew, Pasicha and Penjai Sompongchaiyakul. 2018. “Acid Volatile Sulphide Estimation Using Spatial Sediment Covariates in the Eastern Upper Gulf of Thailand: Multiple Geostatistical Approaches.” *Oceanologia* 60:478–87.

Chamberlain, J. and D. Stucchi. 2007. “Simulating the Effects of Parameter Uncertainty on Waste Model Predictions of Marine Finfish Aquaculture.” *Aquaculture* 272:296–311.

Chang, B. D., F. H. Page, R. J. Losier, and E. P. McCurdy. 2014. “Organic Enrichment at Salmon Farms in the Bay of Fundy, Canada: DEPOMOD Predictions versus Observed Sediment Sulfide Concentrations.” *Aquaculture Environment Interactions* 5:185–208.

Chen, Y. S., M. C. M. Beveridge, and T. C. Telfer. 1999. “Settling Rate Characteristics and Nutrient Content of the Faeces of Atlantic Salmon, Salmo Salar L., and the Implications for Modelling of Solid Waste Dispersion.” *Aquaculture Research* 30(5):395–98.

Chopin, T., S. M. C. Robinson, M. Troell, A. Neori, A. H. Buschmann, and J. Fang. 2008. “Ecological Engineering in Aquaculture: Towards a Better Waste Management in Western World Mariculture.” *Ecological Engineering* 2463–75.

Colt, J. E. and D. A. Armstrong. 1981. *Nitrogen Toxicity to Crustaceans, Fish, and Molluscs.*

Corner, R. A., A. J. Brooker, T. C. Telfer, and L. G. Ross. 2006. “A Fully Integrated GIS-Based Model of Particulate Waste Distribution from Marine Fish-Cage Sites.” *Aquaculture* 258(1–4):299–311.

Crear, David. 1980. “Observations on the Reproductive State of Milkfish Populations (Chanos Chanos) from Hypersaline Ponds on Christmas Island (Pacific Ocean).” *Proceedings of the World Mariculture Society* 11(1–4):548–56.

Cromey, C. J. and K. D. Black. 2005. “Modelling the Impacts of Finfish Aquaculture.” *Handbook of Environmental Chemistry* 5(July):129–55.

Cromey, Chris J., Thomas D. Nickell, and Kenneth D. Black. 2002. “DEPOMOD-Modelling the Deposition and Biological Effects of Waste Solids from Marine Cage Farms.” *Aquaculture* 214:211–39.

Czamanski, Marie, Adi Nugraha, Philippe Pondaven, Marine Lasbleiz, Annick Masson, Nicolas Caroff, Robert Bellail, and Paul Tréguer. 2011. “Carbon, Nitrogen and Phosphorus Elemental Stoichiometry in Aquacultured and Wild-Caught Fish and Consequences for Pelagic Nutrient

Dynamics." *Marine Biology* 158:2847–62.

Demirak, Ahmet, Ahmet Balci, and Mehmet Tüfekçi. 2006. "Environmental Impact of the Marine Aquaculture in Güllük Bay, Turkey." *Environmental Monitoring and Assessment*.

Ern, R., D. T. T. Huong, N. V. Cong, M. Bayley, and T. Wang. 2014. "Effect of Salinity on Oxygen Consumption in Fishes: A Review." *Journal of Fish Biology* 84:1210–20.

FAO. 2016. *The State of World Fisheries and Aquaculture 2016: Contributing to Food Security and Nutrition for All*.

Fossing, Henrik, Peter Berg, Bo Thamdrup, Søren Rysgaard, Helene S. Munk, and Kurt Nielsen. 2004. *A Model Set-up for an Oxygen and Nutrient Flux Model for Aarhus Bay (Denmark)*.

Frankic, Anamarija and Carl Hershner. 2003. "Sustainable Aquaculture: Developing the Promise of Aquaculture." *Aquaculture International* 11:517–30.

Gondwe, Mangaliso J., Stephanie J. Guildford, and Robert E. Hecky. 2012. "Tracing the Flux of Aquaculture-Derived Organic Wastes in the Southeast Arm of Lake Malawi Using Carbon and Nitrogen Stable Isotopes." *Aquaculture* 350–353:8–18.

Grover, John H. and Rogelio O. Juliano. 1976. "Length-Weight Relationship of Pond-Raised Milkfish in the Philippines." *Aquaculture* 7:339–46.

Halwart, Matthias, D. Soto, and James Richard Arthur. 2007. *Cage Aquaculture Regional Reviews and Global Overview*. Rome.

Hammerschmidt, Chad R. and G. Allen Burton. 2010. "Measurements of Acid Volatile Sulfide and Simultaneously Extracted Metals Are Irreproducible among Laboratories." *Environmental Toxicology and Chemistry* 29(7):1453–56.

Hernandez-Llamas, Alfredo and David A. Ratkowsky. 2004. "Growth of Fishes, Crustaceans and Molluscs: Estimation of the von Bertalanffy, Logistic, Gompertz and Richards Curves and a New Growth Model." *Marine Ecology Progress Series* 282:237–44.

Holmer, Marianne, Núria Marbá, Jorge Terrados, Carlos M. Duarte, and Mike D. Fortes. 2002. “Impacts of Milkfish (Chanos Chanos) Aquaculture on Carbon and Nutrient Fluxes in the Bolinao Area, Philippines.” *Marine Pollution Bulletin* 44(7):685–96.

Holmer, Marianne, Dave Wildish, and Barry Hargrave. 2005. “Organic Enrichment from Marine Finfish Aquaculture and Effects on Sediment Biogeochemical Processes.” Pp. 181–206 in *Environmental Effects of Marine Finfish Aquaculture*.

Hopkins, Kevin D. 1992. “Reporting Fish Growth: A Review of the Basics.” *Journal of the World Aquaculture Society*.

Huang, Yuan Chao Angelo, Shou Chung Huang, Hernyi Justin Hsieh, Pei Jie Meng, and Chaolun Allen Chen. 2012. “Changes in Sedimentation, Sediment Characteristics, and Benthic Macrofaunal Assemblages around Marine Cage Culture under Seasonal Monsoon Scales in a Shallow-Water Bay in Taiwan.” *Journal of Experimental Marine Biology and Ecology* 422–423:55–63.

Huiwen, Cai and Sun Yinglan. 2007. “Management of Marine Cage Aquaculture.” *Environmental Science and Pollution Research - International* 14(7):463–69.

Islam, Md Shahidul. 2005. “Nitrogen and Phosphorus Budget in Coastal and Marine Cage Aquaculture and Impacts of Effluent Loading on Ecosystem: Review and Analysis towards Model Development.” *Marine Pollution Bulletin* 50:48–61.

Kishi, Michio J., Masato Uchiyama, and Yoshiyasu Iwata. 1994. “Numerical Simulation Model for Quantitative Management of Aquaculture.” *Ecological Modelling* 72:21–40.

Kodama, Masashi. 2012. *Assessing the Environmental Impact of Milkfish Farming*. Tsukuba, Ibaraki, Japan.

Kumagai, S., T. Bagarinao, and A. Unggui. 1985. “Growth of Juvenile Milkfish Chanos Chanos in a Natural Habitat.” *Marine Ecology Progress Series* 22:1–6.

Lim, Chhorn, Ilda G. Borlongan, and P. Pascual. 2002. “Milkfish, Chanos Chanos.” *Nutrient*

Requirements and Feeding of Finfish for Aquaculture 172–83.

Lugert, Vincent, Georg Thaller, Jens Tetens, Carsten Schulz, and Joachim Krieter. 2016. "A Review on Fish Growth Calculation: Multiple Functions in Fish Production and Their Specific Application." *Reviews in Aquaculture*.

Martinez, Franklin S., Mei-chen Tseng, and Sin-ping Yeh. 2006. "Milkfish (Chanos Chanos) Culture: Situations and Trends." *Journal of the Fisheries Society of Taiwan* 33(3):229–44.

Mawhin, J. 2004. "The Legacy of Pierre-FranÇois Verhulst and Vito Volterra in Population Dynamics." Pp. 147–60 in *The First 60 Years of Nonlinear Analysis of Jean Mawhin*.

McCormick, John. 2001. *Hydrodynamics and Water Quality*.

Middelburg, Jack J. 1989. "A Simple Rate Model for Organic Matter Decomposition in Marine Sediments." 53:1577–81.

Mujib, M., M. Mardiyah, Suherman, R. Rakhmawati, S. Andriani, M. Mardiyah, H. Suyitno, S. Sukestiyarno, and I. Junaidi. 2019. "The Application of Differential Equation of Verhulst Population Model on Estimation of Bandar Lampung Population." *Journal of Physics: Conference Series* 1155(1):1–6.

Nelson, J. A. 2016. "Oxygen Consumption Rate v. Rate of Energy Utilization of Fishes: A Comparison and Brief History of the Two Measurements." *Journal of Fish Biology* 88:10–25.

Noroi, Gunnvor Á., Ronnie N. Glud, Eilif Gaard, and Knud Simonsen. 2011. "Environmental Impacts of Coastal Fish Farming: Carbon and Nitrogen Budgets for Trout Farming in Kaldbaksfjørour (Faroe Islands)." *Marine Ecology Progress Series*.

Okubo, Akira. 1971. "Oceanic Diffusion Diagrams." *Deep-Sea Research and Oceanographic Abstracts* 18:789–802.

Okubo, Akira, Curtis C. Ebbesmeyer, and Brian G. Sanderson. 1983. "Lagrangian Diffusion Equation and Its Application to Oceanic Dispersion." *Journal of the Oceanographical Society of Japan*

39:259–66.

Omori, Koji, Takafumi Hirano, and Hidetaka Takeoka. 1994. “The Limitations to Organic Loading on a Bottom of a Coastal Ecosystem.” *Marine Pollution Bulletin* 28(2):73–80.

Ott, Soren and Jakob Mann. 2000. “An Experimental Investigation of the Relative Diffusion of Particle Pairs in Three-Dimensional Turbulent Flow.” *Journal of Fluid Mechanics* 422:207–23.

Panchang, Vijay, G. Cheng, and Carter Newell. 2006. “Modeling Hydrodynamics and Aquaculture Waste Transport in Coastal Maine.” *Estuaries* 20(14):41.

Pawar, Vaishali, Osamu Matsuda, and Naomi Fujisaki. 2002. “Relationship between Feed Input and Sediment Quality of the Fish Cage Farms.” *Fisheries Science* 68(4):894–903.

Pearson, T. .. and K. D. Black. 2001. “The Environmental Impact of Marine Fish Cage Culture.” Pp. 1–31 in *Environmental Impacts of Aquaculture*.

Piedrahita, Raul H. 2000. “Solids and Nutrient Removal from Aquaculture Waters.” *Suisanzoshoku* 48(2):279–83.

Price, Carol, Kenneth D. Black, Barry T. Hargrave, and James A. Morris. 2015. “Marine Cage Culture and the Environment: Effects on Water Quality and Primary Production.” *Aquaculture Environment Interactions* 6:151–74.

Richardson, Lewis F. 1926. “Atmospheric Diffusion Shown on a Distance-Neighbour Graph.” *Proceedings of the Royal Society of London. Series A, Containing Papers of a Mathematical and Physical Character* 110:709–37.

Rickard, David and John W. Morse. 2005. “Acid Volatile Sulfide (AVS).” *Marine Chemistry* 97:141–97.

Ricker, W. E. 1979. “Growth Rates and Models.” Pp. 677–743 in *Fish Physiology*.

Roden, Eric E. and Jon H. Tuttle. 1992. “Sulfide Release from Estuarine Sediments Underlying Anoxic Bottom Water.” *Limnology and Oceanography* 37(4):725–38.

San Diego-McGlone, Maria Lourdes, Rhodora V. Azanza, Cesar L. Villanoy, and Gil S. Jacinto. 2008. "Eutrophic Waters, Algal Bloom and Fish Kill in Fish Farming Areas in Bolinao, Pangasinan, Philippines." *Marine Pollution Bulletin* 57:295–301.

Silvert, William. 1992. "Assessing Environmental Impacts of Finfish Aquaculture in Marine Waters." *Aquaculture* 107:67–69.

Sorensen, Peter B., Patrik Fauser, Lars Carlsen, and Jorgen Vikelsoe. 2001. "Theoretical Evaluation of the Sediment/Water Exchange Description in Generic Compartment Models (Simple Box)." P. 60 in *NERI Technical Report No. 360*. Copenhagen: Ministry of Environment and Energy National Environmental Research Institute.

Soto, D., J. Aguilar-Manjarrez, C. Brugère, D. Angel, C. Bailey, K. Black, P. Edwards, B. Costa-Pierce, T. Chopin, S. Deudero, S. Freeman, J. Hambrey, N. Hishamunda, D. Knowler, W. Silvert, N. Marba, S. Mathe, R. Norambuena, F. Simard, P. Tett, M. Troell, and A. Wainberg. 2008. "Applying an Ecosystem-Based Approach to Aquaculture: Principles, Scales and Some Management Measures." *Building an Ecosystem Approach to Aquaculture. FAO/Universitat de Les Illes Balears Expert Workshop. 7–11 May 2007, Palma de Mallorca, Spain. FAO Fisheries and Aquaculture Proceedings. No. 14.* 1–232.

Stigebrandt, Anders. 2011. "Carrying Capacity: General Principles of Model Construction." *Aquaculture Research* 42:41–50.

Stucchi, Dario, Terri-Ann Sutherland, Colin Levings, Dave Higgs, and Barry Hargrave. 2005. "Near-Field Depositional Model for Salmon Aquaculture Waste." *Handbook of Environmental Chemistry* 5M(July):157–79.

Sumagaysay-Chavoso, Neila S. 2003. "Nitrogen and Phosphorus Digestibility and Excretion of Different-Sized Groups of Milkfish (Chanos Chanos Forsskal) Fed Formulated and Natural Food-Based Diets." *Aquaculture Research* 34(5):407–18.

Sumbing, JG., Y. Nakamura, M. Kodama, and S. Watanabe. 2019. “Estimation of Milkfish Cage Culture Particulate Waste Dispersion Through Acid Volatile Sulfide Spatial Concentrations.” Pp. 1051–58 in *Proceedings of the 10th International Conference on Asian and Pacific Coasts, 2019, Hanoi, Vietnam*, edited by T. V. Nguyen, D. Xiping, and T. T. Tung. Springer, Singapore.

Swanson, Christina. 1998. “Interactive Effects of Salinity on Metabolic Rate, Activity, Growth and Osmoregulation in the Euryhaline Milkfish (Chanos Chanos).” *Journal of Experimental Biology* 201:3355–66.

Takeoka, Hidetaka and Koji Omori. 1996. “Methods of Determining the Limit of Suitable Fish Culture Based on the Oxygen Consumption Rate by the Sediment.” *水産海洋研究 (Fisheries and Ocean Research)* 60(1):45–53.

Troell, M., C. Halling, A. Neori, T. Chopin, A. .. Buschmann, N. Kautsky, and C. Yarish. 2003. “Integrated Mariculture: Asking the Right Questions.” *Aquaculture* 226(1–4):69–90.

Troell, M., M. C. Hernández-González, C. Aranda, A. Neori, C. Halling, A. H. Buschmann, and T. Chopin. 2009. “Mariculture Waste Management.” in *Encyclopedia of Ecology*.

Tsoularis, A. and J. Wallace. 2002. “Analysis of Logistic Growth Models.” *Mathematical Biosciences* 179(1):21–55.

Urban, N. R., P. L. Brezonik, L. A. Baker, and L. A. Sherman. 1994. “Sulfate Reduction and Diffusion in Sediments of Little Rock Lake, Wisconsin.” *Limnology and Oceanography* 39(4):797–815.

Vogels, Maurice, Rita Zoeckler, Donald M. Stasiw, and Lawrence C. Cerny. 1975. “P. F. Verhulst’s ‘Notice Sur La Loi Que La Populations Suit Dans Son Accroissement’ from Correspondence Mathematique et Physique. Ghent, Vol. X, 1838.” *Journal of Biological Physics*.

Watanabe, S., J. G. Sumbing, and M. J. H. Lebata-Ramos. 2014. “Growth Pattern of the Tropical Sea Cucumber, Holothuria Scabra, under Captivity.” *Japan Agricultural Research Quarterly* 48(4):457–64.

Watanabe, Satoshi, M. Kodama, JG Sumbing, and MJHL Lebata-Ramos. 2014. “Proceedings of the 42nd US-Japan Aquaculture Panel Symposium (Genetics in Aquaculture).” Pp. 80–87 in *Development of Integrated Multi-Trophic Aquaculture Using Sea Cucumber*.

Wongsin, Thongthip, Kangsadan Boonprab, Yuuki Okamoto, and Jintana Salaenoi. 2015. “Hydrogen Sulfide Distribution in Sediments Collected From Cockle Farm at Bandon Bay, Thailand.” in *International Conference on Plant, Marine and Environmental Sciences*.

Wu, R. S. S. 1995. “The Environmental Impact of Marine Fish Culture: Towards a Sustainable Future.” *Marine Pollution Bulletin* 31(4–12):159–66.

Wu, R. S. S., K. S. Lam, D. W. MacKay, T. C. Lau, and V. Yam. 1994. “Impact of Marine Fish Farming on Water Quality and Bottom Sediment: A Case Study in the Sub Tropical Environment.” *Marine Environmental Research* 38:115–45.

Yanagi, Tetsuo, Koso Murashita, and Haruo Higuchi. 1982. “Horizontal Turbulent Diffusivity in the Sea.” *Deep Sea Research Part A, Oceanographic Research Papers* 29(2A):217–26.

Yokoyama, Hisashi. 2000. “Environmental Quality for Aquaculture Farms in Japanese Coastal Areas: A New Policy and Its Potential Problems.” *Bulletin National Research Institute Fro Aquaculture* 29:123–34.

Yokoyama, Hisashi. 2003. “Environmental Quality Criteria for Fish Farms in Japan.” *Aquaculture* 226(1–4):45–56.

Yokoyama, Hisashi, Katsuyuki Abo, and Yuka Ishihi. 2006. “Quantifying Aquaculture-Derived Organic Matter in the Sediment in and around a Coastal Fish Farm Using Stable Carbon and Nitrogen Isotope Ratios.” *Aquaculture* 254:411–25.

Yokoyama, Hisashi, Misa Inoue, and Katsuyuki Abo. 2004. “Estimation of the Assimilative Capacity of Fish-Farm Environments Based on the Current Velocity Measured by Plaster Balls.” *Aquaculture* 240:233–47.

Yokoyama, Hisashi, Yuka Ishihi, Katsuyuki Abo, and Toshinori Takashi. 2010. “Quantification of Waste Feed and Fish Feces Using Stable Carbon and Nitrogen Isotopes.” *Bull. Fish. Res. Agen.* 31:71–76.

Acknowledgement

I would like to extend my sincere and heartfelt gratitude towards all the individuals who have directly or indirectly helped me in this endeavor. Without their presence, the completion of this research would have not been possible.

I am extremely thankful to Professor Yoshiyuki Nakamura for the active guidance, support and encouragement, particularly on providing his expertise for the data analysis of this research. The substantial counsel, comments and interpretations provided by Professor Nakamura are greatly appreciated.

I would also want to extend my utmost regards to Masashi Kodama and Satoshi Watanabe for the never-ending encouragement to pursue graduate studies and for providing the research platform while I was working as research assistant. I am also very thankful for the permission of using the experiment data for this study.

I also appreciate the help of the members of Estuarine and Coastal Engineering Lab more especially to Professor Takayuki Suzuki and Professor Hiroto Higa for the beneficial criticisms and remarks during laboratory seminars and with the help on Japanese translations.

I also acknowledge with deep sense of reverence, my family; Loregem, Joe Lerner and Jean Alexander for the sacrifice, support and motivation during the pursuit of my degree.

I want to extend my eternal appreciation to all my relatives and friends for their moral support and encouragement which served as my inspiration in finishing my degree.

For Tsuyoshi Sugita and Rolando Detoperez Jr, friends and brothers who I valued the company, you will always be remembered.

And last but not the least, I want to thank the Japanese Government thru Monbukagakusho Scholarship for the financial support. I am eternally indebted.